THE THEORY, DEVELOPMENT, AND IMPLEMENTATION OF PARTITIONED ERROR CONTROL

By

Mark Leland Rutherford

Dissertation

Submitted to the Faculty of the

Graduate School of Vanderbilt University

in partial fulfillment of the requirements

for the degree of

DOCTOR OF PHILOSOPHY

In

Chemical Engineering

May 2006

Nashville, Tennessee

Approved:

Professor Kenneth A. Debelak

Professor M. Douglas LeVan

Professor G. Kane Jennings

Professor R. Robert Balcarcel

Professor Nilanjan Sarkar

DEDICATION

To my father whose passion for understanding inspires me to reach for the sky and to my mother whose love is the bedrock on which I build.

ACKNOWLEDGEMENTS

To Dr. Kenneth Debelak for encouraging my exploration of a novel idea, guiding the development of that idea, and most importantly having the patience to allow me to continue to refine that idea as my way of thinking expanded.

To Margarita Talavera for being the heart of the chemical engineering department and for being my unyielding advocate and supporter as I navigated my way through Vanderbilt.

TABLE OF CONTENTS

LIST OF TABLES

LIST OF FIGURES

CHAPTER I

INTRODUCTION

Motivations and Goals

In the search for more efficient, robust control laws it will be necessary to obtain increasing amounts of information about the system to be controlled and the nature of the control problems to be overcome. Different control strategies tend to emphasize one of these approaches to the neglect of the other. This research is concerned with the merging of these issues and is based on the Partitioned Error Control (PEC) system; a novel two-degree-of-freedom control structure which separates servo and regulatory problems. This important feature of PEC only accounts for a fraction of the potential of the PEC system, however. For the purpose of separating servo and regulatory problems, PEC utilizes two controllers. These controllers can be chosen to accentuate each other's strengths and diminish each other's weaknesses. It is the exploration of this synergy that is the primary goal of the research purposed herein.

The current state of industrial processing places very stringent demands on product quality, energy consumption, safety, and environmental accountability. Furthermore, these demands will only grow more stringent with time as economic and regulatory factors are tightened. This has been and will continue to be the driving force behind process control development. This development, however, has come from two distinct aspects of process control: understanding the process, and distinguishing between sources of error.

Historically, more attention has been concentrated on understanding the process. Methods such as linear feedback control, internal model control (IMC), and model predictive control (MPC) attempt to meet regulatory objectives by focusing on how the manipulated variable affects the process output. For example, internal model control does not try to distinguish sources of error, but instead it focuses on predicting the affect of control moves to allow a more aggressive controller that is less susceptible to overshoot. These types of control structures have blossomed in recent years due to advancements in computer modeling. Now that large systems can be modeled with a high degree of detail and accuracy, these types of controllers are ceasing to be limited by our understanding of the process, but instead are being limited by the complexity and non-linearity of the control laws needed for such systems.

On the other hand, control structures, which try to distinguish between sources of error, tend to lead towards systems with multiple relatively simple control laws. A feed forward/feedback control loop is a prime example of this type of architecture. Performance benefits are gained by applying specific control laws to specific error sources. Other systems that take this approach include two-degree-of-freedom controllers and adaptive controllers. Two-degree-of-freedom controllers seek to shape the reference signal, and thus a source of error, so that the primary feedback control law can sufficiently meet both regulatory and tracking objectives. Adaptive controllers take a time variant approach to the problem. For example, self-tuning adaptive controllers attempt to distinguish process dynamics from disturbances, however, instead of implementing multiple control laws simultaneously, adaptive control increases performance by changing a single control law as the dynamics of the process change.

The difficulty with these types of systems is that key information needed to distinguish between sources of error is often unavailable, or in the case of conventional two-degree-of-freedom controllers the controller form itself is not as flexible as would be desired.

The ultimate goals of this research are to 1) develop an understanding of how partitioned error control functions in a SISO setting utilizing common design techniques, 2) develop mixed sensitivity and loop-shaping H∞ controller design in a PEC setting, applying robust stability and robust performance criteria for said controllers in this new setting, and 3) develop a general design procedure for PEC, which will rely heavily on the design procedures for the individual controllers chosen to be placed in the PEC framework.

The following approach outlines the presentation of the theory and implementation of Partitioned Error Control. In chapter two the background and current implementations of two-degree-of-freedom control will be explained. In chapter three the theory of Partitioned Error Control will be developed and compared to inverse model prefilters. In chapter four H_∞ controllers will be placed in the Partitioned Error Control structure. This system will then be compared to two-degree-of-freedom H_∞ control in a single input, single output environment. Chapter five will implement Partitioned Error Control on an inverted pendulum on a cart. The case study of the classic one input, two output problem includes a comparison to two-degree-of-freedom H_∞ controller. Chapter six will implement Partitioned Error Control on a binary distillation column. The case study of the classic two input, two output problem includes a comparison to two-degree-of-freedom H_∞ Internal Model Control. Chapter seven will summarize the results of this research. Finally, Chapter eight will explore future research opportunities.

CHAPTER II

THEORETICAL BACKGROUND OF TWO-DEGREE OF FREEDOM SYSTEMS

Why Is Two-Degree-of-Freedom Control Needed?

Where the operational objectives of a control system include both the suppression of disturbances, and optimal performance to set-point tracking, control is a compromise for any system that does not distinguish between regulatory and servo problems. This compromise occurs because each imposed control objective reduces the degree of freedom of any control system by one. Take for instance the following feedback control system, a one-degree-of-freedom (ODoF) controller. (Figure 1)

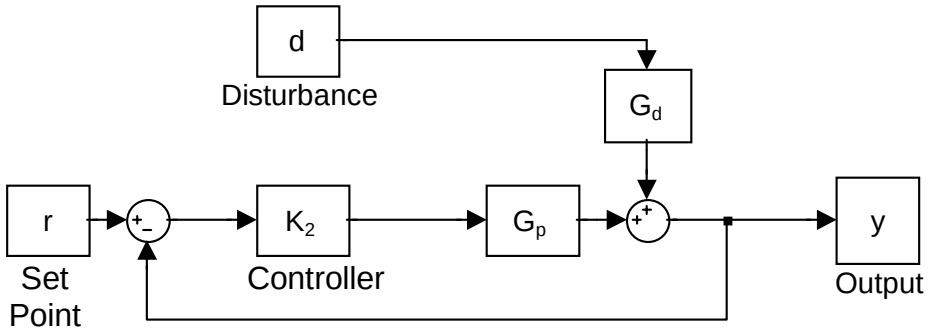

Figure 1: Single Input Single Output (SISO) feedback controller

It can easily be shown that this feedback system becomes over specified if a disturbance rejection objective, $\frac{y}{d}$, and a set-point tracking objective, $\frac{y}{r}$, are both set.

$$\frac{y}{d} = \frac{G_d}{(1 + K_2 G_p)} \qquad (1)$$

$$\frac{y}{r} = \frac{K_2 G_P}{(1 + K_2 G_P)} \qquad (2)$$

In this case, we have 2 equations with one arbitrarily specified variable, K_2. Using classic loop-shaping design techniques for minimum phase systems, we want the set-point tracking controller to be of the form $\frac{1}{s} G_P^{-1}$. This controller, however, has poor disturbance rejection characteristics. The same controller tuned for disturbance rejection would preferably be of the form $\frac{1}{s} G_P^{-1} G_d$. It is obvious that no one controller can be designed to handle both a discontinuous setpoint change, and a continuous disturbance in an optimal fashion without distinguishing between sources of error. To alleviate this problem, it is common to tune the controller for regulatory problems and impose a ramp function on the setpoint variable, in effect giving priority to regulatory objectives to the detriment of set-point tracking objectives. The introduction of a ramp function, or prefilter, however, increases the degrees of freedom in our system by one.

Horowitz[1] first purposed the use of this prefilter or precompensator, as seen in Figure 2, to shape the response of the system to meet set-point control objectives. There are many applications of this type of two-degrees-of-freedom (TDoF) controller in the literature, too many to list. A few examples from chemical engineering include Morari and Zafirou[2] who extended two-degrees-of-freedom controllers into the internal model control (IMC) structure, and Lundstrom and Skogestad[3], Limbeer et al. [4], Van Digglen and Glover[5], and Skogestad et al.[6] who have used two-degrees-of freedom controllers for distillation column control.

A typical block diagram of a TDoF controller is shown in Figure 2. The controller has two components, a feedback controller, K_2, and prefilter, K_r. The prefilter, K_r, shapes the reference signal to enhance performance, while the controller, K_2, handles the shaped tracking error, disturbances, noise, and modeling error. K_2 and K_r can be designed simultaneously and are theoretically capable of achieving two distinct control objectives for minimum phase systems using inverse-based control. However, in practice, the limitations associated with inverse-based design and modeling error lead to a lead-lag prefilter design. Although this type of prefilter does allow some manipulation of the setpoint response, the dynamics are still mainly determined by the feedback loops characteristic equation. Thus, the set-point response of a system with a prefilter is dynamically similar to the setpoint response of an equivalent one-degree of freedom system, as seen in Figure 3. With limited control over set-point dynamics, and the fact that adjustments to the load controller will invariably affect set-point performance, precompensators provide a less than ideal method for meeting multiple control objectives.

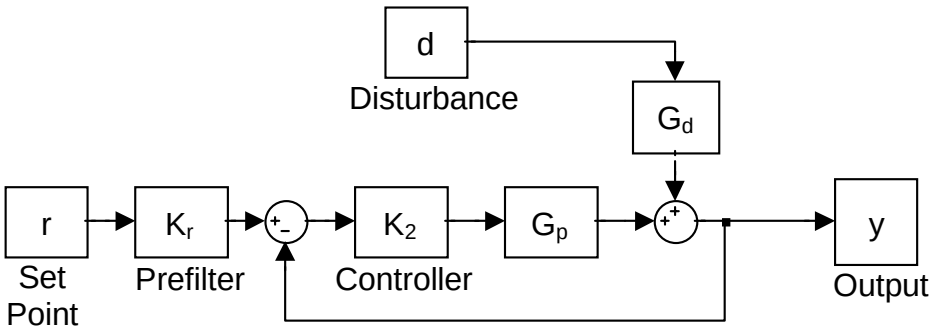

Figure 2: Traditional TDoF control structure

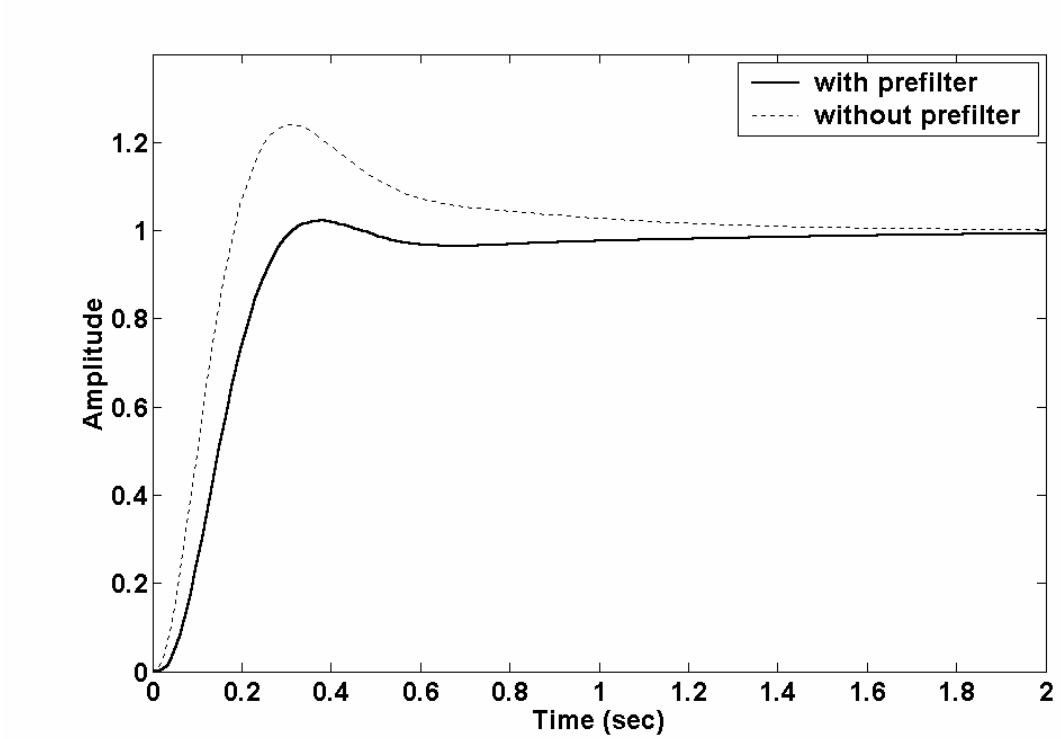

Figure 3: An example set-point response of the TDoF system in Figure 2, and the response of the same system without the use of the prefilter.

It is easily shown that the addition of a precompensator only adds roots to the characteristic equation and has no ability to modify the location of the existing roots. Examine the system in Figure 2, letting the lead-lag compensator, K_r, be written in its general form, $K_r = \frac{\tau_{Lead}s+1}{\tau_{Lag}s+1}$. The response of the TDoF system to a set point change is then as follows:

$$\frac{r}{y} = \frac{(\tau_{Lead}s+1)K_2G_P}{(\tau_{Lag}s+1)(1+K_2G_P)} \quad (3)$$

The same system will have a disturbance response as follows:

$$\frac{d}{y} = \frac{1}{1+K_2G_P} \quad (4)$$

The limited ability of the precompensator to change the characteristic equation for set-point tracking becomes clear. Although it does increase the order of the characteristic equation by one, the root locations are still highly dependant on the feedback controller. Therefore the general dynamics of a setpoint response will be similar to the dynamics of a disturbance response.

Inverse Model Prefilter Design

Consider the SISO system where

$$G_P = G_d = \frac{k_P}{\tau s+1}e^{-\theta s} = \frac{4e^{-3.5s}}{7s+1} \quad (5)$$

Several tuning methods are available for first order plus dead time systems. Table 1 summarizes the controller tunings suggested by 3 such methods.

Table 1. Proportional + Integral Controller Tunings for SISO systems

Murrill K_C/τ_I		Ziegler-Nichols	TLC
Setpoint	Load	K_C/τ_I	K_C/τ_I
0.28/7.39	0.42/6.48	0.43/9.98	0.3/26.4

A suitable controller for disturbance rejection of this system is given by using the proportional-integral (PI) settings according to the tuning rules of Lopez, Murrill et al. [7], and Rovira, Murrill et al. [8], which has the following form

$$K_2 = K_C + \frac{K_C}{\tau_I s}; \quad K_C = 0.42; \quad \tau_I = 6.48; \tag{6}$$

This controller, however, does not provide good set point tracking. An inverse model prefilter can correct for this deficiency by increasing the degrees of freedom of the system by one. Examining the closed loop response of the system in Figure 2 readily shows this increase.

$$\frac{y}{r} = K_r \frac{K_2 G_{nom}}{1 + K_2 G_{nom}} \tag{7}$$

Where G_{nom} is the nominal process model assumed to be equal to the actual process G_P, the designer may specify a reference trajectory, $\frac{y}{r}$, and solve for the prefilter obtaining the control law shown in Equation (8).

$$K_r = \left(\frac{K_2 G_{nom}}{1 + K_2 G_{nom}} \right)^{-1} \left(\frac{y}{r} \right)_{Ref} \tag{8}$$

In general there are three limitations to this design. First, the prefilter will be unstable if the process contains any right hand plane zeros. Second, the controller may be improper if there are an excessive number of poles with respect to zeros in the process. Third, a

process with a state space realization $G_P = \left[\begin{array}{c|c} A & B \\ \hline C & D \end{array}\right]$ will not be invertible for systems where $D \neq 0$. These three constraints limit the family of systems to which inverse prefilter design can be applied. It is also important to note that the order of the prefilter will be at least as large as the order of the process so that the prefilter is proper.

A suitable choice of the reference trajectory for the process in Equation (5) would be as follows

$$\left(\frac{y}{r}\right)_{Ref} = \frac{1}{\lambda s + 1} e^{-\theta_r s} \tag{9}$$

λ can be chosen to obtain the desired response and θ_r is chosen to make sure K_r does not have a predictive element. Finally, we can solve for the form of the prefilter using Equation (5), (6), (8), and (9).

$$K_r = \frac{\frac{\tau_I}{k_C k_P} s(\tau s + 1)}{(\tau_I s + 1)(\lambda s + 1)} e^{-(\theta - \theta_r)s} + \frac{1}{(\lambda s + 1)} e^{-\theta_r s} \tag{10}$$

$$K_r = \frac{\frac{6.48}{(0.42)(4)} s(7s + 1)}{(6.48s + 1)(\lambda s + 1)} + \frac{1}{(\lambda s + 1)} e^{-3.5s} \tag{11}$$

The digital implementation of this prefilter would be feasible: however, it is a nonstandard controller form. Furthermore, any changes in the feedback controller tunings would affect the prefilter design.

Figure 4 shows the step response of this system for various values of λ. Decreasing λ does result in a more tightly tuned controller, which is more susceptible to modeling error.

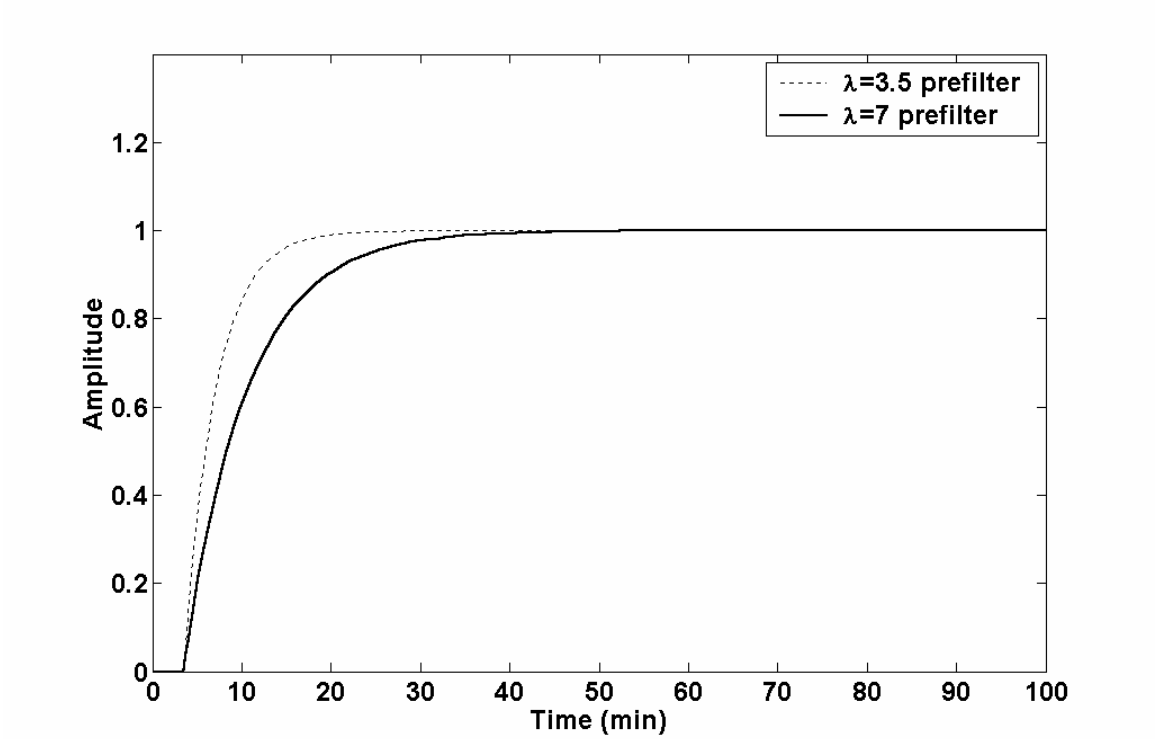

Figure 4: Step response for an inverse base prefilter design with λ=3.5 and λ=7

Lag-Lead Prefilters

An alternative approach is to design the prefilter as a lag-lead element:

$$K_r = \frac{\tau_{lead}s + 1}{\tau_{lag}s + 1} \tag{12}$$

Setting $\tau_{lead} > \tau_{lag}$ will result in a quicker response, while setting $\tau_{lead} < \tau_{lag}$ will result in a slower response. The following example details a typical design procedure for the development of a lead-lag prefilter. The procedure first seeks to find an adequate ODoF solution, however, when that attempt proves inadequate, a prefilter is designed to augment a ODoF controller with good disturbance rejection characteristics. This example is worked out in detail so it may be used as a basis for comparing different TDoF techniques in later chapters.

Consider the following disturbance process defined by Skogestad and Postlethwaite.[9]

$$G(s) = \frac{200}{10s+1}\frac{1}{(0.05s+1)^2}, \quad G_d(s) = \frac{100}{10s+1} \tag{13}$$

For this process, both tracking and disturbance rejection are important objectives and are defined by the following three criteria:

1. Command Tracking: The tracking response should have no greater than 5% overshoot. Furthermore, the response should reach 90% of the final value within 0.3 seconds.
2. Disturbance Rejection: The response of a system to a unit step change in the disturbance should not exceed unity. $|y(t)| \in [-1,1]$ for all t. Furthermore, the response should be less than 0.1 after 3 seconds

3. Input constraints: u(t) should remain within the range of [-1,1].

Obviously, it would be desirable to find a ODoF controller, which meets these objectives. Skogestad and Postlewaite[9] investigated several ODoF designs. These designs are summarized below.

First, a design, which caters to setpoint tracking, was investigated. For setpoint changes a typical plant-inverse controller would be

$$K(s) = \left(\frac{\omega_C}{s}\right) G^{-1} \qquad (14)$$

Since $G_d(0)=100$, the system response without feedback control to a unit step change in the disturbance, d=1, would be 100 times larger than is acceptable given the specifications for disturbance rejection. As the frequency of the disturbance, ω_d, increases the gain will decrease until $G_d(j\,\omega_d) = 1$ around $\omega_d = 10$ rad/s. Hence feedback control will be needed for frequencies up to 10 rad/s to ensure disturbance rejection specifications are met, so we set $\omega_C = 10$rad/s. With ω_C set we change our focus to generating an acceptable inverted plant, G^{-1}. The inverse plant model has an excess of poles making $\left(\frac{\omega_C}{s}\right) G^{-1}$ improper. To alleviate this condition the plant term $(0.05s+1)^2$ is approximated as (0.1s+1). This approximation is then applied over a decade, i.e. we use $\frac{(0.1s+1)}{(0.01s+1)}$ to give the realizable controller design

$$K_1 = \frac{10}{s}\,\frac{10s+1}{200}\,\frac{0.1s+1}{0.01s+1} \qquad (15)$$

The tracking response of the inverse-based controller defined in Equation (15) is shown in Figure 5. The controller exhibits no overshoot and a rise time of about 0.16s, providing excellent tracking. The disturbance response of the inverse-based controller

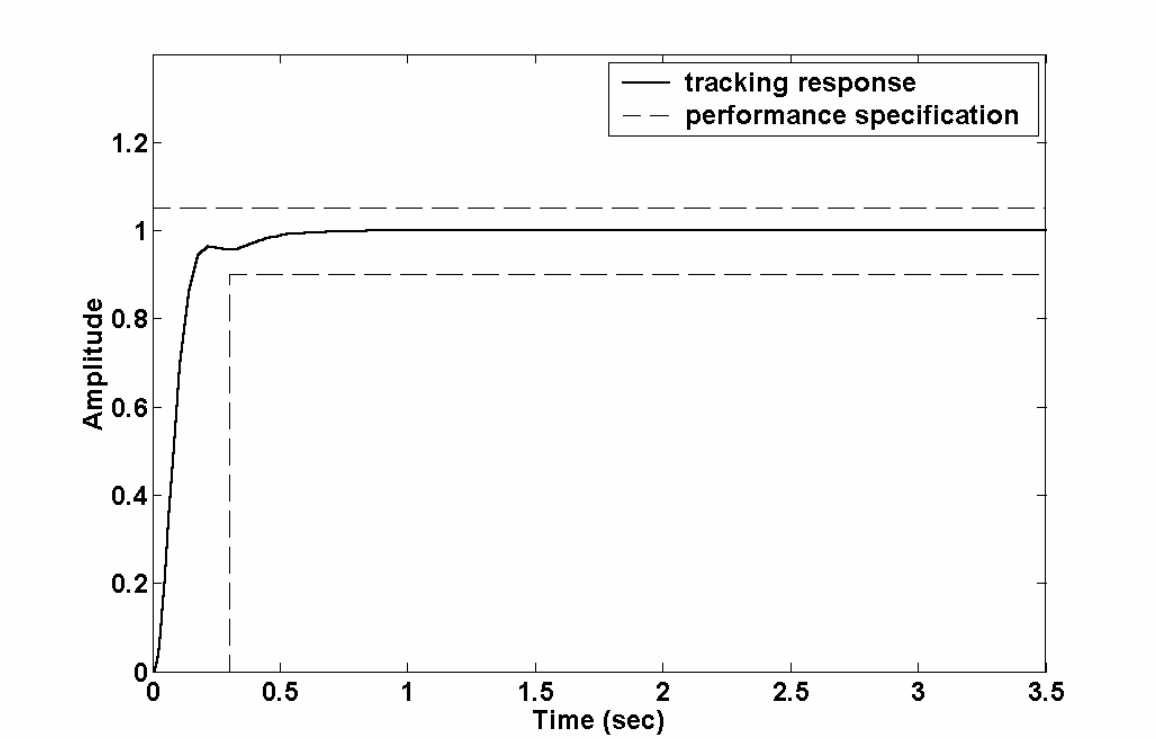

Figure 5: Tracking response to a unit step input of the inverse-based controller, K_1, defined in Equation (15).

defined in Equation (15) is shown in Figure 6. The controller has sluggish disturbance rejection characteristics and fails to meet the disturbance rejection specifications, as the output is about 0.75 at a time of 3 seconds instead of the specified 0.1.

The failure of the first controller to meet design specifications led to the design of a disturbance controller based on loop-shaping design methods. Unlike the tracking example above where the desired form of K was specified in Equation (14), the desired form of a disturbance controller is of the form shown in Equation (16).

$$|K| = \left|\frac{s+\omega_I}{s}\right| \left|G^{-1}G_d\right| \qquad (16)$$

First we will approximate the $|G^{-1}G_d|$ term. Neglecting high frequency dynamics $|G^{-1}G_d|$ is approximately 0.5. Second, we will specify ω_I. The frequency up to which integration is effective is determined by ω_I. For low frequency performance we wish ω_I to be large, yet to maintain an acceptable phase margin we want $\omega_I < \omega_C$. It was deemed that $\omega_I = 0.2\omega_C = 2$ rad/s would be appropriate. This led to the following controller

$$K_2 = 0.5\frac{s+2}{s} \qquad (17)$$

Simulation showed this controller to be more oscillatory than desired, so derivative action was introduced to improve the systems phase margin and transient response. This was achieved by multiplying the controller by a lead-lag term, which is effective over one decade and begins at 20 rad/s. The final form of the controller is shown in Equation (18)

.

$$K_3 = 0.5\frac{s+2}{s}\frac{0.05s+1}{0.005s+1} \qquad (18)$$

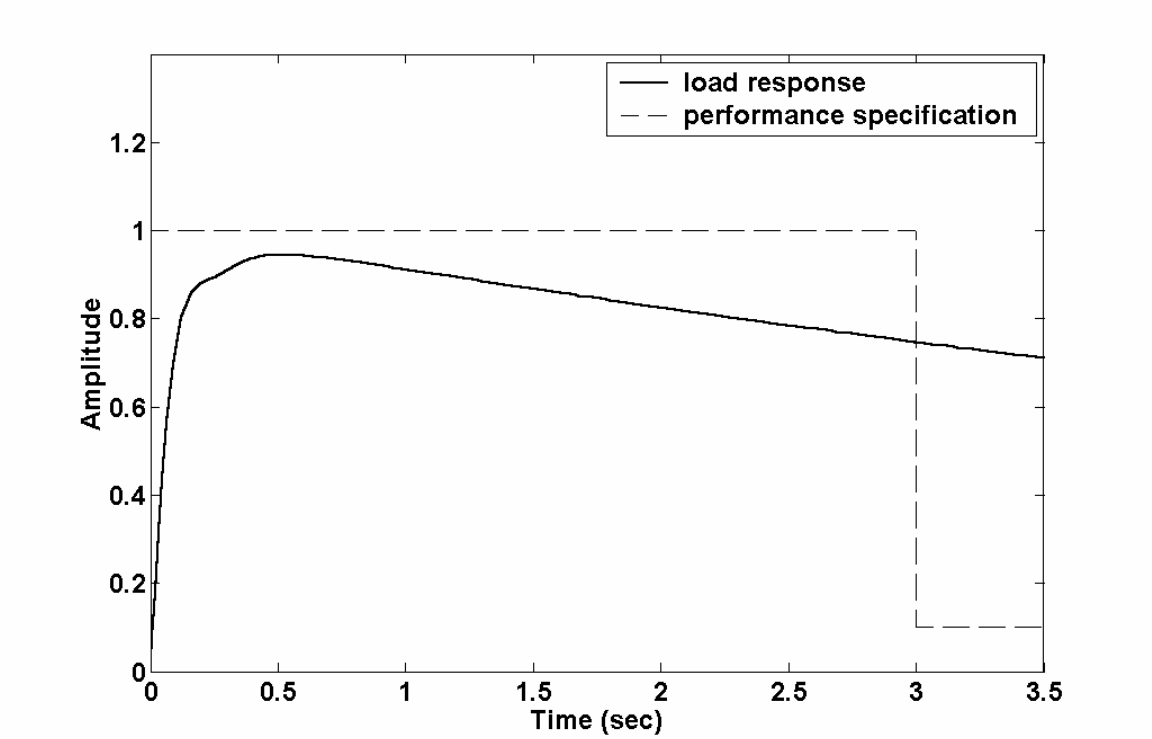

Figure 6: Disturbance response to a unit step input of the inverse-based controller, K_1, defined in Equation (15).

Figure 7 shows the controller K_3 satisfies disturbance rejection criteria. However, Figure 8 shows the tracking performance of K_3 is not satisfactory. The tracking response has an overshoot of 24%, which is well outside the maximum allowed tolerance of 5%.

Since neither controller is sufficient by its self, a TDoF controller was sought. Since the controller K_3 exhibited the best disturbance response characteristics, it will be used as the feedback controller for the process, and a prefilter will be designed to enhance its tracking performance. Skogestad and Postlewaite[9] decided to make a lag-lead prefilter, K_r for this particular problem. The general principle behind lag-lead design is to find a low order approximation of an inverse model prefilter. This is generally accomplished in one of two ways.

1. Solving for an inverse model prefilter directly using Equation (8) and approximating it if possible with a lower order model
2. Finding a low order approximation of $\left(\frac{K_3 G_P^*}{1+K_3 G_P^*}\right)^{-1}$ directly then specifying a reference trajectory and solving for the prefilter.

The later of these design techniques was chosen so the prefilter was designed around an approximation of the inverse model. From a step response test, they approximated $(K_3 G_P)/(1+K_3 G_P)$ by the sum of two transfer functions:

$$\frac{1.5}{0.1s+1}-\frac{0.5}{0.5s+1}=\frac{0.7s+1}{(0.1s+1)(0.5s+1)} \qquad (19)$$

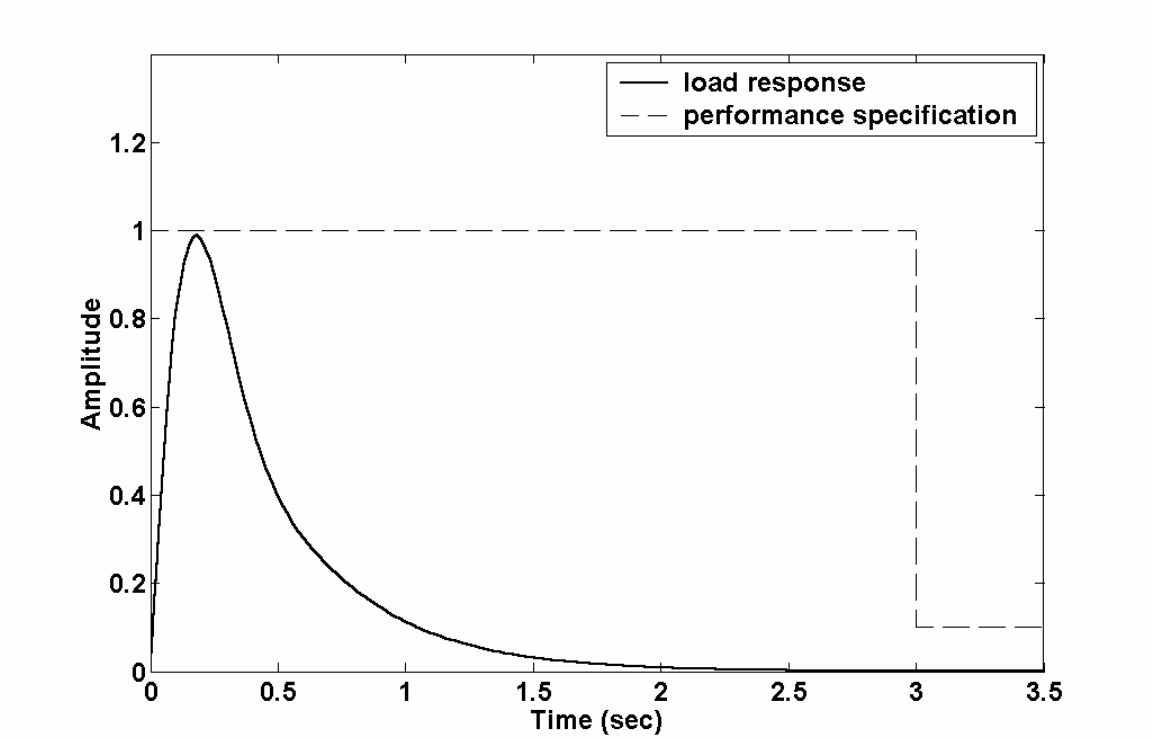

Figure 7: Disturbance response to a unit step input of the inverse-based controller, K_3, defined in Equation (18).

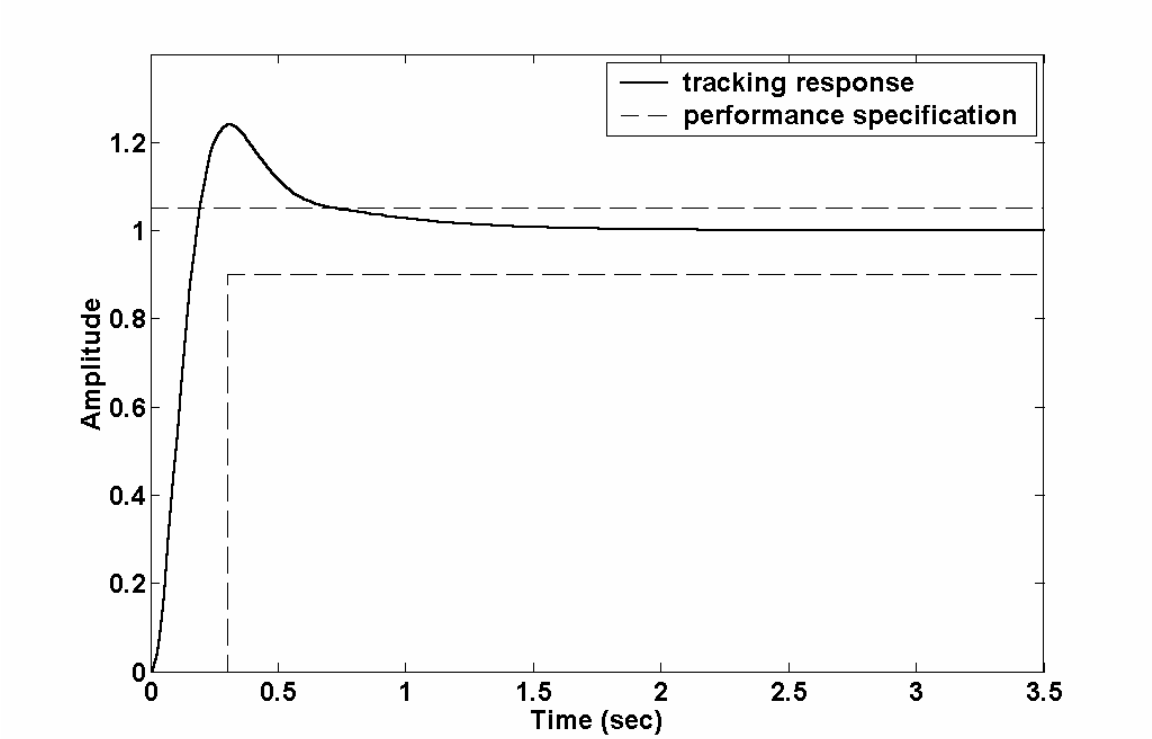

Figure 8: Tracking response to a unit step input of the inverse-based controller, K_3, defined in Equation (18).

A reference trajectory was then chosen, $\left(\frac{y}{r}\right)_{Ref} = \frac{1}{0.1s+1}$. This provides a first-order response with no overshoot. The resulting prefilter for the TDoF controller is

$$K_r = \frac{0.5s+1}{0.7s+1} \tag{20}$$

This controller was then slightly modified to prevent the control signal from exceeding 1, such that the final form of the prefilter is given as

$$K_r = \frac{0.5s+1}{(0.65s+1)(0.03s+1)} \tag{21}$$

Figure 9 details how the feedback controller K3 and the prefilter Kr are implemented.

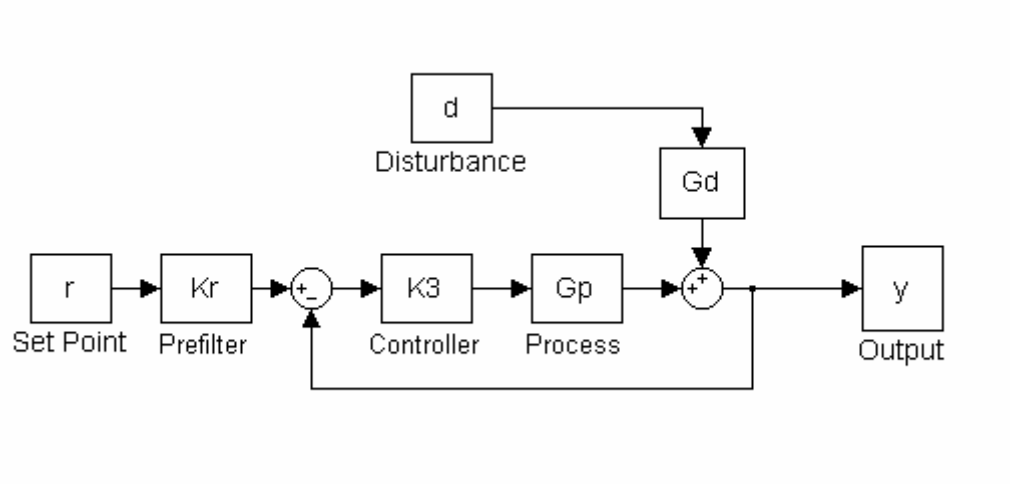

Figure 9: Diagram specifying the implementation of the TDoF controller utilizing controller K_3 from Equation (18) and the prefilter K_r from Equation (21).

The nominal response for the TDoF controller to a unit step change in the setpoint is shown in Figure 10. The response is not as desirable as the one obtained from the ODoF controller specifically designed for tracking responses (Equation (15)), but meets

all the design specifications nonetheless. The response has a rise time of approximately 0.25s and exhibits an overshoot slightly greater then 2%.

The nominal response for the TDoF controller to a unit step change in the disturbance is shown in Figure 11. As we would expect, this response is the same one generated from the ODoF controller specified in Equation (18), since disturbance responses are independent from prefilter dynamics.

Summary

The TDoF controller was able to satisfy all design criteria, yet the design expressed a heavy reliance on the inverse process model. This dependence complicates prefilter design for non-minimum phase systems, which are systems that have time delays or Right Hand Plane zeros. Additionally it should be noted that the tracking performance of the TDoF controller was less desirable than the response of the ODoF controller specifically designed for servo tracking. This result stems directly from the fact that the prefilter is unable to change the location of poles in the characteristic Equation defined by the regulatory controller, but is only able to add additional poles to change process dynamics.

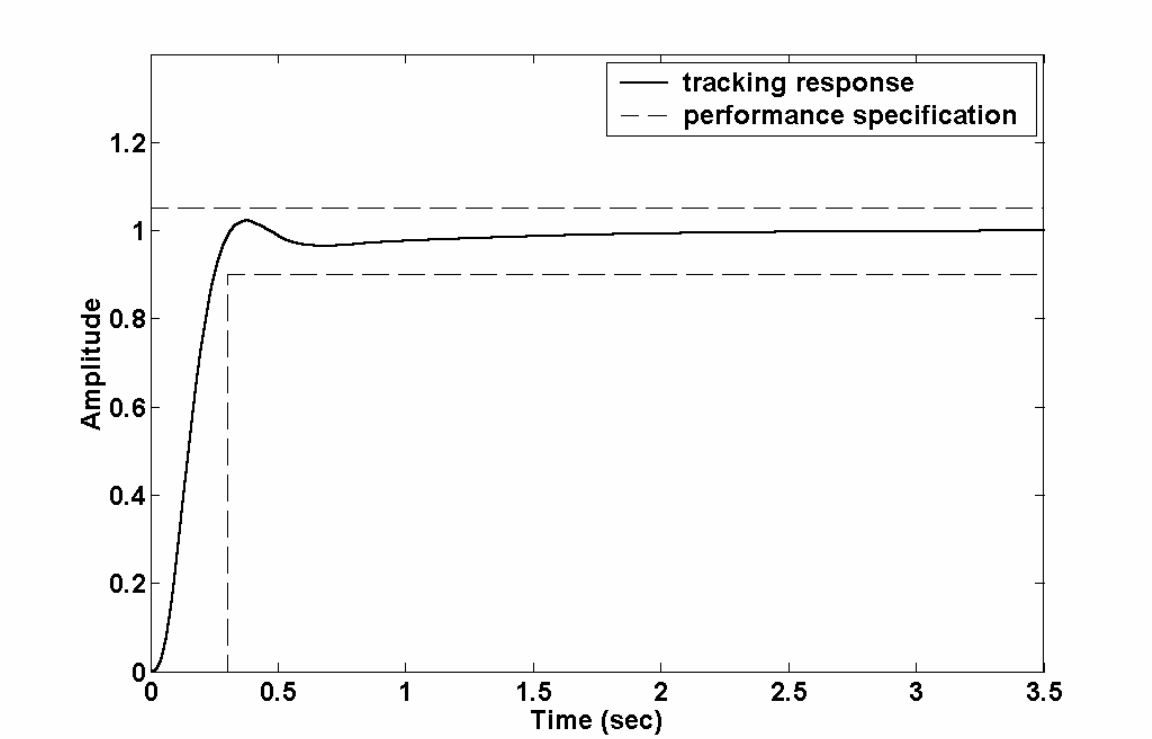

Figure 10: Tracking response to a unit step input of the TDoF controller shown in Figure 9.

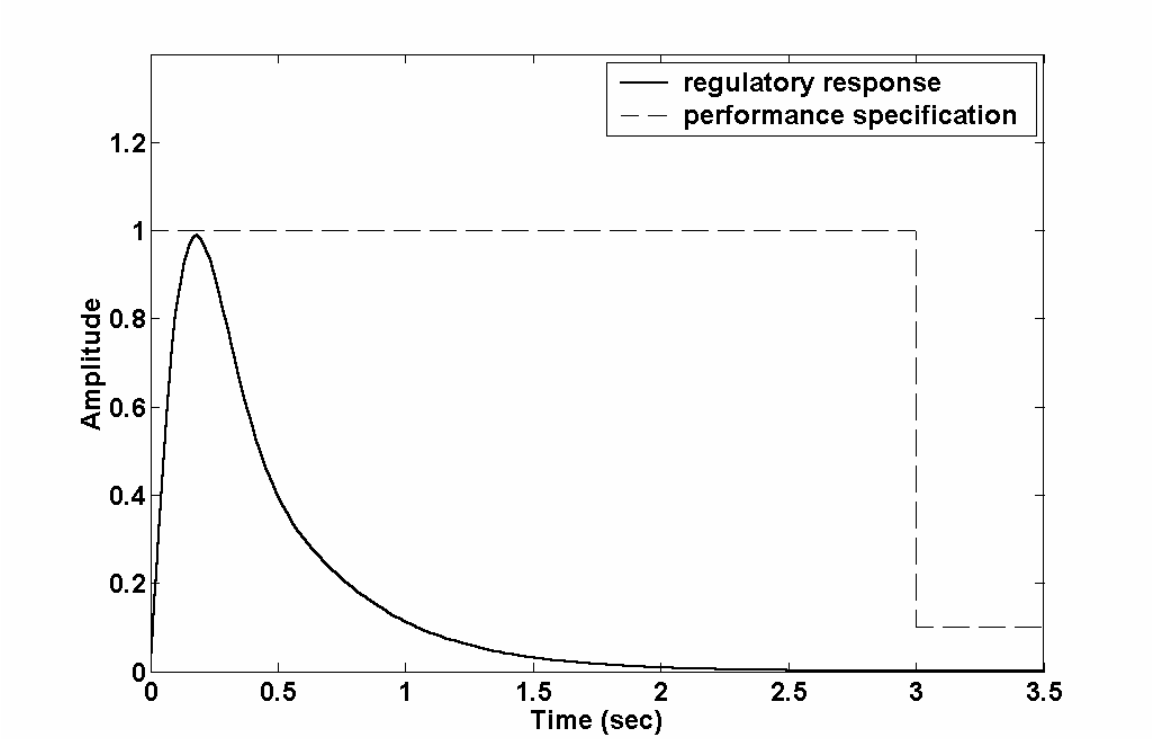

Figure 11: Disturbance response to a unit step input of the TDoF controller shown in Figure 9

CHAPTER III

THEORY OF PARTITIONED ERROR CONTROL

Partitioned Error Control

A TDoF control system in which the controllers can be independently designed would be desirable. The controllers should be capable of distinguishing between set-point changes and load disturbances. Debelak and Rutherford[10] proposed the following control structure (see Figure 12) to meet these criteria. This control structure includes the nominal process model, G_{nom}, and two controllers, K_1 and K_2, which can be independently tuned to handle both setpoint changes and load disturbances. This configuration is called Partitioned Error Control (PEC), because instead of using an error signal based on a measured output, $[r - y_m]$, as an input to a single controller, the PEC structure utilizes a process model to generate a nominal output, y', which is used to separate tracking considerations based on the following equation:

$$u = \begin{bmatrix} K_1 & K_2 \end{bmatrix} \begin{bmatrix} r - y' \\ y' - y_m \end{bmatrix} \tag{22}$$

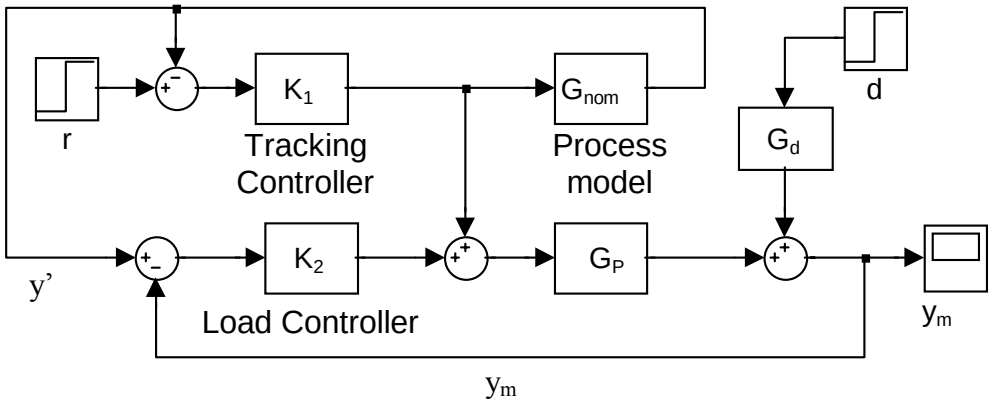

Figure 12: Partitioned Error Control structure

Partitioned error control belongs to the family of model-based controllers, which includes direct synthesis control, internal model control, and generic model control. It is also a two-degrees-of-freedom controller. The closed-loop transfer function for this system is given by

$$y = \left[\frac{K_2 G_P}{1 + K_2 G_P} + \frac{(K_1 - K_2) G_P}{(1 + K_2 G_P)(1 + K_1 G_{nom})} \right] (r) + \frac{G_d}{1 + K_2 G_P} (d) \qquad (23)$$

For the nominal case, i.e., $G_P = G_{nom}$, the closed-loop transfer function reduces to:

$$y = \frac{K_1 G_P}{1 + K_1 G_P} (r) + \frac{G_d}{1 + K_2 G_P} (d) \qquad (24)$$

The characteristic equation for each response is only dependent on the controller designed specifically for that response. This is one of the fundamental differences between PEC and traditional TDoF methods. Thus, the two controllers can be tuned independently for set-point changes and load disturbances. The tuning process is also made significantly easier, because both controllers can be designed using classic feedback design procedures, making PEC more intuitive than other TDoF controllers.

If $K_2 = K_1$, then the closed-loop transfer function reduces to

$$y = \frac{K_2 G_P}{1 + K_2 G_P}(r) + \frac{G_d}{1 + K_2 G_P}(d) \qquad (25)$$

The system behaves like an ordinary feedback system regardless of the model used.

Lets reconsider the system defined in Equation (5). Table 1 gives the PI controller settings according to the tuning rules put forth by Lopez, Murrill et al. [7], and Rovira, Murrill et al. [8], the Zielger-Nichols (ZN) settings, and the TLC("tender loving care") settings of Tyreus and Luyben[11] for this process. The closed-loop setpoint and load responses of these controllers are given in Figure 13 and Figure 14. Obviously, choosing the Murrill controllers to place in the PEC system would result in the best nominal response for both servo and regulatory problems.

Now let us compare the PEC design utilizing the Murrill set-point tunings defined in Table 1 with the conventional inverse-model TDoF controller, which uses the prefilter defined in Equation (11) using a λ of 3.5. Figure 15 shows the conventional inverse model based prefilter provides slightly improved performance for this simple system. Yet, PEC is capable of utilizing many design techniques; so in fact, the prefilter is being compared to the Murrill tunings for set point changes, not the PEC structure in general. This comparison to a specific design technique does not give full understanding of PEC. As such, it is helpful to examine how PEC utilizes other design techniques.

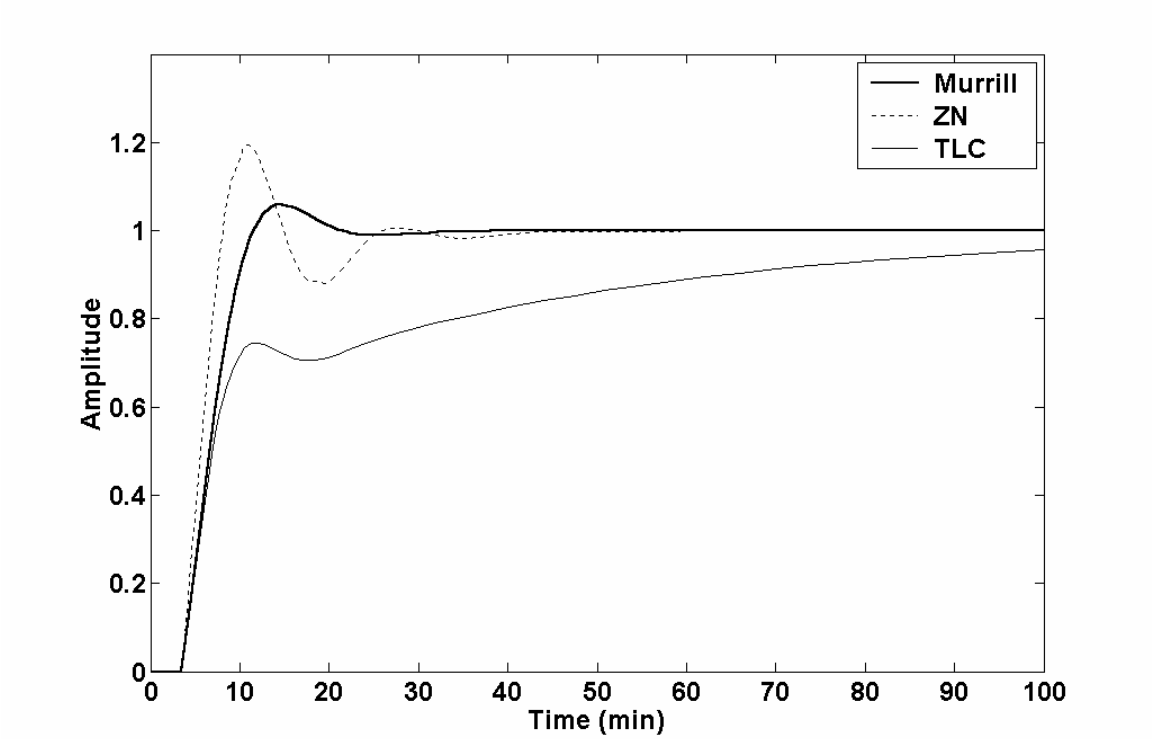

Figure 13: The set point step response of the Murrill set-point controller, the Zielger-Nichols controller, and the TLC settings of Tyreus and Luyben[11] in a one degree-of-freedom structure

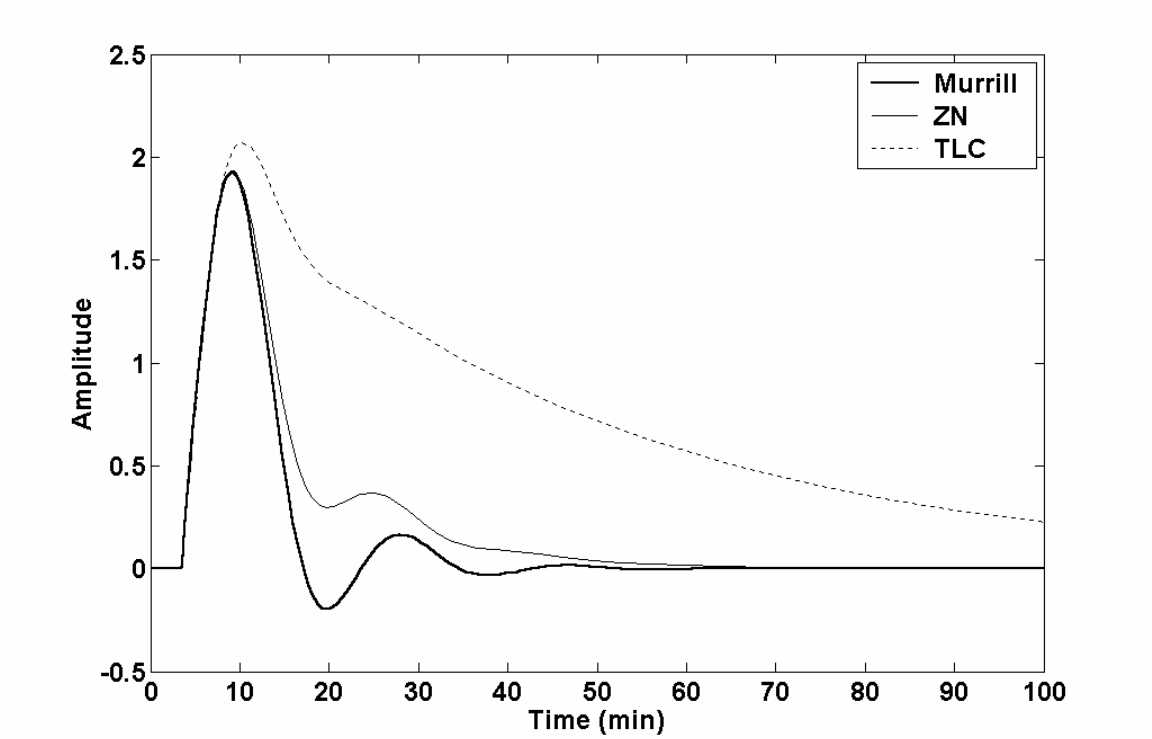

Figure 14: The disturbance response of the Murrill load controller, the Zielger-Nichols controller, and the TLC settings of Tyreus and Luyben[11] in a one degree-of-freedom structure

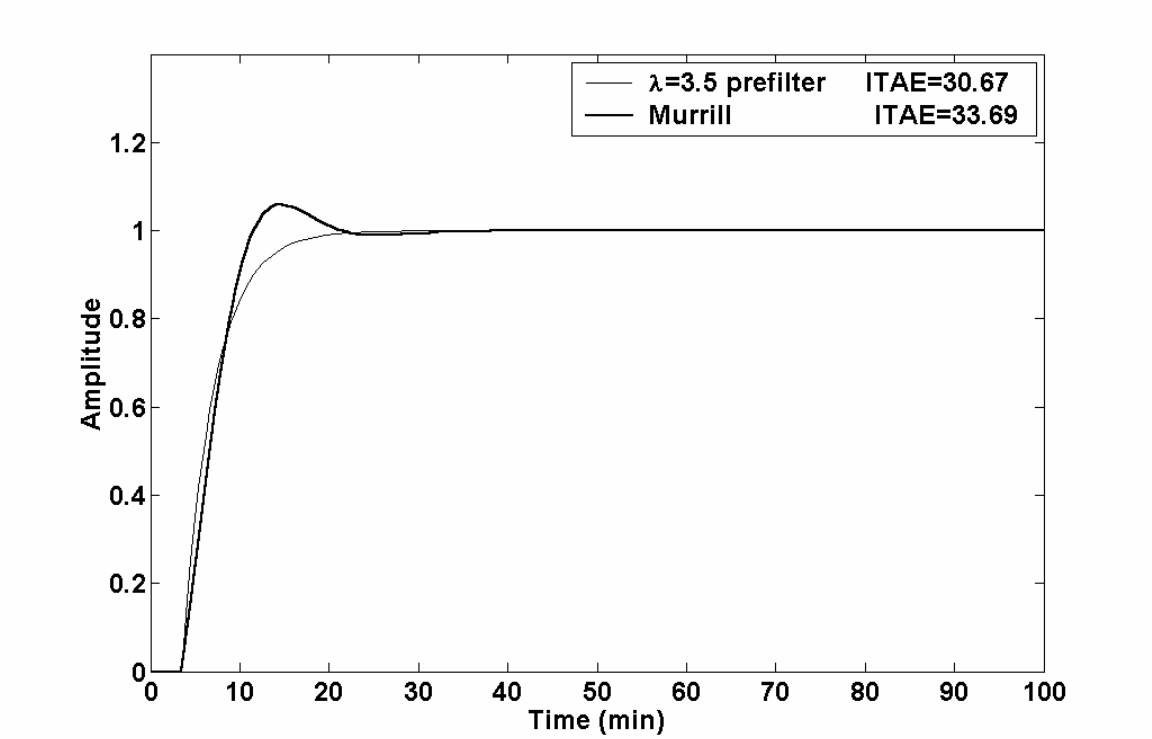

Figure 15: Nominal step response comparison of PEC using Murrill tunings and an inverse based prefilter.

We will now reexamining the process defined in Equation (13). A comparison will be made between the lead-lag prefilter design from chapter 2 and PEC. Recall that the lead-lag prefilter design utilized the feedback controller from Equation (18) and the prefilter from Equation (21). The block diagram of the implementation of the controller and prefilter can be seen in Figure 9. The PEC system will also utilize the feedback controller in Equation (18). Instead of using a prefilter, PEC will make use of the tracking controller from Equation (15) and a process model from Equation (13). Because we are using Equation (13) as our model, PEC will be operating with a perfect model $G_{nom} = G_P$. The block diagram of the implementation of these controllers can be seen in Figure 12. Since it has already been shown that the tracking controller meets the tracking objective, and the feedback controller meets regulatory objectives, Equation (24) ensures that under nominal conditions the PEC system will meet both tracking and regulatory objectives.

The nominal response to a unit step change in the reference of the prefilter and PEC systems is presented in Figure 16. The Integral of the Time weighted Absolute value of the Error (ITAE) for the step response of the PEC system, 0.009, is much smaller than that for the prefilter design, 0.056. It reaches the setpoint more quickly and is less oscillatory.

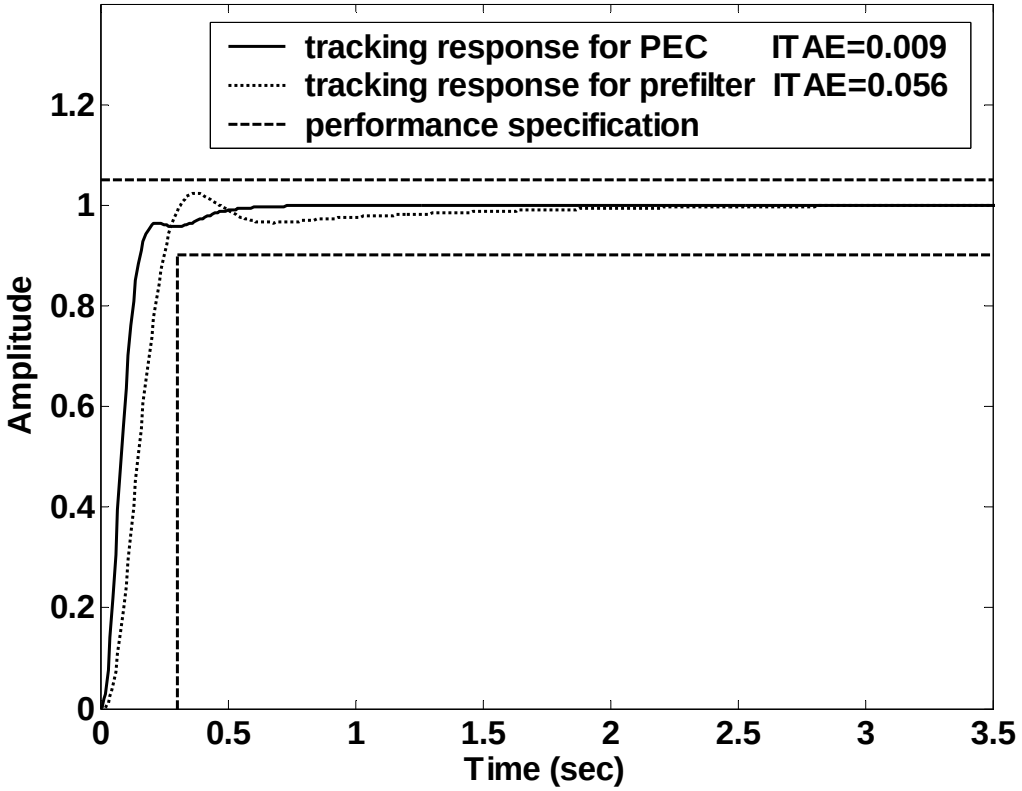

Figure 16: Tracking response to a unit step change of PEC and the prefilter for the system defined in Equation (13).

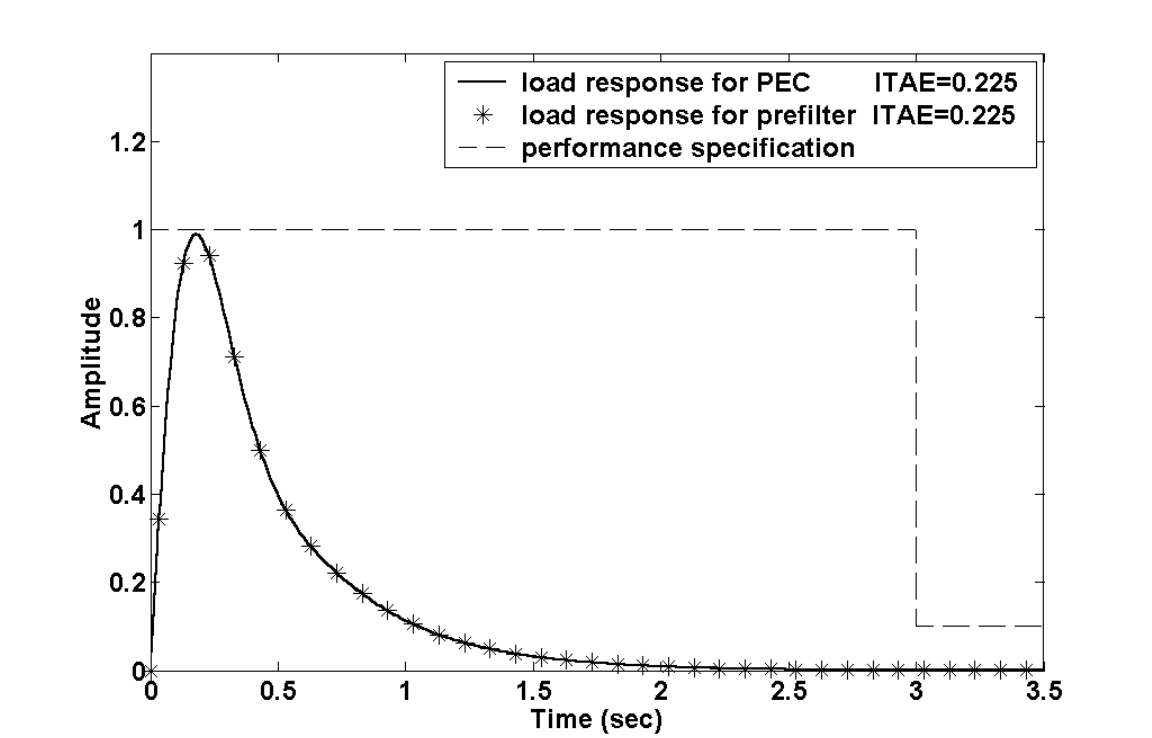

Figure 17: Regulatory response to a unit step change of PEC and the prefilter for the system defined in Equation (13).

The nominal response to a unit step change in the disturbance of the prefilter and PEC systems is presented in Figure 17. The load responses for the prefilter design and the PEC design are identical as expected since they both use the same controller to regulate disturbances. Neither the prefilter, nor the partitioning loop in the PEC structure have any influence on the dynamics of the system when there is no change in the reference signal, as is the case when examining a disturbance response.

Both controllers possess a second degree of freedom, yet this example shows that limitations imposed by design techniques can hinder the ability of a designer to take advantage of that second degree of freedom. The prefilter design in this example had to make an approximation to obtain a proper design, due to an excessive number of poles with respect to zeros in the process model, which made the inverse process improper. This approximation had a direct, all be it small, impact on the performance of the system in two ways. First, modeling error was generated in order to approximate an inverse process model. All models have modeling error, but the more approximations we make the more this problem is exacerbated. Second, the control laws, and thus the designers ability to manipulate the system, suffer from all approximations. Examine the poles of the prefilter system under the perfect model assumption. The poles of the regulatory response are located at (-201.09, -20.00, -8.24 ± 9.45i, -2.53). The poles of the servo response for the prefilter system are (-201.09, -33.33, -20.00, -8.24 ± 9.45i, -2.53, -1.54). Without using a perfect inverse model the prefilter can not manipulate the location of the poles of the servo response. It can only add additional poles. This is in sharp contrast to PEC which has the same poles as the prefilter system for its regulatory response at (-201.09, -20.00, -8.24 ± 9.45i, -2.53), but the poles of the servo response under nominal

conditions are located at (-105.01,-0.13.86 ± 18.22i, -7.27, -0.10). The PEC servo response has a totally independent set of poles from the regulatory response. This is the freedom that designers are able to take advantage of through the use of the PEC system, and this is the reason PEC can be used to achieve better tracking performance than inverse model based prefilters, even though both systems are two-degree-of-freedom systems an under ideal conditions both systems should be able to manipulate the second degree of freedom equally well.

Not only has PEC provided a superior TDoF controller in this case, but it has also done so with less design effort. In the original design procedure by Skogestad and Postlewaite[9], ODoF controllers were pursued first. Of the two controllers that were designed under this procedure only the design work done for the regulatory controller was used to design the TDoF prefilter system. However, PEC did not require any additional design effort beyond that done for the ODoF controllers. PEC was able to successfully incorporate both designs to give superior performance with reduced design effort in this case.

PEC would also be more applicable to processes that exhibit an inverse response or a response with difficult dynamics. For such processes it is either difficult to discern a good reference trajectory or system dynamics make process inversion impossible. For such processes, it is easier to design a good controller, by following deterministic feedback loop design procedures, than it is to specify and implement a more arbitrary reference trajectory, thus giving PEC an advantage over prefilter designs.

Model Mismatch

In all model-based systems the question of process model mismatch arises. How does PEC handle plant model mismatch? There are two parts to this answer; one is trivial, while the other is more complex. First, the trivial answer explains how PEC handles modeling error in the presence of a disturbance. The feedback controller, K_2, solely handles modeling error propagated by disturbances. Thus the analysis of modeling error can directly apply current feedback control theory, which includes determining stability margins by use of pole locations for a set of perturbed plants. This is readily apparent, because the characteristic equation of the disturbance response involves only the load controller, K_2, and the process transfer function, G_P (eq 26).

$$y = \frac{G_d}{1 + K_2 G_P}(d) \qquad (26)$$

This is true for both PEC and the conventional inverse model prefilter, thus we know for certain that PEC processes disturbances in the presence of modeling error in the exact same way prefilter systems do. Therefore we can neglect the trivial case where modeling error is propagated by disturbance responses since we have a good understanding from existing theory of how the single feedback controller handles error.

The second answer to how PEC handles modeling error is more complex, because control of setpoint changes involves both the partitioning and feedback loops, as indicated in Equation (23), when modeling error is present. The stability of the PEC system for tracking problems is determined by the characteristic equation defined in Equation (27), which was obtained through simple rearrangement of Equation (23):

$$y = \frac{K_1 G_P (1 + K_2 G_{nom})}{(1 + K_2 G_P)(1 + K_1 G_{nom})} r \qquad (27)$$

The characteristic equation includes the tracking controller(K_1), the load controller(K_2), the actual process(G_P), and the process model(G_{nom}). One way to estimate the effect of process model mismatch is to plot the closed-loop frequency diagram for the conventional control structure and for the PEC structure for different errors in the estimates of the process gain, time constant, and time delay. As the process approaches its limit of stability, the maximum closed-loop log modulus will approach infinity. Essentially, as the maximum closed-loop log modulus approaches infinity, the process is approaching the point (-1,0) of a Nyquist plot. After the limit of stability is reached the system is unstable. The maximum closed-loop modulus ceases to have significant meaning and can actually begin to decrease. This occurs because the maximum log modulus is an indication of how close a system is to the point (-1,0) on the Nyquist plot, though it does not indicate which direction we are approaching it from.

A ODoF feedback controller was constructed using the setpoint tunings suggested by Murrill from Table 1 for the process defined in Equation (5). Figure 18 is a closed-loop frequency plot of that system for errors in the process gain of 0%, 10%, 25%, and 40%. The Maximum closed loop modulus increases as the error in the process gain increases, characteristic of an increasingly oscillatory response. The process does not reach its limit of stability until the error in the process gain reaches about 63%.

Although simulations showed this controller provides satisfactory tracking for gain estimation error of up to at least 40% in the gain, we must remember that it does not provide satisfactory disturbance regulation even for the nominal process.

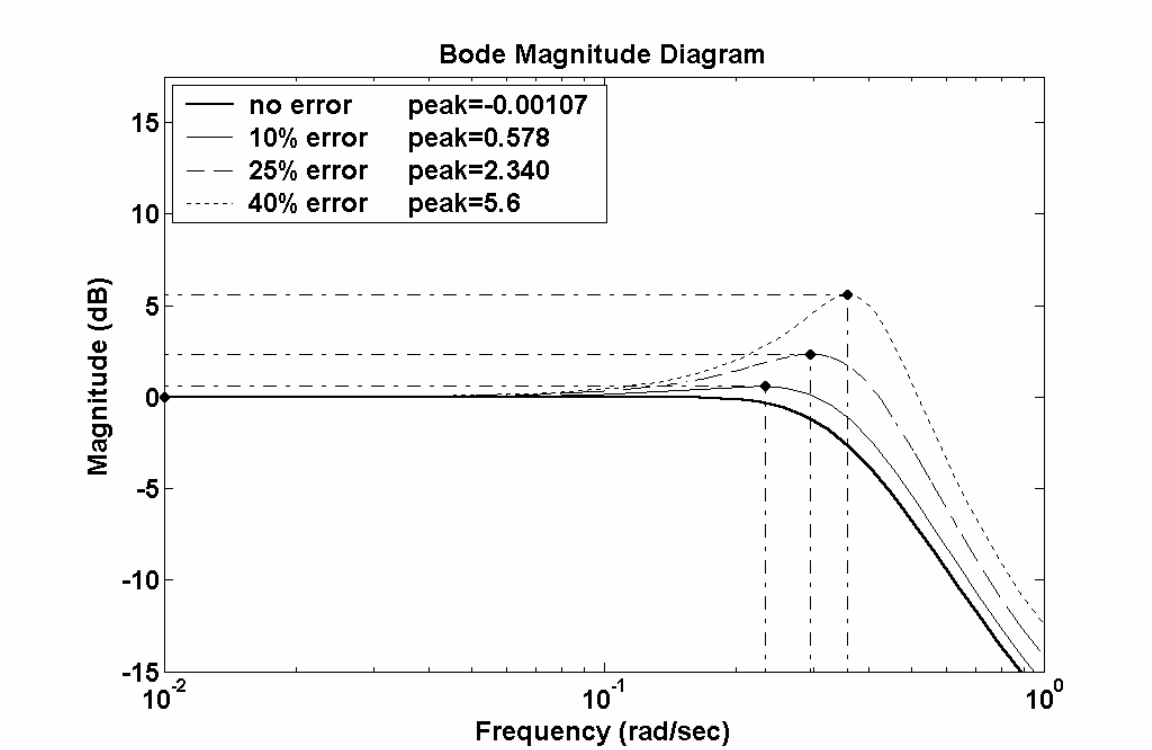

Figure 18: Frequency response for the process described by Equation (5) of a Murrill set-point controller in a ODoF setting for gain estimation errors of 0%, 10%, 25%, and 40%.

Similarly Figure 19 shows the closed-loop frequency plot for the conventional ODoF control structure using the load settings suggested by Murrill from Table 1. It is evident from this figure that the oscillations found in the nominal response are quickly magnified by moderate amounts of modeling error. This is expected, because we are viewing the response of a controller we tuned specifically for a regulatory objective to a sinusoidal tracking input.

Figure 20 shows the closed-loop frequency plot for the PEC structure with the same errors in the estimate of the process gain. Murrill's set point tunings are used for the controller in the partitioning loop, while Murrill's load tunings are used for the controller in the feedback loop. For no error in the estimate of the gain, the closed-loop frequency response of the Murrill set-point controller (Figure 18) is identical to the response of the PEC system (Figure 20) as expected. However, as modeling error is introduced the response of the PEC system begins to look less like the response of the Murrill set-point controller, and more like the response of the Murrill load controller. This occurs because the load controller provides the only mechanism for handling modeling error in the PEC system. The controller in the partitioning loop does not receive feedback from the process. As such, when the relative amounts of modeling error compared to tracking error becomes significant, the load controller has a noticeable impact on process dynamics.

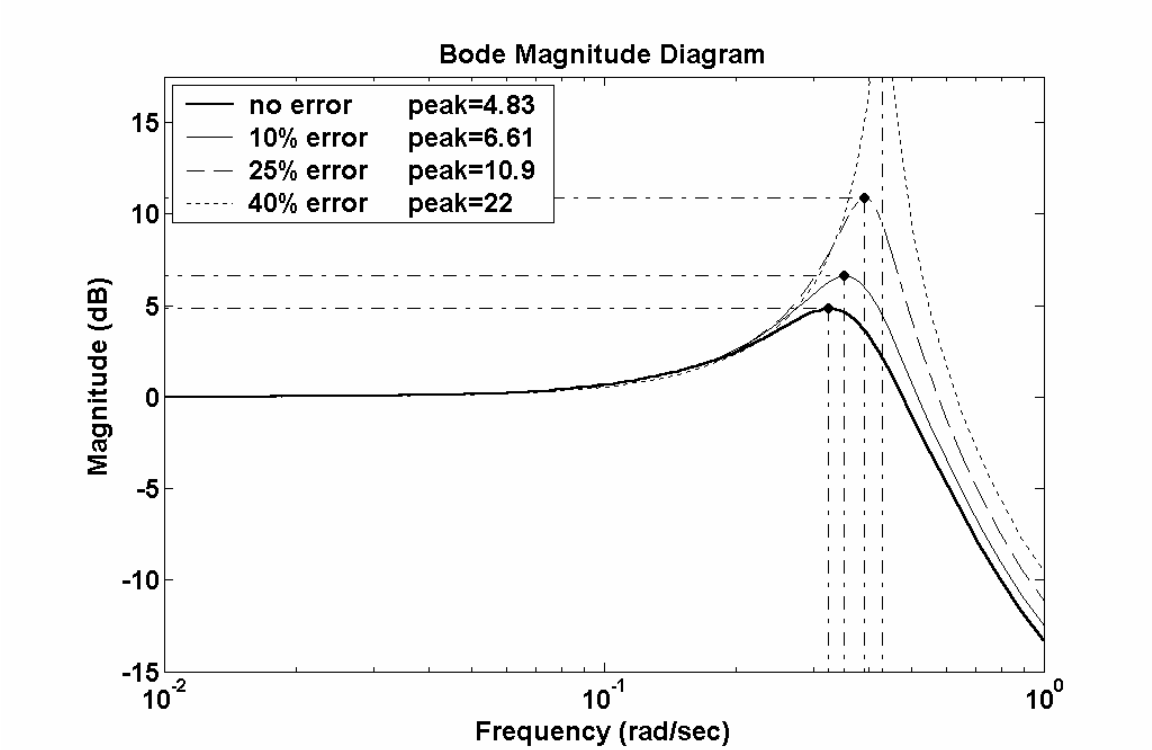

Figure 19: Frequency response for the process described by Equation (5) of a Murrill load controller in a ODoF setting for gain estimation errors of 0%, 10%, 25%, and 40%.

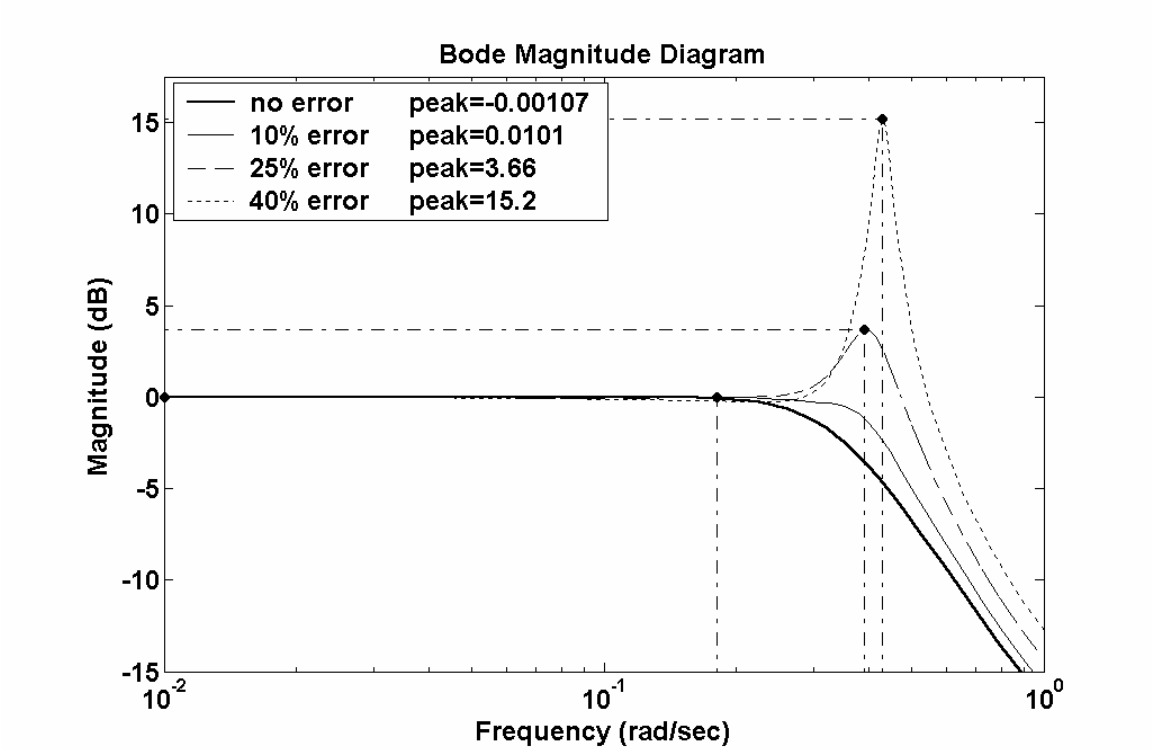

Figure 20: Frequency response for the process described by Equation (5) of the PEC system utilizing a Murrill set-point controller in the partitioning loop and a Murrill load controller in the feedback loop for gain estimation errors of 0%, 10%, 25%, and 40%.

For very poor models, where the modeling error exceeds tracking error, the response of the PEC system becomes dominated by the load controller. In this particular case, the controller tunings chosen for the load controller, the Murrill load settings, have a significant oscillation for tracking even at the nominal level. Better choices for the load controller can improve the response of the PEC significantly as will be shown in the following chapter. Similar plots could be made for errors in the estimates of the time constant and dead time, showing similar results with varying degrees of severity. Like all model based control systems modeling error is particularly sensitive to the inaccuracies in the estimation of dead times. This sensitivity will be addressed in a case study of a binary distillation column in a later chapter.

Activity from the feedback controller

If you look at the outputs from both controllers in the PEC configuration for a setpoint change, you will find that when $G_{nom} = G_P$, the output from controller K_2 is zero. As the mismatch between G_{nom} and G_P increases, the output from controller K_2 increases. The control action becomes the sum of the outputs from controllers K_1 and K_2. The transfer function from a reference signal, r, to the output of the controller K_2, m, is given by the following equation:

$$\frac{m}{r} = \frac{K_1 K_2 (G_{nom} - G_P)}{(1 + K_2 G_P)(1 + K_1 G_{nom})} \qquad (28)$$

If $G_{nom} = G_P$, then the output from controller K2 will be equal to zero, for any input r. The output from controller K_2 can be monitored during setpoint changes. If K_2's output deviates from zero, it is an indication of plant model mismatch, i.e., $G_{nom} \neq G_P$. The

deviation of K_2's output from zero can be used as an indicator by an adaptive controller, e.g., Foxboro's Exact and Control Soft's Intune, of when to update the model. This feature of the PEC structure could be easily incorporated into an adaptive controller. Astrom and Wittenmark[12] have established techniques for identifying models, which can be used by an adaptive controller. Adjustments of the model parameters in G_{nom} can be made through a series of on-line setpoint tests until the output from controller K_2 is zero.

Noise effects

Noise in process control can arise from the measuring devices, the surroundings, or the process. How does PEC compare with a conventional controller in a noisy environment? To compare the effect of noise on PEC and a conventional controller, band-limited white noise was included in the feedback signal to the controller. The primary difference between band-limited white noise and white noise is that the band-limited white noise produces output at a specific sample rate, which is related to the correlation time of the noise. Theoretically, continuous white noise has a correlation time of 0, a flat power spectral density (PSD), and a covariance of infinity. In practice, physical systems are never disturbed by white noise, although white noise is a useful theoretical approximation when the noise disturbance has a correlation time that is very small relative to the natural bandwidth of the system.

Figure 21 thru Figure 23 compare setpoint changes for the process described by Equation (5) for PEC using the tracking and regulatory tunings of Murrill specified in Table 1, with a control system using an inverse prefilter from Equation (10) with λ=7 and PI controller utilizing ZN tunings for different levels of error in the estimate of the

process gain. The noise power and sampling time for the band-limited white noise are set at 0.005 and 0.1 minutes, respectively. Nominal responses without noise are included in the plots.

With 0% error in the estimate of the gain, i.e. $G_P=G_{nom}$, PEC performs better than the prefilter with ZN tunings, both with respect to ITAE and rise time (Figure 21). This is expected since the step response of the PEC system without noise has better performance characteristics then the prefilter system.

With a 10% error in the estimate of the process gain, PEC still performs better than the prefilter with ZN tunings (Figure 22). Again this is expected since PEC exhibits better performance characteristics then the prefilter with 10% error in the gain.

However, as the error in the estimate of the gain increases to 40%, the performance of the PEC deteriorates below that of the prefilter with ZN tunings (Figure 23). Again this coincides with our expectations of the system. PEC has a significantly more aggressive nominal tracking response, and we would expect aggressive control in the presents of modeling error to lead to aggressive overshoot with the perturbations we are simulating in the gain. Similar results are also found when comparing the prefilter design with the PEC design for the process defined in Equation (13).

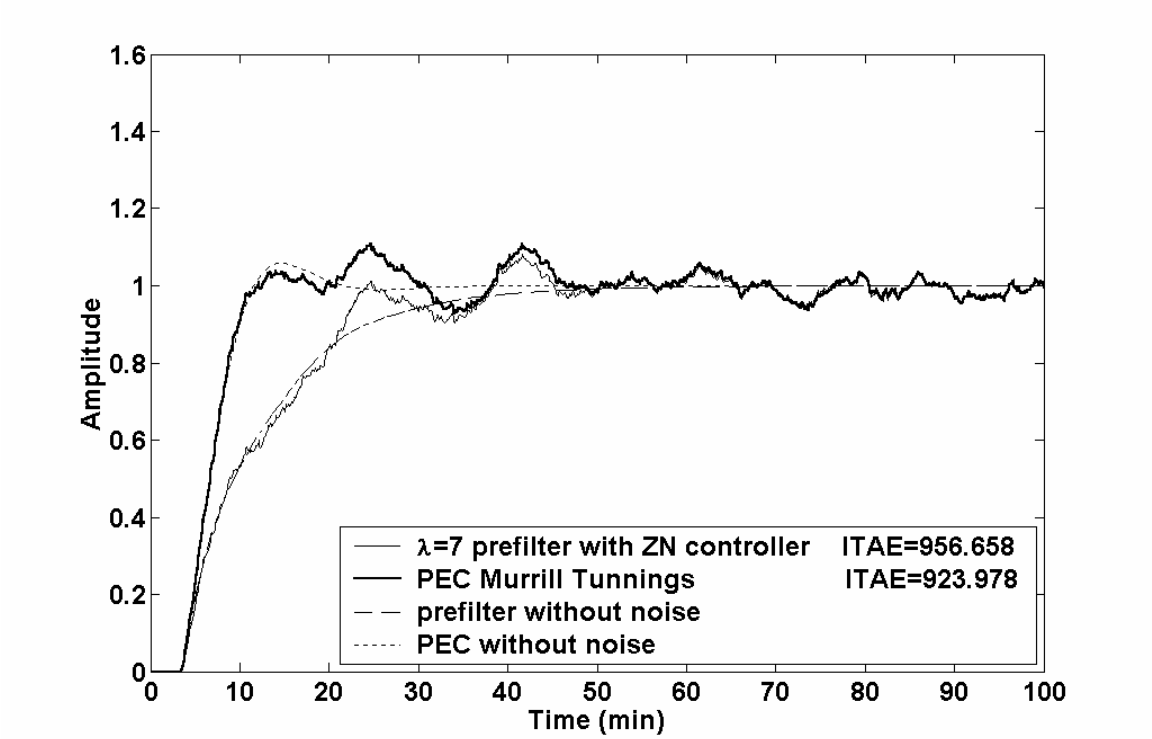

Figure 21: Step response of PEC using Murrill tunings, and a prefilter design using Zielger-Nichols under the influence of white noise.

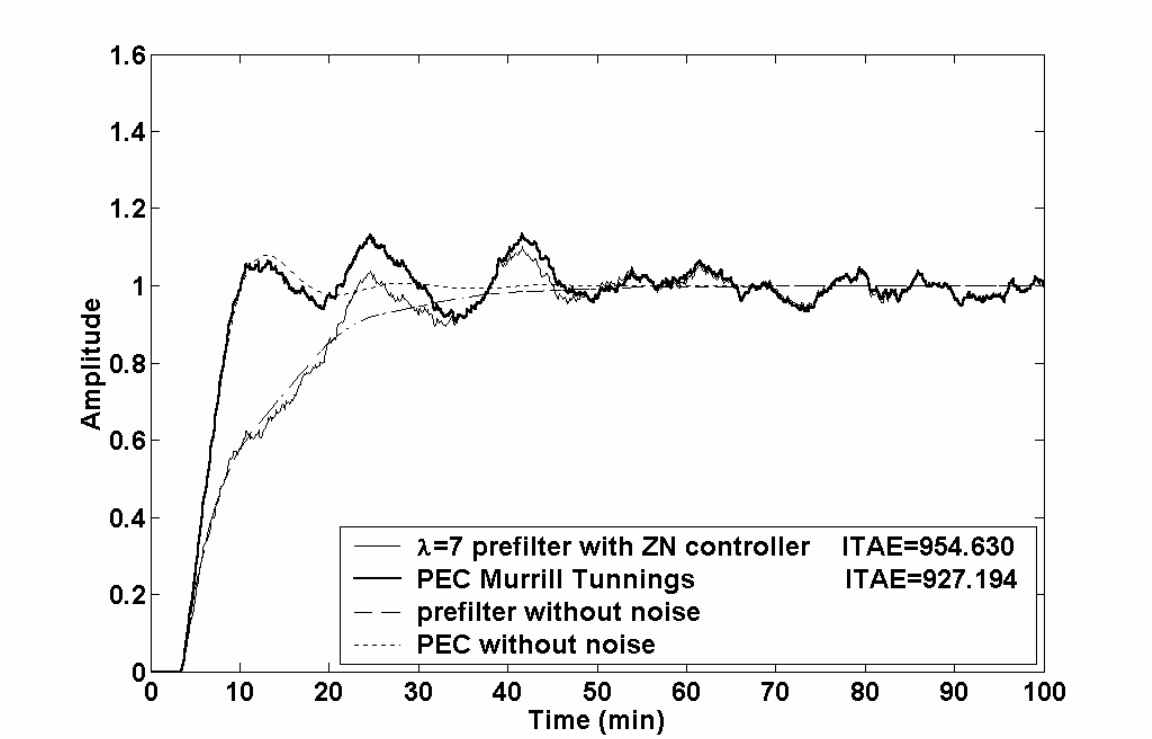

Figure 22: Step response of PEC using Murrill tunings, and a prefilter design using Zielger-Nichols under the influence of white noise and 10% error in process gain estimation.

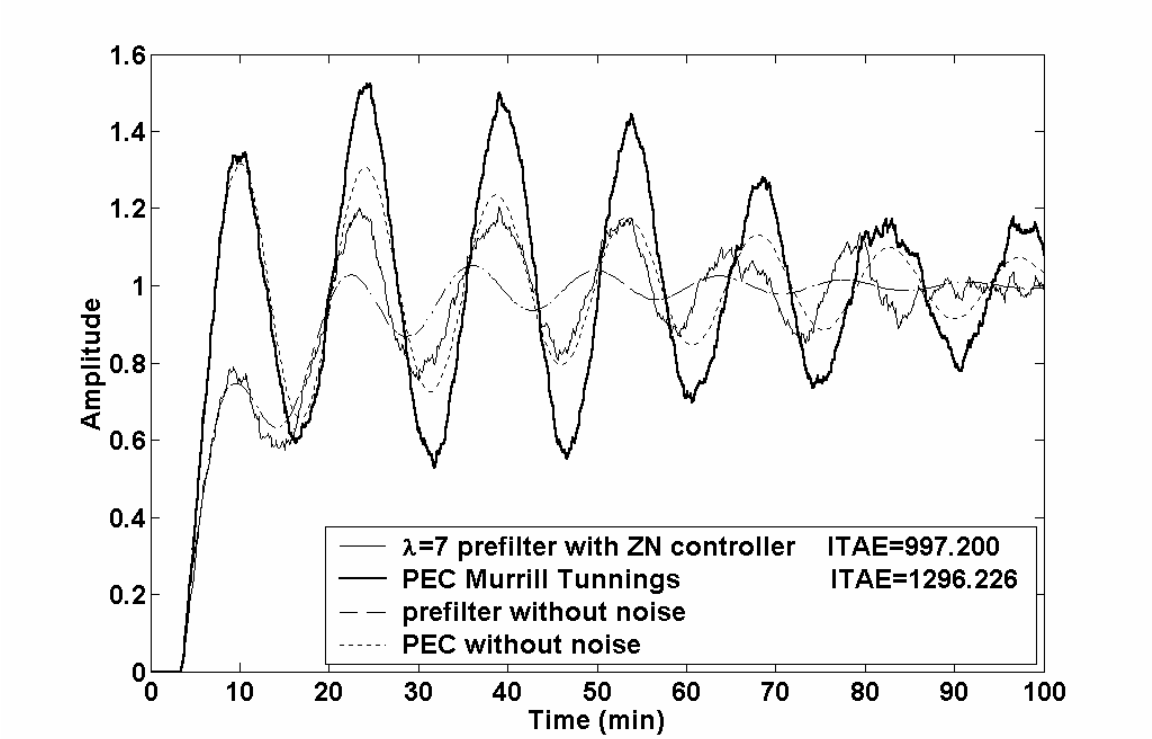

Figure 23: Step response of PEC using Murrill tunings, and a prefilter design using Zielger-Nichols under the influence of white noise and 10% error in process gain estimation.

It should be noted that direct comparison of PEC and the prefilter design is affected by the differences in the nominal response of these systems. Considering that, it is still apparent that the PEC system adjusted for the affects of noise in much the same fashion as the prefilter system. This is because noise is a disturbance, which is solely regulated by the feedback controller of the TDoF system in question.

Model Mismatch TDoF Comparison

So far we have addressed the relationship between model uncertainty and the activity of the controller in the feedback loop. We have also addressed the effects of noise on the PEC system. This analysis gave us qualitative insights regarding PEC, but very little quantitative understanding of Equation (27) was achieved. Because of this, we are going to change our approach to understanding modeling error in the PEC system. We are not going to analyze modeling error in PEC as a stand-alone system. Instead we will seek to understand how PEC handles modeling error RELATIVE to how prefilter designs handle modeling error. For purposes of this comparison, the PEC system for the now familiar process defined in Equation (13) will be compared to the prefilter design for that same system in the presence of various gain estimation errors. The PEC system will use the controller defined in Equation (15) for tracking, the controller defined in Equation (18) for disturbance rejection and a process model defined in Equation (13). The block diagram, which shows how these various elements fit into the PEC structure, can be seen in Figure 12. The prefilter system will also use the controller defined in Equation (18) for feedback control, and will use the prefilter defined in Equation (21). Figure 9 shows the block diagram for the implementation of these various elements.

First we will examine the frequency responses of these systems in the presence of modeling error. Figure 24 shows the closed-loop log modulus for the prefilter designed under loop-shaping techniques by Skogestad and Postlewaite9, which was summarized in chapter 2. Plots are shown for errors in the process gain of 0%, 10%, 25%, and 40%. The peak in the closed-loop log modulus is minimal, even at an error of 40% in the process gain. Figure 25 shows the peaks of the corresponding plot of the PEC system for the same errors in the estimate of the gain. At a 10% error in the process gain, the difference between the two structures is minimal. However, as the error increases, the PEC structure is more sensitive to errors in the gain, as indicated by the increasing size of the peak in the closed-loop log modulus curve.

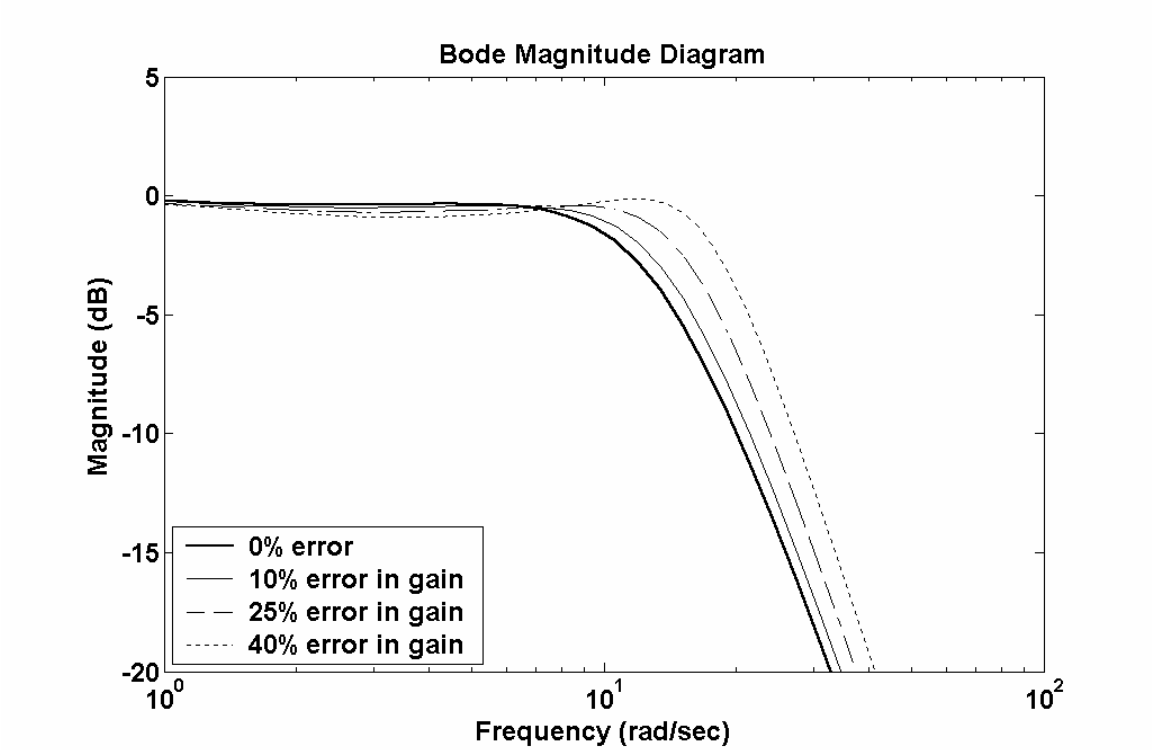

Figure 24: Frequency response for the process described by Equation (13) of a prefilter system using the controller found in Equation (18) and prefilter from Equation (21) for gain estimation errors or 0%, 10%, 25%, and 40%.

For this specific case, it is not unexpected that PEC is more sensitive to modeling error. The tracking controller in the PEC structure is significantly more aggressive than the prefilter and yields superior nominal performance. The highly aggressive nature of the partitioning controller, Equation (15), implies that any error in modeling will cause the system to aggressively deviate from the nominal response. This phenomenon can be seen by comparing Figure 26 and Figure 27. Figure 26 shows the tracking response of the prefilter system to various degrees of modeling error in the gain, while Figure 27 shows the tracking response of PEC exposed to the same modeling error. Upon first inspection it would appear that the PEC system, Figure 27, does not handle modeling error as efficiently as the prefilter design. However, that analysis is ultimately inaccurate, because these two control systems have been designed to handle tracking error with significantly different levels of aggression. The prefilter has a rise time of 0.184s, while the PEC system has a rise time of 0.123s. This means the prefilter is taking 50% more time to reach 90% of the final value than the PEC system. This significant dissimilarity serves as a strong indication that the difference between how these two particular systems handle modeling error is related to differing controller tunings, a difference that clouds our ability to perceive the role which the control structures, PEC and prefilter control, play in error propagation.

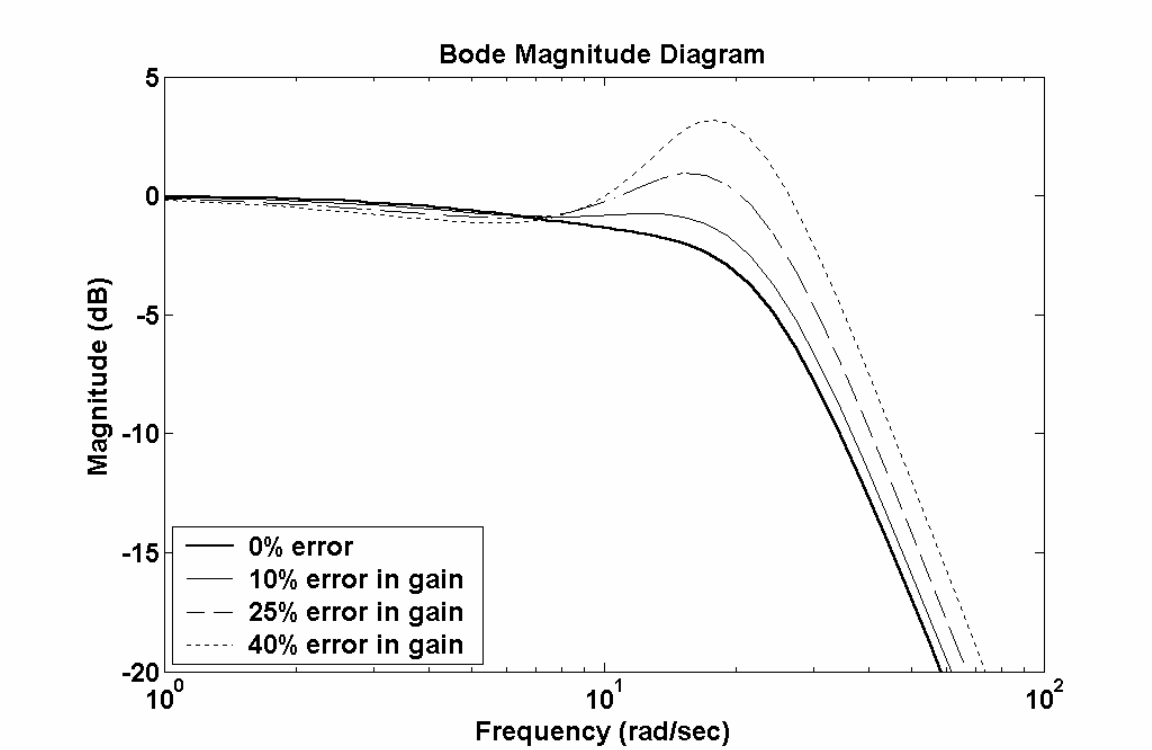

Figure 25: Frequency response for the process described by Equation (13) of a PEC using the controllers found in Equation (15) and (18) for gain estimation errors or 0%, 10%, 25%, and 40%.

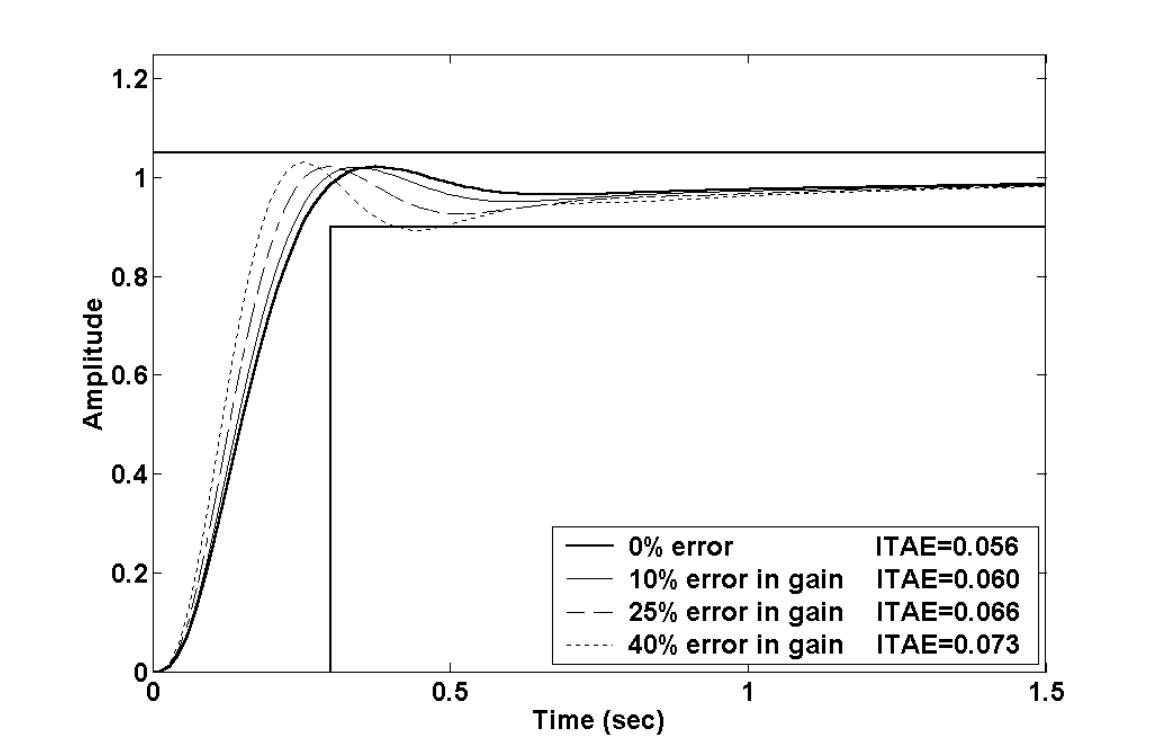

Figure 26: Step response for the process described by Equation (13) of a prefilter system using the controllers found in Equation (17) and (18) for gain estimation errors or 0%, 10%, 25%, and 40%.

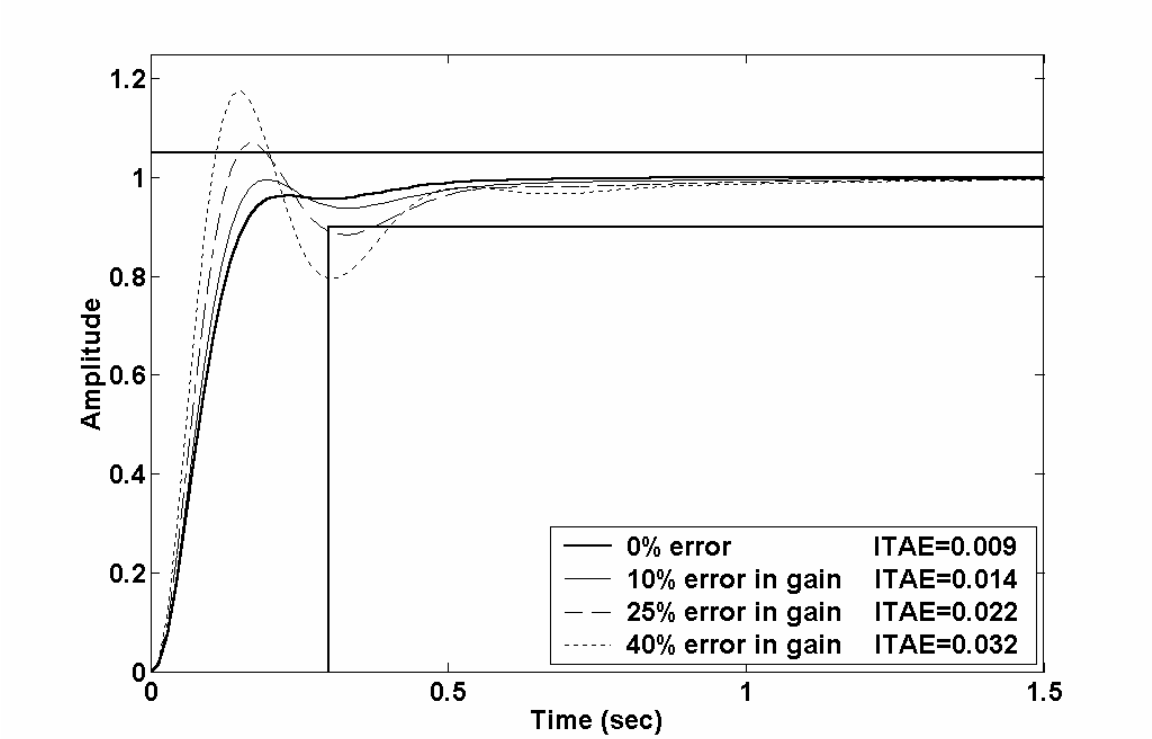

Figure 27: Frequency response for the process described by Equation (13) of a PEC system using the controllers found in Equation (15) and (17) for gain estimation errors or 0%, 10%, 25%, and 40%.

Since it is difficult to discern what properties of the system are determined by the controllers and what properties are determined by the PEC framework in which they were implemented, a method of analysis is needed which does not rely on any specific controller tunings. However, in order to achieve a meaningful result from this generalization, the analysis must occur as a comparison between PEC and a benchmark system, the inverse model prefilter. Unfortunately, the response of a system with an arbitrarily set reference trajectory like the prefilter is almost always different from the closed-loop response of a system that has been designed using tuning guidelines. This is simply a result of the different design procedures used in each case, and is the main reason analysis of specific systems tends to yield inconclusive data. This can be compensated for by artificially setting the reference trajectory used in the prefilter design to be equal to the nominal closed-loop response of the PEC system. With this assumption we can contrive a very simple proof to demonstrate how PEC is identical to inverse model based control with regards to how plant/model mismatch is processed. Let us assume we want to control some process G_P with model G_{nom}. The design process for a PEC system would require us to find suitable tracking and load controllers. Regardless of the process or the controllers chosen, the nominal closed loop tracking response of the PEC system can be generalized as:

$$\left(\frac{y}{r}\right)_{PEC^*} = \frac{K_1 G_{nom}}{1 + K_1 G_{nom}} \tag{29}$$

The response in Equation (27) can be used as the reference trajectory needed to design a prefilter.

$$\left(\frac{y}{r}\right)_{Ref} = \left(\frac{y}{r}\right)_{PEC^*} \tag{30}$$

This yields the following prefilter design

$$K_r = \frac{1+K_2G_{nom}}{K_2G_{nom}}\left(\frac{y}{r}\right)_{Ref} = \frac{1+K_2G_{nom}}{K_2G_{nom}}\frac{K_1G_{nom}}{1+K_1G_{nom}} \qquad (31)$$

From the PEC design Equation, (23), the step response for the actual system will be

$$\left(\frac{y}{r}\right)_{PEC} = \frac{K_2G_p}{1+K_2G_p} + \frac{(K_1-K_2)G_p}{(1+K_2G_p)(1+K_1G_{nom})} \qquad (32)$$

Similarly the calculated response for the prefilter system as determined by Equation (7) will be as follows

$$\left(\frac{y}{r}\right)_{Prefilter} = \frac{1+K_2G_{nom}}{K_2G_{nom}}\frac{K_1G_{nom}}{1+K_1G_{nom}}\frac{K_2G_P}{1+K_2G_P} \qquad (33)$$

Though these responses are in different forms it is simply a matter of algebra to show that they are identical regardless of the process or the controllers. Unfortunately, the normal design methods for these two types of systems prevents a direct comparison like this for all but the most trivial systems, because controller design is often excessively complicated if the assumption in Equation (30) is maintained.

There are several conclusions that can be drawn from this proof. The lower degree of performance exhibited by the PEC systems in the presence of modeling error in this chapter was not due to the PEC structure itself, but the controllers which were placed in the structure. Similarly, the high degree of nominal performance exhibited by the PEC system was determined by whether or not controller design for servo problems yielded a better trajectory than the reference trajectory used in prefilter design which is often arbitrarily chosen. This means PEC may have a distinct performance advantage for systems where the best reference trajectory is not easily defined. This issue will be covered in the following two chapters.

Conclusions

The theoretical understanding of PEC laid out in this chapter has highlighted many desirable characteristics, which are currently unavailable to designers using existing two-degree of freedom techniques.

- PEC allows for implementation of independently designed conventional controllers with little additional design effort
- PEC can be applied to noninvertible systems making it a more flexible two-degree of freedom controller.
- PEC can utilize preliminary ODoF controller designs, often reducing the design load relative to other TDoF techniques
- Modeling error propagation is identical to prefilter systems, meaning robust performance issues are results of controller tunings and not due to the PEC framework itself
- One major distinction in performance between PEC and other TDoF controllers is how the desired reference trajectory is chosen. In general TDoF controllers specify the reference trajectory, while the PEC step response is generally found by minimizing more general design criteria

For simple SISO systems, inverse prefilter designs provide an adequate method for two-degree of freedom control, but as systems become more complicated the design and implementation of those controllers becomes very cumbersome. PEC provides an alternative two-degree of freedom method, which being based on feedback design techniques, is more intuitive and more flexible than inverse based methods.

CHAPTER IV

THE USE OF H_∞ CONTROLLERS IN A PARTITIONED ERROR CONTROL STRUCTURE

Goals and Motivations

Chapter three was able to demonstrate the capabilities of the novel two-degree-of-freedom system, but not all of the nuances of PEC were brought forth in the original analysis. This Chapter will complete the development of PEC in a SISO setting, and will primarily be used to establish a design procedure for the use of H_∞ controllers in the PEC system and demonstrate potential benefits from the use of different controller designs in the PEC structure.

Chapter three correctly defines the closed loop response of the PEC system to be.

$$y = \left[\frac{K_2 G_p}{1 + K_2 G_p} + \frac{(K_1 - K_2) G_p}{(1 + K_2 G_p)(1 + K_1 G_{nom})} \right] (r) + \frac{G_d}{1 + K_2 G_p} (d) \qquad (34)$$

By simple inspection it is easily shown that the stability of the system is determined by two characteristic equations,

$$1 + K_2 G_P = 0 \qquad (35)$$

and

$$\left(1 + K_2 G_P\right)\left(1 + K_1 G_{nom}\right) = 0 \qquad (36)$$

Due to the deterministic nature of the partitioning loop designers are free to establish and manipulate the location of the poles in the partitioning loop in a nominal setting, $(1 + K_1 G_{nom})$, by manipulating K_1. Therefore, robust stability criteria are solely dependant

on the feedback controller parameters to stabilize the characteristic equation $1 + K_2 G_P = 0$. This dependence on the feedback controller for robust stability is also paralleled in standard TDoF designs, yet the ability to take advantage of wider latitude in tracking control is not available. There are several reasons for this. First, two-degree-of-freedom prefilters that use an inverse model often require approximations and are only available for systems that are invertible. Every approximation made increases modeling error and thus increased the use of the regulatory controller for servo responses. Second, prefilters that do not use an inverse model attempt to shape the feedback controllers servo response to look more like the desired reference trajectory. This shaping is generally done with the step response of the system, and regardless of what tuning parameters are used, this process is not well formalized and is often complicated by attempting to shape the step response of the system as well as the actuator usage of the controller at the same time. As this chapter unfolds, these characteristics will be demonstrated.

The theoretical introduction of partitioned error control in chapter three demonstrates the adaptability of the PEC system to commonly used PID control techniques. What this work failed to do was demonstrate the benefit of using different controller design techniques in the partitioning loop and the feedback loop, taking full advantage of the freedom in design that PEC has to offer in order to achieve enhanced performance. The emphasis of that chapter was on the use of similar controllers tuned for either servo or regulatory concerns. For example, a PI controller tuned under Murrill's tracking rules was only paired with a PI controller tuned under Murrill's regulatory rules. It needs to be made clear that a designer is free to mix performance controllers with

robust controllers regardless of how those controllers were derived, thus taking advantage of the best a particular design has to offer to enhance performance in the process.

To demonstrate the flexibility of PEC in this chapter, two advanced controller types will be introduced. H_∞ mixed sensitivity controllers and H_∞ loop-shaping controllers. These controllers have very distinct strengths and weaknesses that make them well suited for PEC. Only a general introduction and explanation of key features of these controllers will be presented in this paper. For a more comprehensive understanding of the vast field of H_∞ control, the reader is directed to the works of Skogestad and Postlethwaite[9]. The general principle of all H_∞ designs is to minimize the maximum singular value of the transfer function of exogenous inputs to outputs as a function of frequency. The distinction between the various types of H_∞ control is based on what inputs and what outputs are used to determine the transfer function. A brief overview of the H_∞ norm will be defined, followed by a more detailed description of the general H_∞ control algorithm, after which it will be shown how the favorable servo characteristics of the H_∞ mixed sensitivity controller and the favorable regulatory characteristics of the H_∞ loop-shaping controller can be combined for enhanced performance in the Partitioned Error Control structure.

H_∞ norm definition

The H_∞ norm of a systems singular value decomposition is defined as the maximum value of the frequency response, $G(j\omega)$, of the system times the upper bound of the singular value, $\bar{\sigma}$.

$$\left\|G(s)\right\|_{\infty} \triangleq \max_{\omega} \bar{\sigma}(G(j\omega)) = \lim_{p\to\infty}\left(\int_{-\infty}^{\infty}\left|\bar{\sigma}(G(j\omega))\right|^{p} d\omega\right)^{1/p} \quad (37)$$

The interpretation of this equation in the time domain yields a better understanding of the functionality of the norm. The maximum value, the H_∞ norm, corresponds to the worst-case steady–state gain for a sinusoidal input at any frequency. Therefore lowering the H_∞ norm lowers the worst-case steady–state gain and increases system stability. For SISO systems, the norm is simply the peak of the frequency response of a transfer function. The H_∞ norm is well documented, having roots in Linear Quadratic Gaussian (LQR) and H_2 control, and generalized for wide use in controller design by Glover and Doyel[13].

The H_∞ norm can be used with any proper linearly stable system. That is to say that in the state-space realization in the standard A,B,C,D notation, D does not have to equal 0, making this controller applicable to a wide variety of systems.

H_∞ norm general control algorithm

There are three basic ways to design a controller using the H_∞ norm. They are mixed-sensitivity H_∞ control, signal-based H_∞ control, and H_∞ loop-shaping control. Of these, mixed-sensitivity H_∞ control and H_∞ loop-shaping control are of interest to this research. The reason signal-based H_∞ control is not suitable will be made clear below. All H_∞ controller techniques discussed in this research are based on the general control configuration shown in Figure 28, where P is the generalized plant. The signals of the general control configuration are: *u* the control variables, *v* the measured variables, *w* the exogenous signals such as disturbances *d*, commands *r*, and noise *n* such that $w = \begin{bmatrix} d & r & n \end{bmatrix}^{T}$, and *z* which contains outputs to be minimized for example the error

signal $z = [y - r]$. The General plant P is normally composed of the process being controlled, a series or weights on the inputs and outputs, and algebraic manipulations on the various signals to obtain the desired outputs. Equations (38) and (39) define the transfer functions for the general plant, P, and controller, K. The generalized plant can be realized in many ways. Two realizations that are often used are the $\begin{bmatrix} P_{11}(s) & P_{12}(s) \\ P_{21}(s) & P_{22}(s) \end{bmatrix}$ partitioned form and the two-port state space model form. These forms are defined in Equations (40)-(41).

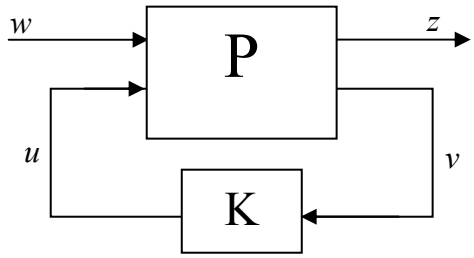

Figure 28: General control configuration

$$\begin{bmatrix} z \\ v \end{bmatrix} = P(s) \begin{bmatrix} w \\ u \end{bmatrix} \tag{38}$$

$$u = K(s)v \tag{39}$$

$$\begin{bmatrix} z \\ v \end{bmatrix} = P(s) \begin{bmatrix} w \\ u \end{bmatrix} = \begin{bmatrix} P_{11}(s) & P_{12}(s) \\ P_{21}(s) & P_{22}(s) \end{bmatrix} \begin{bmatrix} w \\ u \end{bmatrix} \tag{40}$$

$$\begin{bmatrix} z \\ v \end{bmatrix} = P(s) \begin{bmatrix} w \\ u \end{bmatrix} = \left[\begin{array}{c|cc} A & B_1 & B_2 \\ \hline C_1 & D_{11} & D_{12} \\ C_2 & D_{21} & D_{22} \end{array}\right] \begin{bmatrix} w \\ u \end{bmatrix} \tag{41}$$

The closed loop transfer function from *w* to *z* is given by the linear fractional transformation

$$z = \mathrm{F}_l\left(P, K\right) w \tag{42}$$

where

$$F_l\left(P, K\right) \triangleq P_{11} + P_{12} K \left(I - P_{22} K\right)^{-1} P_{21} \tag{43}$$

The goal of H_∞ optimization is to find all stabilizing controllers, K, which minimize γ.

$$\left\| F_l(P,K) \right\|_\infty = \max_\omega \bar{\sigma}(F_l(P,K)(j\omega)) = \gamma_{\min} \tag{44}$$

For SISO systems we are seeking to minimize the peak of the frequency response of the transfer function from *w* to *z*, or the H_∞ norm from *w* to *z*. Note the lowest achievable H_∞ norm is defined as γ_{min}, however, it is often simpler both theoretically and computationally to find a sub optimal controller with $\gamma > \gamma_{\min}$. The significance of γ varies depending on how the problem is framed, therefore explanations of its significance will be held off till the distinctions between various types of H_∞ controllers are described. This sub optimal problem can be efficiently solved using the algorithm of Doyle et al.[14] by reducing γ iteratively assuming the following assumptions summarized by Skogestad and Postlethwaite[9] are true.

List 1 System criteria for the application of H_∞ control

1. (A,B_2,C_2) is stabilizable and detectable
2. D12 and D21 have full rank
3. $\begin{bmatrix} A - j\omega I & B_2 \\ C_1 & D_{12} \end{bmatrix}$ has full column rank for all ω
4. $\begin{bmatrix} A - j\omega I & B_1 \\ C_2 & D_{21} \end{bmatrix}$ has full row rank for all ω
5. $D_{11}=0$ and $D_{22}=0$
6. $D_{12} = \begin{bmatrix} 0 \\ I \end{bmatrix}$ and $D_{21} = \begin{bmatrix} 0 & I \end{bmatrix}$
7. $D_{12}^T C_1 = 0$ and $B_1 D_{21}^T = 0$
8. (A,B_1) is stabilizable and (A,C_1) is detectable

The stabilizing controller may then be calculated given the three conditions below exist

1. $X_\infty \geq 0$ is a solution to the algebraic Riccati equation

$$A^T X_\infty + X_\infty A + C_1^T C_1 + X_\infty (\gamma^{-2} B_1 B_1^T - B_2 B_2^T) X_\infty = 0 \qquad (45)$$

such that Re $\lambda_i \left[A + (\gamma^{-2} B_1 B_1^T - B_2 B_2^T) X_\infty \right] < 0, \forall i;$ and

2. $Y_\infty \geq 0$ is a solution to the algebraic Riccati equation

$$A Y_\infty + Y_\infty A^T + B_1 B_1^T + Y_\infty (\gamma^{-2} C_1^T C_1 - C_2^T C_2) Y_\infty = 0 \qquad (46)$$

such that Re $\lambda_i \left[A + Y_\infty (\gamma^{-2} C_1^T C_1 - C_2^T C_2) \right] < 0, \forall i;$ and

3. $\rho(X_\infty Y_\infty) < \gamma^2$

All such controllers are then given by $K = F_l(K_C, Q)$ where

$$K_C(s) \overset{s}{=} \left[\begin{array}{c|cc} A_\infty & -Z_\infty L_\infty & Z_\infty B_2 \\ \hline F_\infty & 0 & I \\ -C_2 & I & 0 \end{array}\right] \tag{47}$$

$$F_\infty = -B_2^T X_\infty; \quad L_\infty = -Y_\infty C_2^T; \quad Z_\infty = \left(I - \gamma^{-2} Y_\infty X_\infty\right)^{-1} \tag{48}$$

$$A_\infty = A + \gamma^{-2} B_1 B_1^T X_\infty + B_2 F_\infty + Z_\infty L_\infty C_2 \tag{49}$$

where Q(s) is any stable proper transfer function such that $\|Q\|_\infty < \gamma$. For Q(s)=0, we get

$$K(\mathrm{s}) = K_{C11}(\mathrm{s}) = -Z_\infty L_\infty \left(\mathrm{s}I - A_\infty\right)^{-1} F_\infty \tag{50}$$

K(s) is referred to as the "central" controller. One important characteristic of the central controller is that it has as many states as the generalized plant P(s).

Most applications of H_∞ control require an iterative procedure for solving the two Riccati equations (Equations (44) and (45)), because γ_{min} cannot be solved for directly. There are a few exceptions to this rule, however, in practice the general control algorithm is performed by commercially available software such as MATLAB. The Designer simply has to specify the general plant configuration P and call upon a routine which will solve for the controller K(s). The vast majority of discussion involving H_∞ design from this point on will focus on how the generalized plant, P, is chosen. Since setting up the generalized plant appropriately is the major design element in H_∞ controller design problems.

General Principles of Frequency Responses

The general H_∞ algorithms we will examine are best analyzed in the frequency domain. This is in contrast to simpler controller designs like PID controllers, which tend to focus on the time response of a system. Because of this it is helpful to refresh ourselves on some of the typical shapes seen in frequency responses, and the significance of those shapes in terms of time domain performance. This review will provide some insight into possible performance objectives we may seek in H_∞ design and help us better understand how choices in setting up the generalized plant, P, will determine controller characteristics.

Recall for feedback control systems of a process G, under the influence of a controller K that the relationship between the systems output y, the controller output u, and process inputs such as references, disturbances, and noise (r, d, and n) is given as follows:

$$y(s) = \underbrace{(I+GK)^{-1}GK}_{T(s)}[r(s)] + \underbrace{(I+GK)^{-1}}_{S(s)}[d(s)] - \underbrace{(I+GK)^{-1}GK}_{T(s)}[n(s)] \qquad (51)$$

$$u(s) = \underbrace{K(I+GK)^{-1}}_{KS(s)}[r(s) - n(s) - d(s)] \qquad (52)$$

Where S is the sensitivity function equal to $(I+GK)^{-1}$, and T is the complementary sensitivity function equal to $(I+GK)^{-1}GK$. To facilitate the discussion, objectives will be framed in terms of the open loop transfer function L=GK. It should be remembered, however, that any objective specified for L has a direct impact on the both the sensitivity function and the complimentary sensitivity function. Equation (51) rewritten in terms of L can be seen in Equation (53).

$$y(s) = \underbrace{(I+L)^{-1}L}_{T(s)}[r(s)] + \underbrace{(I+L)^{-1}}_{S(s)}[d(s)] - \underbrace{(I+L)^{-1}L}_{T(s)}[n(s)] \qquad (53)$$

We can determine general values of L, and thus S, T, and KS, based on how we wish certain inputs, r, d, and n, to effect outputs y and u as per Equations (51) and (52). For instance, y = r would give us perfect tracking. In order to approach perfect tracking we would need $\sigma(L(j\omega))$ to be large for all ω, $y = \frac{L}{1+L} * r \approx 1 * r$. This in turn requires σ(S) to be small, and σ(T) =1. However, making $\sigma(L(j\omega))$ large at all frequencies also means that noise will have a considerable effect on our system. Thankfully, these contradicting objectives can be separated into distinct frequency bands. For instance the specification of perfect tracking at all frequencies, requiring $\sigma(L(j\omega))$ to be large for all ω, is not plausible. A better objective is to make $\sigma(L(j\omega))$ large or $\sigma(S(j\omega))$ small below the crossover frequency, ω_C, for better control at lower frequencies where noise is not a significant problem. In conjunction with this objective, it can also be specified that $\sigma(L(j\omega))$ should be small or $\sigma(S(j\omega)) = 1$ for high frequencies to mitigate noise.

We can view these specifications in more practical terms by looking at a plot of the sensitivity function, S, for a system under aggressive control, see Figure 29. For good tracking we require σ(S) to be small at low frequencies, this is equivalent to requiring integral action to prevent steady state offset. By inspection we see this system does meet that requirement. For noise mitigation we require σ(S) to be 1 at high frequencies. This desensitizes the system to the effects of high frequency inputs such as noise. By inspection of Figure 29 we see that the system also meets this requirement.

Another important characteristic of this response is the bandwidth. The bandwidth of a system, ω_B, is defined as the frequency at which the system crosses $1/\sqrt{2} \approx -3\text{dB}$ from below. A higher bandwidth signifies a more aggressive response and is associated with faster rise times in the time domain.

The last characteristic we will discuss is the peak gain. Through experience, rule of thumb has determined that peaks of up to about $2 \approx 6\text{dB}$ for a systems sensitivity plot provide good tracking. The controller in Figure 29 has a peak of 8.95 dB. Since the system in Figure 29 exceeds this recommendation, it is expected that the time response of this system will be very oscillatory. The actual time response of this system can be seen in Figure 30, and validates that expectation. Another reason the peak gain in Figure 29 is significant is that it represents the $\|S\|_\infty$. Therefore if we find a controller, which minimized $\|S\|_\infty$, we are finding a controller, which "pushes" this peak down. By pushing this peek down, the system is actually becoming more stable. To illustrate the "pushing" effect, Figure 31 shows the sensitivity response of the system in Figure 29 along with the sensitivity response of the same system when the controller gain has been reduced by a factor of 4. The result of reducing the controller gain is that it will make the system less aggressive and more stable. The peak response of the new system is 2.54 dB, well within the limits defined by the rule of thumb. The reduction of the peak gain has another significant effect. "Pushing" the peak of the response down has what is called a "waterbed" effect. Just as pushing down on one spot of a waterbed will cause other areas to rise up, so will pushing down on one spot of the frequency response of a sensitivity function cause other areas of the function to rise up. Lowering the peak of the response has pushed the bandwidth of the system to the left or decreased it, slowing down the

responses rise time. Hence nothing is gained for free, but an acceptable balance between the systems overshoot and bandwidth has been achieved.

Figure 32 shows the step response of the balanced controller relative to the aggressive controller. It is obvious that by adjusting the $\|S\|_\infty$ to coincide with general guidelines more sensible control was achieved.

This review has given a brief description of some of the characteristics and design objectives of frequency response based controller design. The sensitivity function is just one of many functions which may be used in H_∞ controller design, and these functions come in a variety of forms depending on process dynamics. This does tend to require more understanding of the process from designers then simpler controllers, but can lead to higher performance controllers as well.

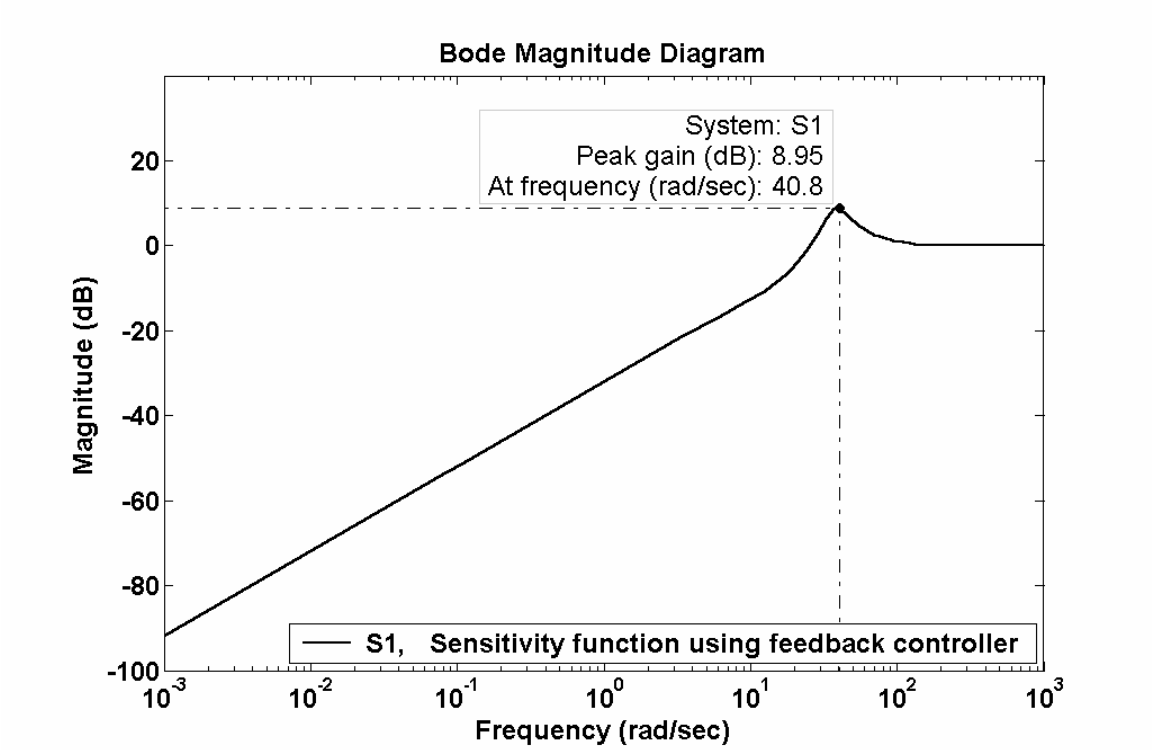

Figure 29: Typical plot of sensitivity function under aggressive control

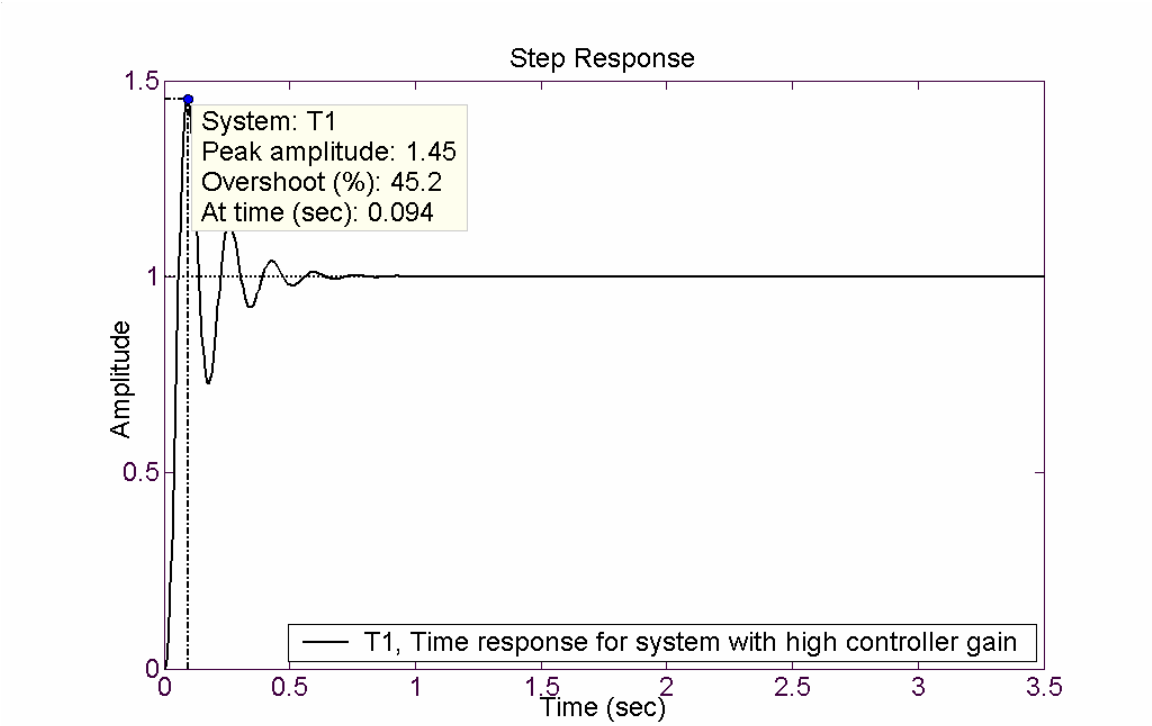

Figure 30: Plot of Time response for the system under aggressive control presented in Figure 29.

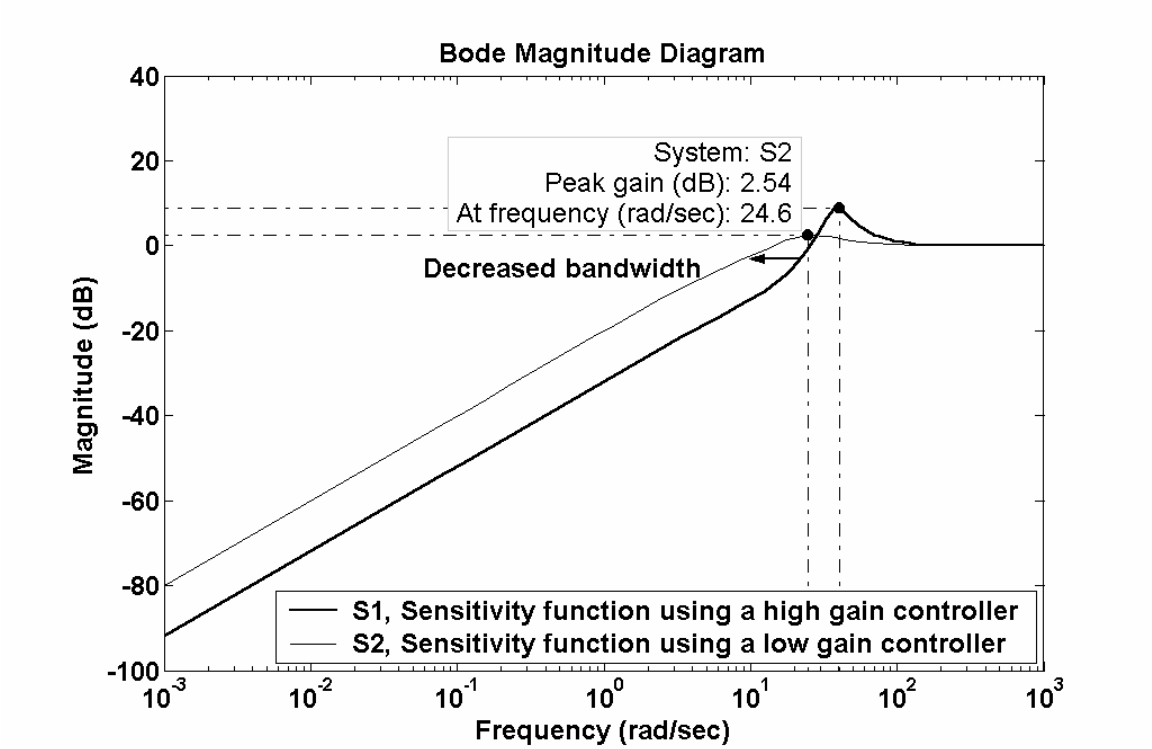

Figure 31: Frequency response of the sensitivity function under aggressive control (high controller gain) and under reasonable control (low controller gain)

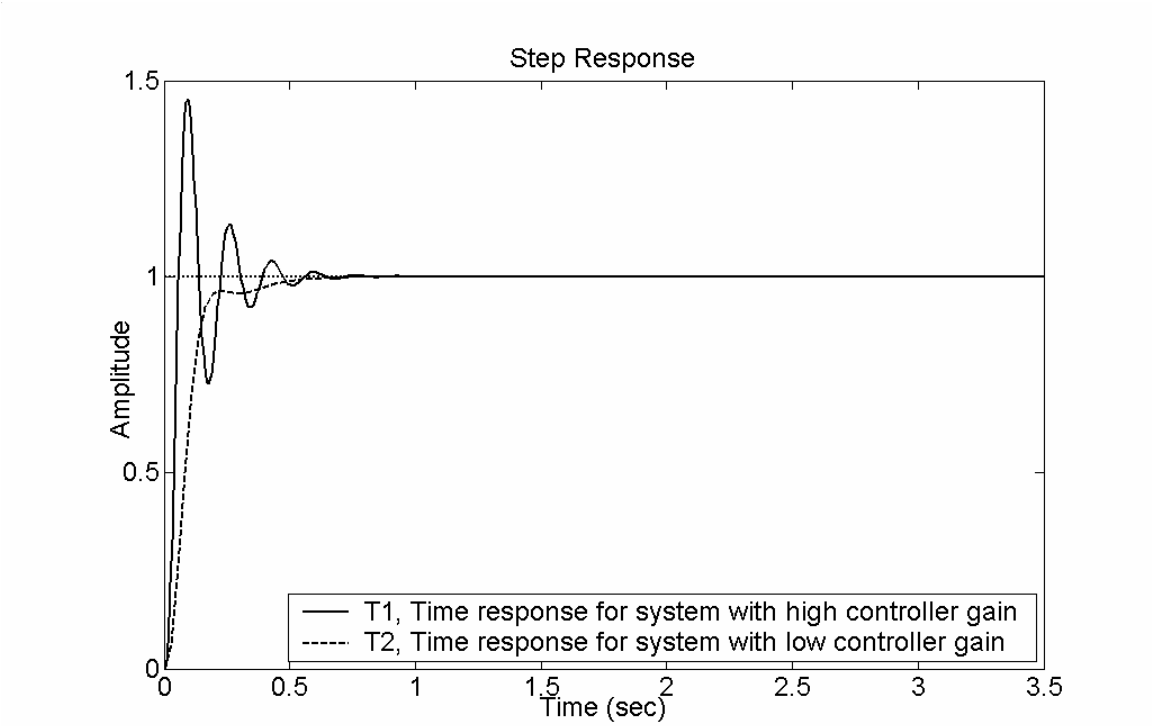

Figure 32: Step response of the same system under high gain control as well as low gain control

Mixed-Sensitivity H_∞ Control

The objective of mixed-sensitivity control is to shape the sensitivity function $S = (I + GK)^{-1}$ and either KS or the complimentary function $T = I - S = \frac{GK}{I + GK}$. The minimization of the sensitivity function's norm at low frequencies benefits disturbance rejection and tracking. The minimization of the complimentary sensitivity functions norm benefits tracking and noise attenuation. The minimizing a closed-loop transfer function like KS serves to limit controller effort. In general it is not very effective to minimize just one of these functions. As such mixed sensitivity H_∞ control tends to minimize them in pairs. For example mixed sensitivity H_∞ controller design could be set up to minimize the following function:

$$\left\| \begin{matrix} W_P S W_R \\ W_U K S W_R \end{matrix} \right\|_\infty < \gamma \qquad (54)$$

where W_P, W_U, and W_R are weighting functions and $\gamma > 0$ is the parameter to be minimized. W_P, W_U, and W_R are chosen to weight the input signal over the desired frequencies, and not to directly shape S or KS. For instance the weight W_P in Equation (54) could be selected to place more emphasis on the bandwidth frequency to emphasize the importance of higher bandwidth in the final design. The corresponding generalized process for Equation (54) is shown in Figure 33.

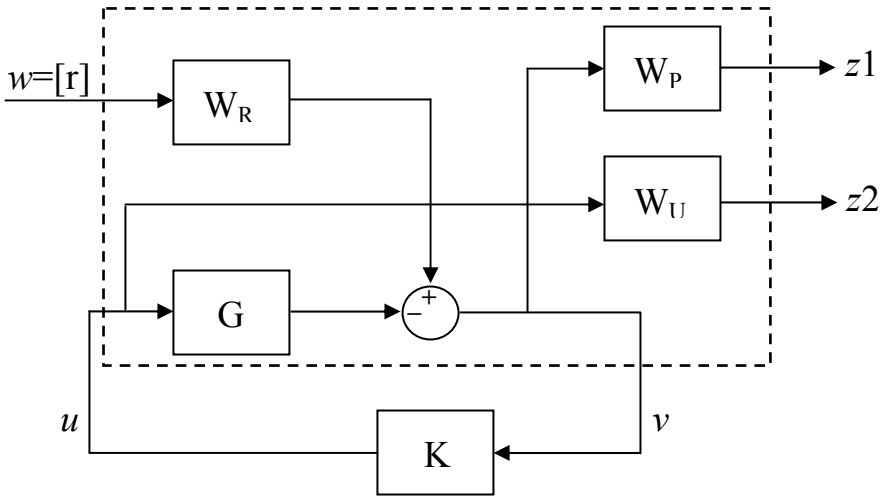

Figure 33: S/KS mixed sensitivity configuration

More than two norms can be minimized using this technique, but the problem becomes very cumbersome, and the solution is not often worth the design effort. For this reason mixed sensitivity is well suited for specific problems, but does not provide a comprehensive controller in and of its self. It can be designed for servo problems or regulatory problems but not both. This particular conclusion is pertinent to the Partitioned Error Control research objectives because the partitioning loop provides and environment where the limited breadth of mixed-sensitivity H_∞ controllers are inconsequential as each controller in the PEC structure is exposed to isolated sources of error (tracking or disturbance rejection). Therefore, a mixed sensitivity controller can be designed specifically for tracking or disturbance rejection, thus full advantage can be taken of what mixed-sensitivity H_∞ control has to offer. For instance in the examples presented later in this chapter, a mixed sensitivity controller will be used in the partitioning loop where it will be designed for setpoint tracking and controller action

minimization. In this setting the controller will be isolated from disturbances, thus negating any deficiencies the controller may have to disturbance rejection.

Weight Selection for Mixed Sensitivity H_∞ Controllers

In the previous section reference, performance, and controller weights (W_R, W_P, and W_U) were introduces as part of the mixed-sensitivity H_∞ controller. These weights are used to express performance objectives for the controller. In this section we will discuss some of the principles surrounding weight selection. Choosing the appropriate weights is straight forward if performance objectives are defined in the frequency domain. One performance objective that is often defined in terms of frequency is the desired bandwidth of the system. Unfortunately, many objectives are specified in the time domain, such as maximum allowable overshoot. We will need to evaluated these time domain objectives and determine their frequency response implications. Once those implications are determined then the weights can be defined.

Reference Weight, W_R: The purpose of the reference weight is to give designers the ability to determine the relative importance of input signals. For instance let us examine a system containing an inverted pendulum on a horizontally moving cart. When trying to simultaneously stabilize the attitude of the inverted pendulum and the horizontal position of the cart a reference signal can be supplied for both the position of the cart on which the pendulum rests, and for the pendulum. However, as a matter of practical application, it is not necessary to have the pendulums attitude track a reference signal aggressively. In fact, optimal control requires the pendulum to move away from the set point signal to accommodate lateral cart movement commands. It is simply desired for

the pendulum to stay upright. This goal can be achieved by de-emphasizing the reference signal for the pendulums attitude relative to the reference signal of the carts position. An adequate choice of the reference weight for this particular problem might look like

$$\underbrace{\begin{bmatrix} 1 & 0 \\ 0 & 0.01 \end{bmatrix}}_{W_R} \begin{bmatrix} r_{cart} \\ r_{pendulum} \end{bmatrix} \tag{55}$$

For most applications the reference weight is generally not needed. When this occurs a reference weight of W_R=I is chosen effectively removing the reference weight from the problem. An example of such a problem would be the multivariable control of a distillation column where distillate and bottoms outputs are both of equal concern.

Performance Weight, W_P: As it's name implies, the performance weight sets the performance standard on the sensitivity function in the form of upper bounds at both low and high frequencies, and for the bandwidth of the system. The general idea behind weight selection in the context of an H_∞ norm problem is illustrated by the following example. Figure 34 shows the sensitivity function, S, of a process G, under the control law of K. The upper bounds on S as specified by W_P are also shown in Figure 34 by plotting $|1/W_P|$. If these bounds are met then $|1/W_P| \geq |S|$ for all frequencies. The control law that is currently being applied to the system is unable to meet this condition at frequencies around 17.5 rad/s. The inability of the current control law to meet this requirement causes $|W_PS|$ to have a peak at 17.5 rad/s as shown in Figure 35. The H_∞ optimization of $\|W_PS\|_\infty$, assuming W_R=I, seeks to find a new control law, which minimizes this peak, and thus tries to bring the system into compliance with the performance specifications set in W_P.

A common choice for the form of the performance weight is $W_P = \mathrm{diag}\{w_{Pi}\}$

where

$$w_{Pi} = \frac{s/M_i + \omega_{Bi}^*}{s + \omega_{Bi}^* A_i}, \quad A_i \ll 1 \tag{56}$$

and $M_i > 0$, $A_i > 0$, and $\omega_B > 0$

- A_i specifies the upper bound on S at $\omega \le A_i \omega_B^*$. Selecting $A_i \ll 1$ gives the system approximate integral action by setting the upper bound at low frequencies.
- M_i specifies the upper bound on S at $\omega \ge M_i \omega_B^*$. As per the rule of thumb discussed in the section on general principles of loop shaping, M_i=2 sets this upper bound at approximately 6dB. For this reason M_i=2 is a standard initial choice and is used to set the upper bound at high frequencies.
- ω_B^* specifies the upper bound on S at $A_i \omega_B^* \le \omega \le M_i \omega_B^*$. ω_B^* is the frequency where the performance weight crosses –1 dB, and is approximately the bandwidth requirement of the system.

With this general understanding of the significance of performance weight parameters, a designer can translate time domain performance objectives into the frequency domain fairly easily.

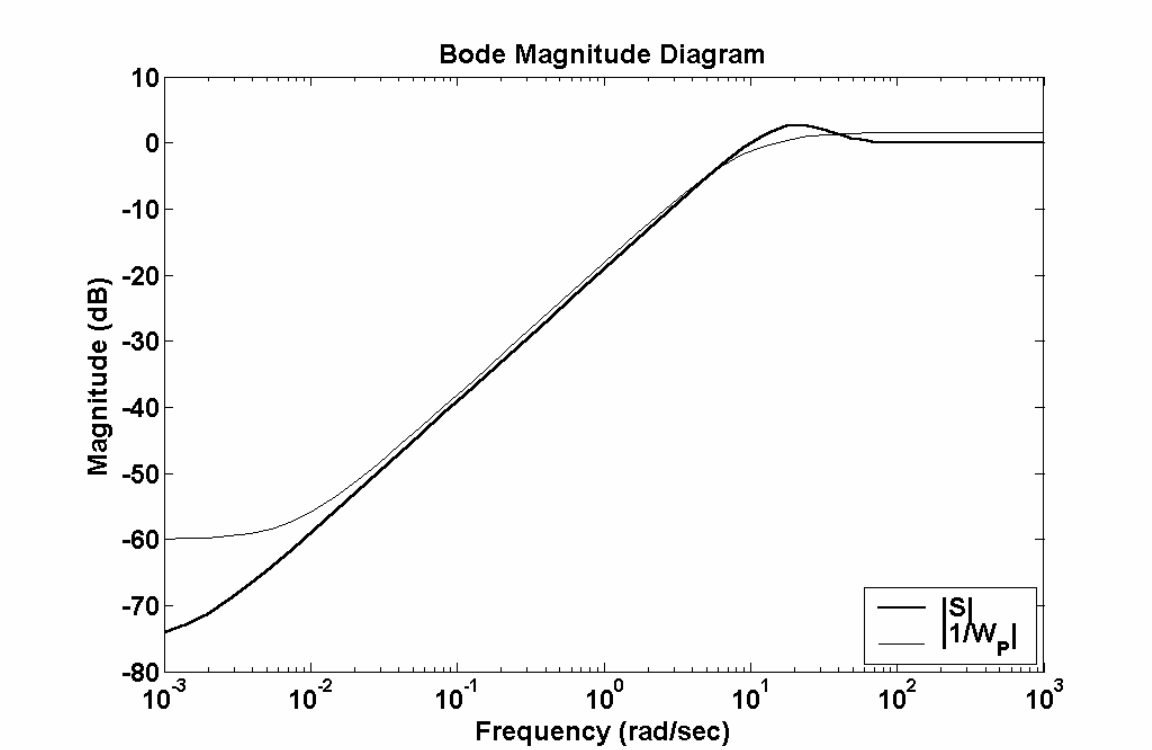

Figure 34: Frequency response of a sensitivity function, S, and the inverse of its performance weight, $1/W_P$.

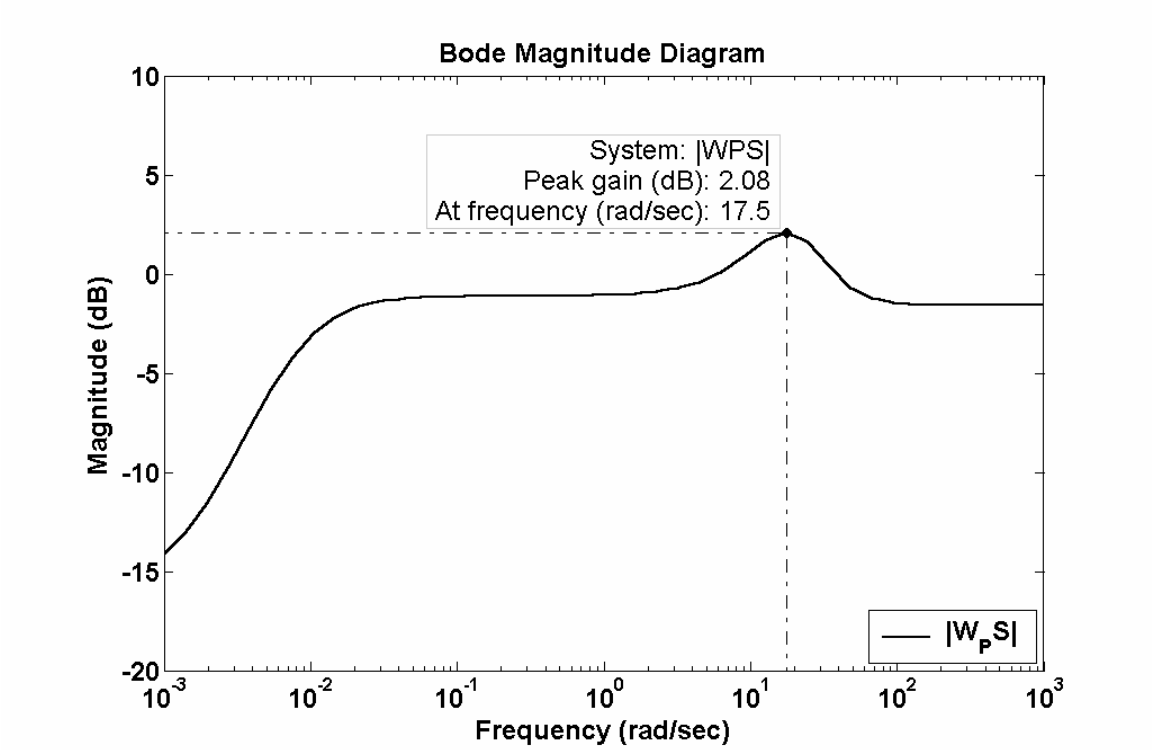

Figure 35: Frequency response of a system in which $|1/W_P| \geq |S|$ is not met for all frequencies.

Controller Weight, W_U: The controller weight seeks to place upper bounds on control energy. Typically W_U is chosen to be the identity matrix, such that W_U=I. Choices of W_U where the diagonal elements are less than 1 encourage controller usage, while values of the diagonal elements greater than 1 tend to discourage controller usage. The controller weight is used by designers who seek to limit the bandwidth of |KS|. A typical form of W_U for SISO systems is given in Equation (57).

$$W_U = \frac{1}{A_U}\left[\frac{s+\omega_U M_U}{s+\frac{\omega_U}{A_U}}\right] \qquad (57)$$

where $\omega_U>0$, $M_U>0$, and $A_U>0$. With typical parameter values of $0 < A_U \ll M_U < 1$. Small values of A_U encourage controller usage at low frequencies were noise is less of a problem, while values near one for M_U tend to discourage the effects of noise on controller usage at high frequencies. ω_U is the frequency at which the controller weight crosses –1dB and is approximately equal to the bandwidth requirement on |KS|. A typical plot of |KS| and $|1/W_U|$ can be seen in Figure 36

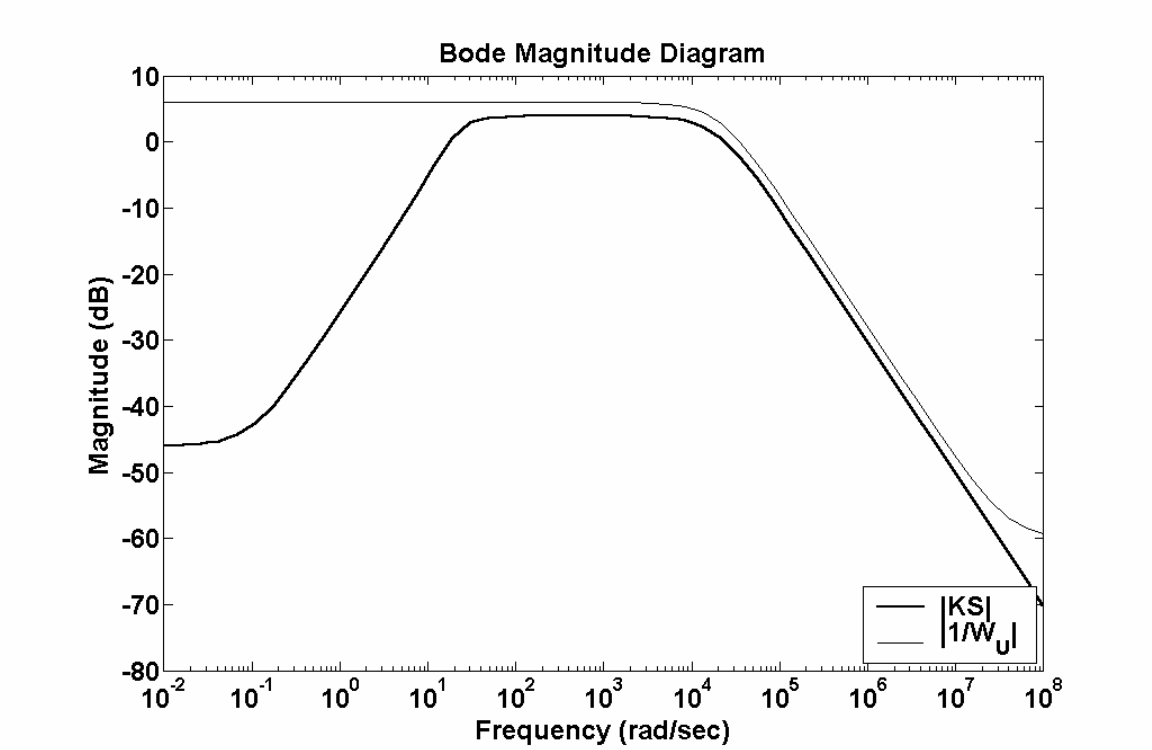

Figure 36: Frequency response of controller action, KS, and the inverse of the controller weight, $1/W_U$.

Depending on the physical limitation of the system and the severity of the requirements placed on it by W_P, the H_∞ optimization can meet with various levels of success. For mixed sensitivity H_∞ control the cost function, γ, which is minimized, is a direct measure of that success.

- γ=1: This indicates that all of the weight specifications have been met, such that $\left\| \begin{matrix} W_P S W_R \\ W_U K S W_R \end{matrix} \right\|_\infty < \gamma = 1$. This implies for W_R=I that $|S|<|1/W_P|$ and that $|KS|<|1/W_U|$ at all frequencies.
- γ>1: This indicates that all of the weight specifications have NOT been met. This signifies that $|S|<\gamma|1/W_P|$ and $|KS|<\gamma|1/W_U|$. Therefore as γ increases in value the designed controller is failing to meet the weight specifications more and more. γ quantifies the maximum peak of the infinity norm of the system after minimization. This allows designers to adjust the weight specifications by using the value of γ in specific situations.
- γ<1: This indicates that the H_∞ optimization problem was able to meet all weight specifications easily. Generally when small values of γ are achieved, it is a signal for the designer to adjust weights by making them more demanding.

A design procedure for a mixed-sensitivity H_∞ (S/KS) control has been developed by Skogestad and Postlethwaite[9]. The five step procedure included both disturbance and tracking problems, yet since the intention is to use the mixed-sensitivity H_∞ controller in

the partitioning loop where only tracking is a consideration, a simplified procedure is adequate for our needs. With this in mind the three relevant design steps are paraphrased:

1. Specify W_U and W_R: for a well scaled system, a reasonable initial choice for these weights are W_U=I and W_R=I.
2. Specify W_P: A common choice for the performance weight is $W_P=\mathrm{diag}\{w_{Pi}\}$ Selecting $A_i \ll 1$ ensures approximate integral action with $S(0) \cong 0$. Often we select M_i, the maximum peak magnitude of S_i, to be about 2 for all outputs , whereas ω_{Bi} may be different for each output. A large value of ω_{Bi} yields a faster response for output i.

$$w_{Pi} = \frac{s/M_i + \omega_{Bi}^*}{s + \omega_{Bi}^* A_i}, \quad A_i \ll 1 \tag{58}$$

3. To find a reasonable initial choice for the weight W_P, one can first obtain a controller with some other design method, plot the magnitude of the resulting diagonal elements of S as a function of frequency, and select $w_{Pi}(s)$ as a rational approximation of $1/|S_{ii}|$.

The problem is then placed in the generalized configuration, Figure 33, and a controller is synthesized which minimizes the H_∞ norm of the outputs.

The reliance of the weight selection, W_P, on a controller obtained with "some other design method" is a distinct drawback for mixed-sensitivity H_∞ control, requiring the development of an additional controller or a high degree of intuition about the process. Once this initial guess is achieved, an iterative procedure is used to fine-tune the weight until the desired performance is achieved. Though there are some drawbacks to

the design procedure, the performance of this controller is often significantly better than lower order methods.

H_∞ Loop-Shaping Control

Classical loop-shaping design procedures combined with H_∞ robust stabilization led to the proposal of H_∞ loop-shaping design by McFarlane and Glover[15]. H_∞ loop-shaping control introduces uncertainty into the general control configuration and attempts to stabilize various transfer functions in the face of that uncertainty. Due to the limitations of classical phase and gain margins as indicators of robustness for multivariable loops, uncertainty is modeled by norm-bounded dynamic matrix perturbations. Using such perturbations allows robustness to be quantified by the maximum singular value of the various closed loop transfer functions[9]. The objective of H_∞ loop shaping control is to then minimize the maximum singular value. Unfortunately the introduction of a single perturbation requires that the perturbation is stable. A more general uncertainty model uses two perturbations which are comprised of the coprime factorization of the plant. This uncertainty model has been shown to be very general and useful to H_∞ loop shaping problems even if it less intuitive than other models.

The idea of coprime uncertainty is to describe a family of processes based on uncertainty in the location of zeros and poles in the nominal plant. To get a better understanding of how this works, it is helpful to recall the details of the left coprime factorization of a process, which is defined as:

$$G(s) = M_l^{-1}(s)N_l(s) \qquad (59)$$

$N_1(s)$ should contain all the RHP zeros of the process G(s), while $M_1^{-1}(s)$ should contain all the RHP poles of the process G(s). Since $M_1(s)$ is inverted, these poles are described as zeros in the transfer function. The simplified left coprime factorization for processes where D=0 in the standard state space realization is:

$$\begin{bmatrix} N & M \end{bmatrix} = \left[\begin{array}{c|cc} A+HC & B & H \\ \hline C & 0 & I \end{array}\right] \tag{60}$$

where $H = -YC^t$ and where $Y = Y^t \geq 0$ is the stabilizing solution to the algebraic Riccati equation

$$AY + YA^t - YC^tCY + BB^t = 0 \tag{61}$$

which can be solved in conjunction with the second Riccati equation

$$A^TX + XA - XBB^TX + C^TC = 0 \tag{62}$$

by finding γ_{min}

$$\gamma_{min} = \varepsilon_{max}^{-1} = \left\{1 = \left\| \begin{matrix} N & M \end{matrix} \right\|_H^2 \right\}^{-1/2} = \left(1 + \rho(XY)\right)^{1/2} \tag{63}$$

Figure 37 shows how uncertainty can be expressed in terms of coprime factorization, defining the family of processes $G_P = (M_1 + \Delta_M)^{-1}(N_1 + \Delta_N)$. The benefit of H_∞ loop shaping controller is the ease in which robust stability can be ensured for this broad family of processes. The H_∞ closed solution finds a stabilizing controller, K, for the specified γ according to the following function.

$$\gamma = \left\| \begin{bmatrix} K \\ I \end{bmatrix} (I - GK)^{-1} M^{-1} \right\|_\infty \tag{64}$$

Stability is then guaranteed for all processes provided

$$\left\| \begin{bmatrix} \Delta_N \\ \Delta_M \end{bmatrix} \right\|_\infty < \gamma^{-1} \qquad (65)$$

Hence the minimization of γ allows for the widest latitude in process uncertainty.

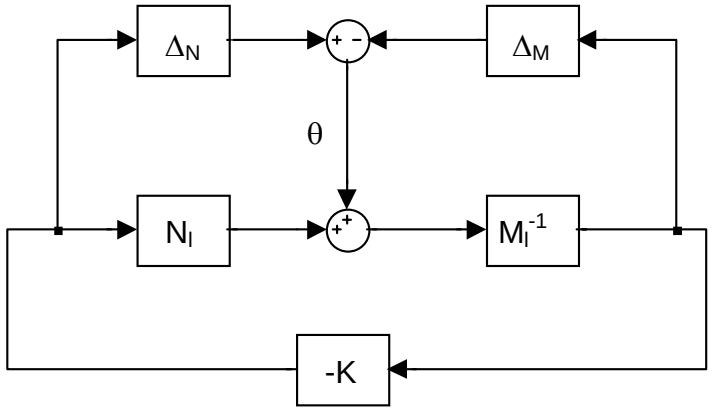

Figure 37: Block diagram describing coprime uncertainty

However, before coprime factorization of the plant can begin, the plant must be "shaped", thus H_∞ controller design is a two step process. The first step is to shape the plant, and the second step is to find a stabilizing controller in the face of coprime uncertainty. "Shaping" the plant consists of augmenting it by pre and post compensators, $Gs = W_2GW_1$. The main objective of compensator selection is to stabilize the nominal process. The selection of the weights W_1 and W_2 requires some skill, but there are general guidelines, which can help the design process. For instance, $W_2 = I$ is a good initial choice for the post compensator, W_2. If a particular output is deemed more important, then W_2 can be used to express the relative importance of the outputs. The selection of the preweight, W_1, is a little more complicated. W_1 should be chosen such

that the shaped plant, Gs, has desirable characteristics. For example, the shaped plant should have high gains at low frequencies, a roll off rate of approximately 20dB/decade at the desired bandwidth, and integral action to enhance low frequency performance. These guidelines may require some trial and error, but have been applied successfully to a wide variety of systems from the robust control of VSTOL (vertical and/or short take-off and landing) aircraft by Hyde[16], to the control of high performance helicopters by Walker and Postlethwaite[18]. The pre weight often takes the shape of a PI controller and as such design can be aided by using tuning rules for PI controllers.

Once the plant is shaped, the second step is to robustly stabilize it via H_∞ optimization in the presents of coprime uncertainty resulting in a controller K_∞. The actual controller is then derived by cascading K_∞ with the weights, $K = W_1 K_\infty W_2$. Walker[19] clearly stated the advantages offered by this design procedure as:

1. Relative simplicity owing to similarities with classical SISO loop-shaping methods;
2. Existence of closed formulation for H_∞ optimal cost $\gamma_{opt} (= 1/\varepsilon_{max})$ [*where* ε_{max} *is the optimum stability margin*];
3. Existence of controllers with an observer/state-feedback structure;
4. Absence of pole-zero cancellation between plant and controller;

What was not stated was that this method is ill suited for solving tracking problems without modification. Since H_∞ loop-shaping controllers are not explicitly designed to handle reference tracking, implementing an H_∞ controller without modification often results in derivative kick. In order to reduce this effect the reference signal is fed directly

into the pre weight W_1 as seen in Figure 38. The addition of a constant to the reference signal insures there will be no steady state offset.

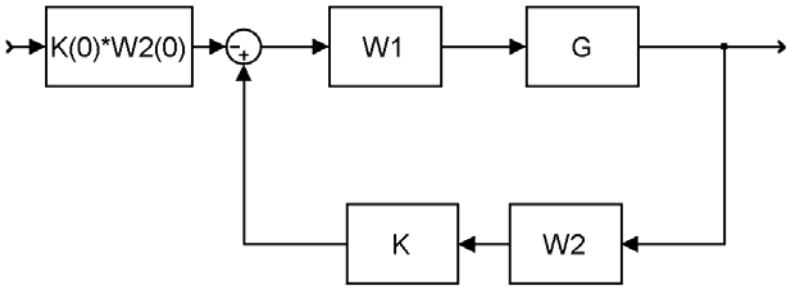

Figure 38: Block diagram describing the implementation of one-degree of freedom H_∞ loop-shaping control. In this implementation the control signal is scaled to prevent steady state offset and fed directly into the pre weight W_1 to prevent derivative kick.

Adaptations have been made expanding H_∞ loop-shaping into two-degree-of-freedom techniques so that tracking considerations can be addressed, but the one degree of freedom design does not consider these tracking issues. Having a controller designed for robust disturbances, however, is not a problem in the PEC architecture where the stability benefits of an H_∞ loop-shaping controller can be fully utilized in the feedback loop while tracking concerns can be handled by a separate controller.

Now the beginnings of design approach for PEC are becoming visible. We will use a Mixed sensitivity controller in the partitioning loop were it is shielded from disturbances, and we will use an H_∞ loop-shaping controller in the feedback loop where it

is shielded from tracking issues. In this way we are using the strengths of each controller and mitigating their respective weaknesses. A full direct comparison between the two-degree of freedom extension of H_∞ loop-shaping control and partitioned error control will be touched upon later in this chapter.

Signal Based H_∞ Control

Signal based H_∞ control attempts to design a single controller capable of handling multiple design objectives by taking advantage of the distinct frequencies in which these design criteria exist. The selection of weights, which separates out these frequencies, requires a high degree of intuition about the process, while the performance benefits of the design are marginal. Since we desire to find simple controllers, which deal with specific problems, Signal based H_∞ control is not suitable to our needs and will not be considered in PEC design.

PEC H_∞ Loop Shaping/Mixed Sensitivity Design Procedure

Now that it has been established that H_∞ loop shaping has qualities that are beneficial to disturbance control and H_∞ mixed sensitivity has qualities that are beneficial to tracking controller, we can formulate a design procedure for the two controllers in the PEC system and see if any benefits arise from the use of these controllers jointly.
The Procedure for the design of PEC using H_∞ loop-shaping/Mixed Sensitivity Control from a modeled plant is as follows:

1. Scale the inputs and outputs of the plant. Scaling helps better formulate control problems and is generally the first step in any controller design. Inputs should be scaled to reflect relative actuator capabilities. For instance, all actuators could be scaled to 10% of their expected ranges, making relative actuator usage comparisons straightforward. Outputs are scaled so that cross-coupling between outputs is equally undesirable. Then the process should be ordered such that it is as diagonal as possible.
2. Decouple the process if necessary
3. Shape the process by defining pre and post weights, W_1 and W_2
4. Synthesize the H_∞ loop-shaping feedback controller
5. Validate controller meets performance and robustness objectives for disturbance problems. Repeat steps 3 and 4 until satisfied
6. Determine if two-degree of freedom control is necessary.
7. Find the frequency response of the sensitivity function, S_{ii}, of the feedback controller, and select the performance weights W_{Pii}. Initially $\frac{1}{|W_{Pii}|} \cong |S_{ii}|$
8. Select the actuator weights, W_U
9. Synthesize the partition loop controller
10. Validate controller performance and stability for nominal tracking problems. Repeat steps 7-10 until satisfied.
11. Validate PEC system as a whole for robust performance.
12. Use model reduction techniques on the total PEC controller if desired

Recall that one of the drawbacks to H_∞ Mixed sensitivity control was in the selection of the performance weight, Wp. It is helpful to have a preexisting controller in order to

generate |Sii| and thus an initial Wp. By designing the feedback controller first, we are giving ourselves that preexisting controller, and a simple and effective way of deriving |Sii|. Of course the sensitivity function of the feedback controller will not meet performance objectives, hence the need for two degree of freedom control in the first place, but it still provides a starting point for an iterative weight selection process.

The Application of the PEC H_∞ Design Procedure

The PEC H_∞ loop shaping/mixed sensitivity controller design procedure will be applied to the now familiar process of Skogestad and Postlewaite[9], Equation (66). A variety of controllers were designed for this process by Skogestad and Postlewaite[9]. Since these controllers were developed for SISO use and were never indented to be used in conjunction with each other, they provide a bias free means of testing the interaction between tracking and regulatory controls in the PEC system.

The process under consideration is defined as follows:

$$G(s) = \frac{200}{10s+1}\frac{1}{(0.05s+1)^2}, \quad G_d(s) = \frac{100}{10s+1} \qquad (66)$$

For this process, both tracking and disturbance rejection are important objectives and are defined by the following three criteria.

1. Command Tracking: The tracking response should have no greater than 5% overshoot. Furthermore, the response should reach 90% of the final value within 0.3 seconds.
2. Disturbance Rejection: The response of a system to a unit step change in the disturbance should not exceed unity. $|y(t)| \in [-1,1]$ for all t. Furthermore, the response should be less than 0.1 after 3 seconds.
3. Input constraints: u(t) should remain within the range of [-1,1].

An additional optimization criteria will be added to showcase some of the differences between different two-degree-of-freedom techniques.

4. Optimize the controller to obtain the lowest Integral of the Time-weighted Absolute value of the Error (ITAE) possible while meeting the first three criteria.

Three controllers will be compared by the end of this study, One-Degree-of-Freedom H_∞ Loop-Shaping control, PEC using H_∞ Mixed Sensitivity and H_∞ Loop-Shaping Control, and Two-Degree-of-Freedom H_∞ Loop-Shaping control. A One-Degree-of-Freedom solution will be sought first. It is expected from previous experience with the system that the one-degree-of-freedom controller will provide an adequate solution to this problem. The minimum phase system that is being used as an example is not the best candidate to challenge two-degree-of-freedom design. However, the simplicity of this system does benefit in the analysis of the tuning procedures used to optimize the process. Once the ODoF design has reached the limits of its capabilities, a

Partitioned Error Controller will be developed. Finally, a Two-Degree-of-Freedom H_∞ Loop-Shaping controller will be developed to highlight the differences in obtaining an optimal solution using alternative techniques. While reviewing the different designs keep in mind that both Two-Degree-of-Freedom controllers will end up with almost identical performance characteristics. The difference between the controllers will be found in the relative subjectiveness or objectiveness of their respective tuning procedures. The system responses to a ±40% error in the gain will be shown to not only demonstrate nominal similarities in performance but to demonstrate robust similarities as well.

From previous experience with this system we know it is well scaled and balanced, we also know that there are no loop interactions in a SISO system. This satisfies steps 1 and 2 of the design procedure.

For step 3 of the procedure we begin to design a ODoF H_∞ loop-shaping controller by selecting pre and post weights to shape the plant. Skogestad and Postlewaite[9] argued that the shaped plant would have the following form: $|G_s| = |GW_1| \approx |G_d|$. This argument is by no means trivial. The design is specifically attempting to give the shaped system characteristics of the disturbance so that the system will respond better to regulatory problems. This standard technique in H_∞ loop-shaping designs helps disturbance rejection to the detriment of setpoint tracking. Neglecting high frequency dynamics, $s \to 0$, they started with W_1=0.5 to match the desired form. They then added integral action for better low frequency performance giving $W_1 = \frac{0.5}{s}$. A phase advance term, s+2, was then added to reduce the slope to about –1 at the crossover frequency. Then to increase the response time the gain was then multiplied by a factor of 2, resulting in the following pre weight.

$$W_1 = \frac{s+2}{s} \qquad (67)$$

A post weight, W_2, could be selected to weight the relative importance of disturbance rejection over actuator usage, but at this time there is no need for such a weight so a value of W_2=1 will be used

In step 4 of the procedure the shaped plant Gs was sub optimally "robustified" to tolerate maximum coprime uncertainty. The resulting 5 state controller has a gamma of 2.34.

$$K_2 = \frac{-1.258e004\ s^4 - 5.707e005\ s^3 - 7.599e006\ s^2 - 2.231e007\ s - 1.859e007}{s^5 + 6011\ s^4 + 3.965e005\ s^3 + 1.061e007\ s^2 + 1.967e007\ s} \qquad (68)$$

Figure 39 shows the robust disturbance rejection plots of the controller in Equation (68). It is readily apparent from that figure that the controller meets all disturbance rejection design criteria satisfactorily, satisfying step 5 of the design procedure.

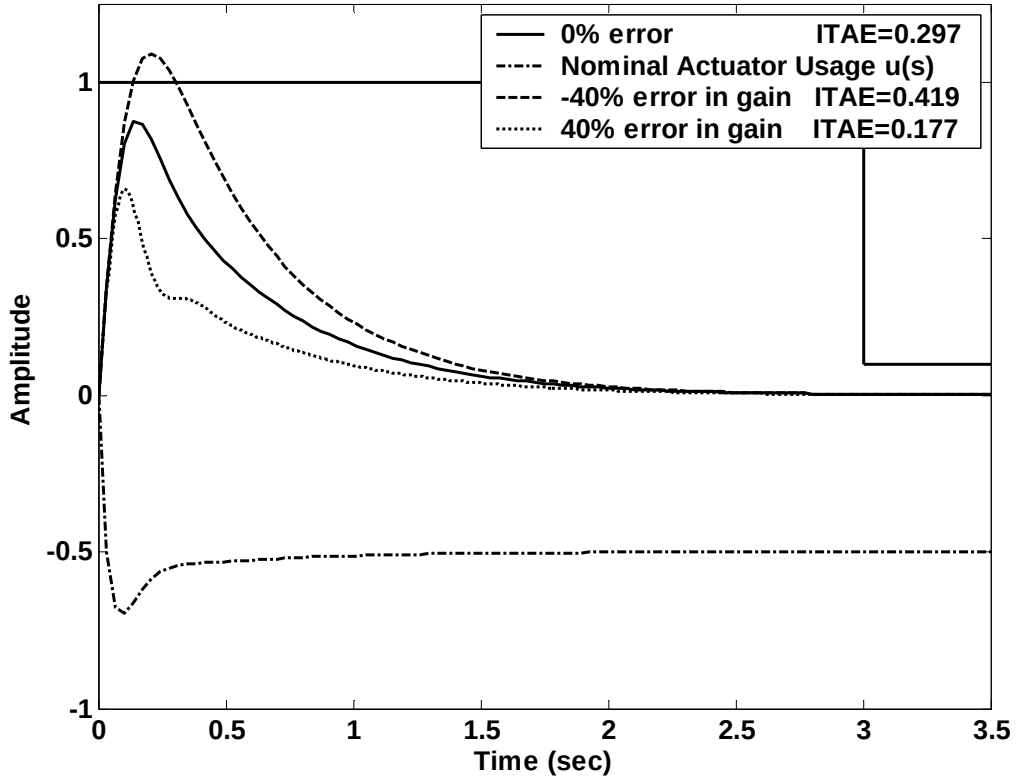

Figure 39: Initial regulatory response of the ODoF H_∞ loop-shaping controller for the process defined in Equation (66) for gain estimation error of 0% (with actuator usage), -40%, and 40%. Performance objectives are defined by solid lines.

Step 6 in the design procedure we determine if two-degree of freedom control is necessary. To do this, we can subject the controller, Equation (68), to a step test under nominal conditions, or we can test the performance of the controller under robust conditions. Since an algorithm was developed for testing the disturbance response for a perturbed process, it is a fairly simple matter to subject the tracking response to the same perturbations in the process gain. Figure 40 shows a plot of this test. The response was not only able to meet performance criteria under nominal conditions, but nearly meets those same criteria under robust conditions. At this point we have found a one-degree of freedom controller which passes the first 3 acceptance criteria. The actuator usage of the servo and regulatory response is well within the allowed limits. This indicates that we can optimize the controller to achieve better performance. This optimization will be the next step in the design.

Recall that ODoF H_∞ loop shaping controller design seeks to minimize the H_∞ norm of 2 functions, one disturbance rejection function and one actuator usage function. In order to optimize the controller design we will shift the relative weighting of these two functions to emphasize the importance of disturbance rejection and allow more actuator usage. This is very simply done by increasing the value of the post weight of the shaped plant, W_2. The value of W_2 was increased iteratively to a value of 2.1 which gives us a peak actuator usage for disturbance rejection of -1. The regulatory and servo responses of this new controller can be seen in Figure 41 and Figure 42 respectively. The ITAE of both responses have been enhanced, there are however some characteristics of the responses that leave room for improvement. The actuator usage of the regulatory response is oscillatory. This is a characteristic of excessive integral action. Ideally this

integral action could be reduced. Additionally, the actuator usage of the servo response has not been maximized, yet overshoot on the servo response is approaching our acceptance criteria boundary.

The next step in the optimization will be to add derivative action to the preweight W_1 in order to reduce the oscillation in actuator usage. This modification is in line with the loop shaping technique used to define the control law presented in Equation (18). The new value of W_1 can be seen in Equation (69).

$$W_1 = \frac{s+2}{s}\frac{0.05s+1}{0.005s+1} \qquad (69)$$

The preweight W_1 was used and the post weight was once again iteratively increased to a value of 2.7 until the maximum actuator usage was obtained resulting in the final ODoF design with regulatory and tracking responses found in Figure 43 and Figure 44 respectively. The ITAE regulatory response of the ODoF H_∞ controller was reduced from an initial value of 0.297 to 0.177 during the optimization process. The ITAE tracking response of the controller was reduced from an initial value of 0.025 to 0.015 during the optimization process. Unfortunately, the initial control action exceeds the limits imposed by criteria #3, u(t) should remain within the range of [-1,1]. Obviously this could be adjusted by the use of a lead-lag prefilter with the following side effects.

- Lower Performance: Slowing down the initial response will increase the ITAE of the response.
- Larger Size. The current ODoF controller has 7 states, adding a prefilter will increase the total number of states of the controller to 8.

- Better Scalability: The addition of a prefilter may be an acceptable technique for SISO systems, but for MIMO processes it would be preferable to find a technique that looked at the total system response.

This solution would work, but there is a better alternative. Using PEC a systematic procedure can be followed to find an easy to obtain solution that will increase the systems performance without increasing the number of states of the controller, and provide better scaling.

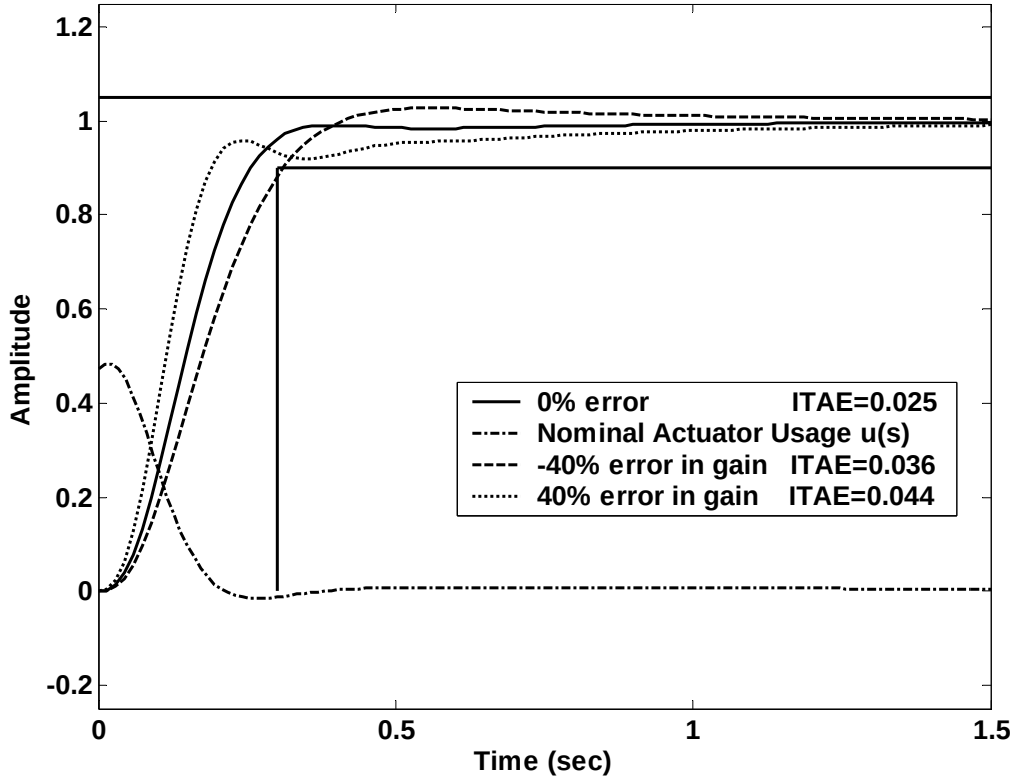

Figure 40: Initial tracking response of the ODoF H_∞ loop-shaping controller for the process defined in Equation (66) for gain estimation error of 0% (with actuator usage), -40%, and 40%. Performance objectives are defined by solid lines.

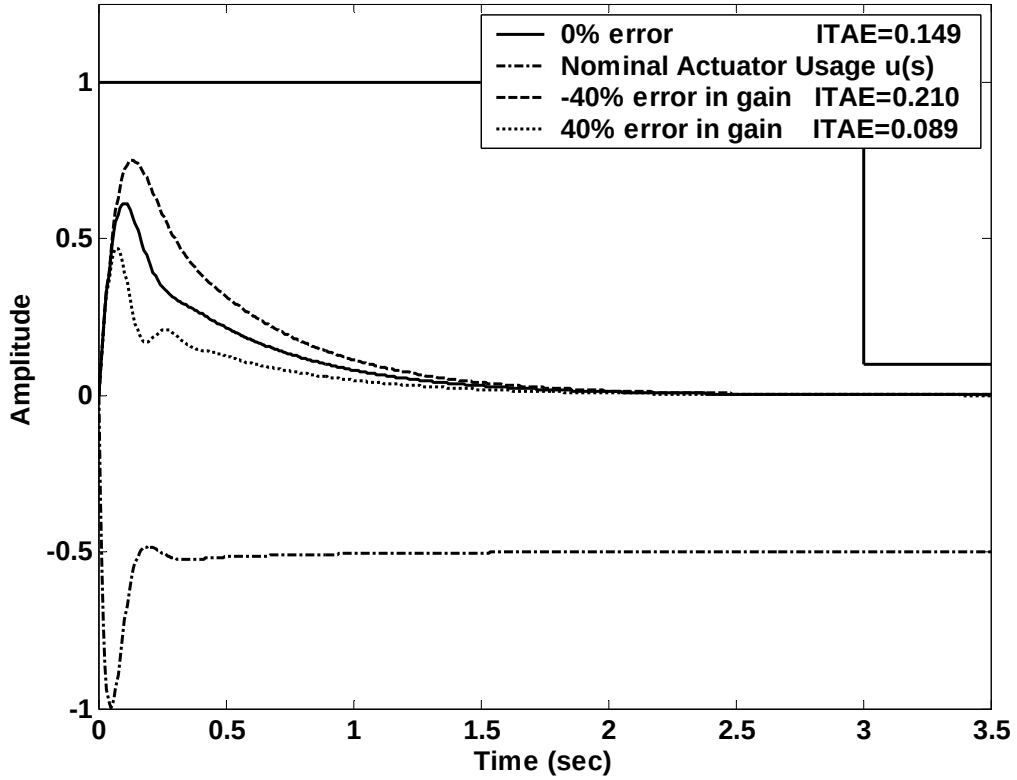

Figure 41: Intermediate regulatory response of the ODoF H_∞ loop-shaping controller for the process defined in Equation (66) for gain estimation error of 0% (with actuator usage), -40%, and 40%. Performance objectives are defined by solid lines.

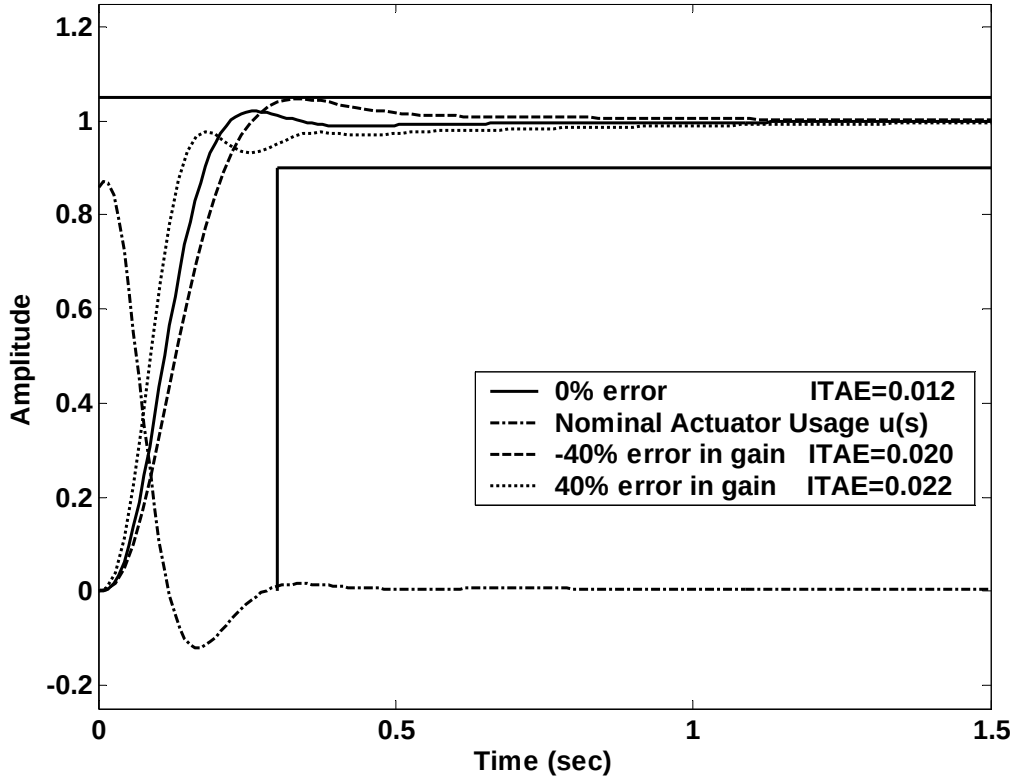

Figure 42: Intermediate tracking response of the ODoF H_∞ loop-shaping controller for the process defined in Equation (66) for gain estimation error of 0% (with actuator usage), -40%, and 40%. Performance objectives are defined by solid lines.

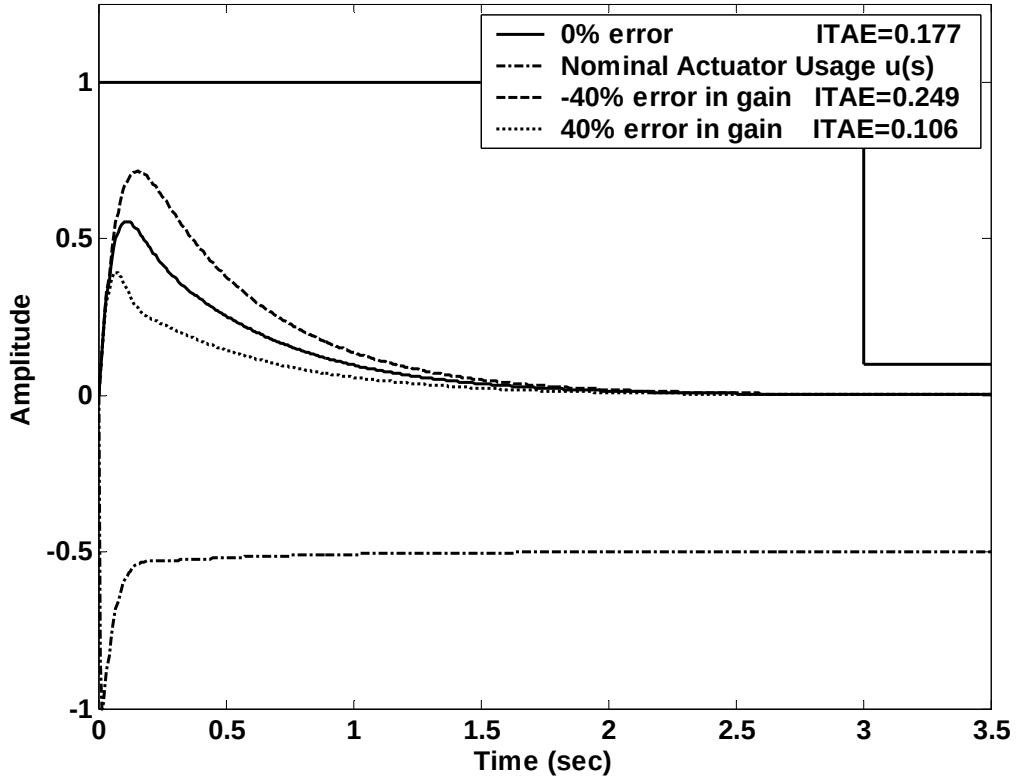

Figure 43: Final regulatory response of the ODoF H_∞ loop-shaping controller for the process defined in Equation (66) for gain estimation error of 0% (with actuator usage), -40%, and 40%. Performance objectives are defined by solid lines.

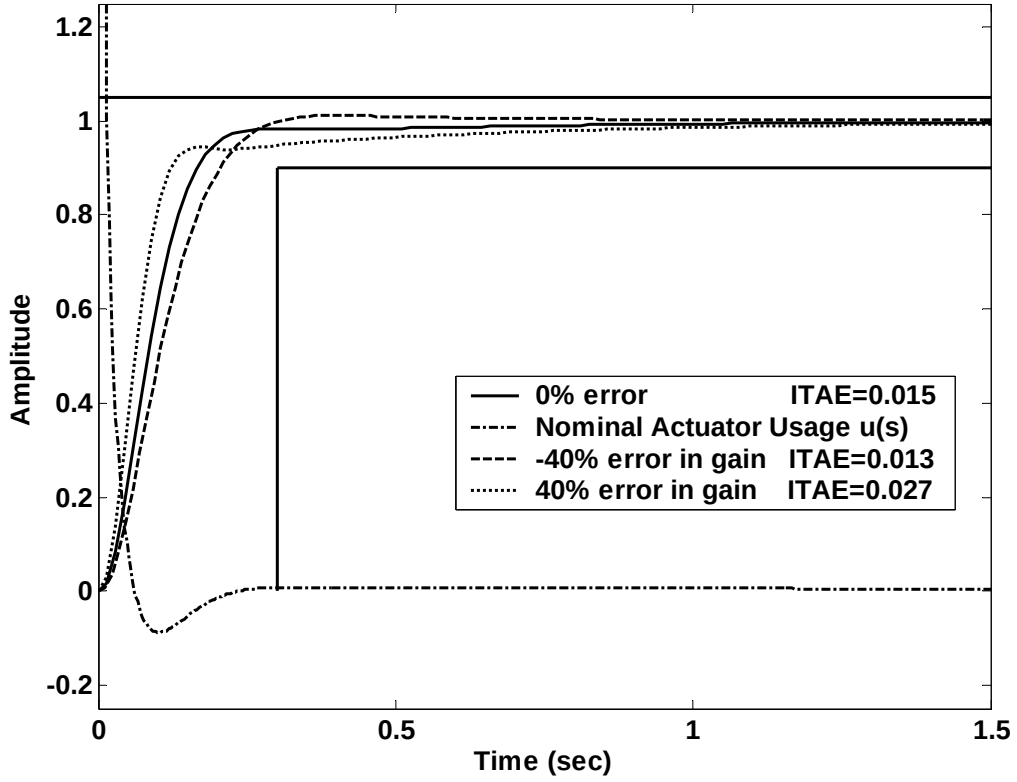

Figure 44: Final tracking response of the ODoF H_∞ loop-shaping controller for the process defined in Equation (66) for gain estimation error of 0% (with actuator usage), -40%, and 40%. Performance objectives are defined by solid lines.

In Step 7 of the PEC design procedure we will begin the design of a H_∞ Mixed Sensitivity tracking controller. The first step of which is to determine performance weights by using a preexisting controller, in this case the we will use the ODoF H_∞ loop-shaping controller described in Equation (68). This was the initial ODoF controller and has the worst tracking response of all the controllers that were examined. It represents the worst choice that is available. This controller may be used to aid in the initial selection of the three parameters in the performance weight, A, M, and ω_b, in Equation (58). The bode magnitude diagram of the sensitivity function, S, of the ODoF controller is shown in Figure 45 along with inverse of the performance weight $|1/W_P|$ with A=1e-4, M=2, and ω_b=15. Of these 3 parameters, A was chosen to be small to approximate integral action at low frequencies, M was chosen as the default initial value of 2, and only ω_b was adjusted to match the bandwidth characteristics of the sensitivity function.

Using the initial performance weight as shown in Figure 45 and W_U=1 the default initial guess for the actuator weight, a H_∞ mixed sensitivity controller is synthesized. The tracking performance of this controller is shown under nominal conditions in Figure 46. The controller gives a slight overshoot, and meets the performance specifications with ITAE=0.009, lower then the final ODoF controller (ITAE=0.015). The increased performance of the H_∞ mixed sensitivity controller demonstrates that the use of the H_∞ loop shaping controllers' sensitivity function for the design of a tracking controller provides an acceptable initial guess, and significantly reduces the design effort for the performance controller. This figure also shows that the actuator usage exceeds the design criteria, however, we now have a very specific tool for controlling our actuator usage, the actuator weight W_U. With this tool, we can specify the desired performance

characteristics of the tracking response and the desired characteristics for actuator usage, and find the best solution which balances these considerations. In this case the performance weight is acceptable and we merely need to increase the value of the actuator weight until the design criteria is met. The final value of W_U=1.8 was found from this iterative procedure. The final tracking controller can be seen in Figure 47. With an ITAE of 0.012 the performance of this controller exceeds the ODoF controller. In the end very little effort was exerted to achieve this response, we were able to leverage the work done on the regulatory controller, and we were able to use a tracking controller with tunable parameters that had clear significance to the problem at hand. The finalized H_∞ Mix Sensitivity controller completes steps 8, 9 and 10 of the PEC design procedure.

Since this H_∞ mixed sensitivity controller will function in the partitioning loop where no modeling error exists, there is no need to examine the robustness of this controller. The feedback controller solely determines the robustness of the PEC system. Therefore, the next logical step is to determine the robust performance characteristics for the integrated PEC system.

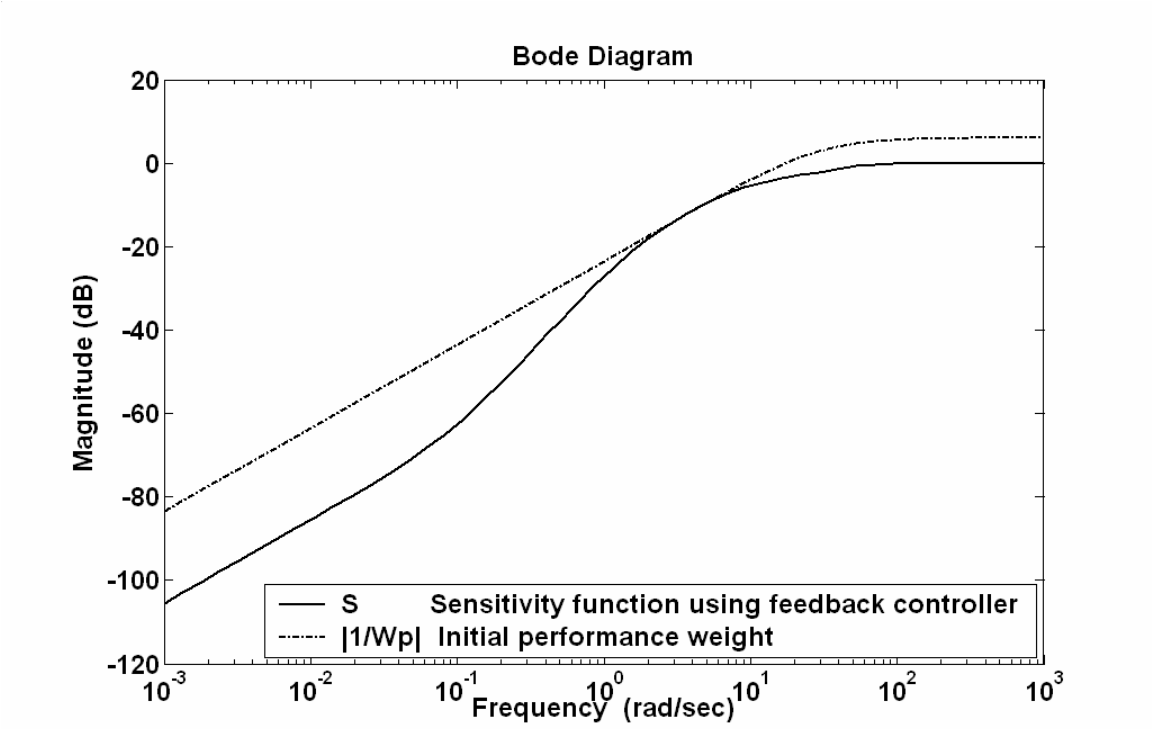

Figure 45: Initial guess of the inverse of the performance weight $|1/W_P|$ as an approximation of the sensitivity function for the process defined in Equation (66) under feedback control defined by Equation (68).

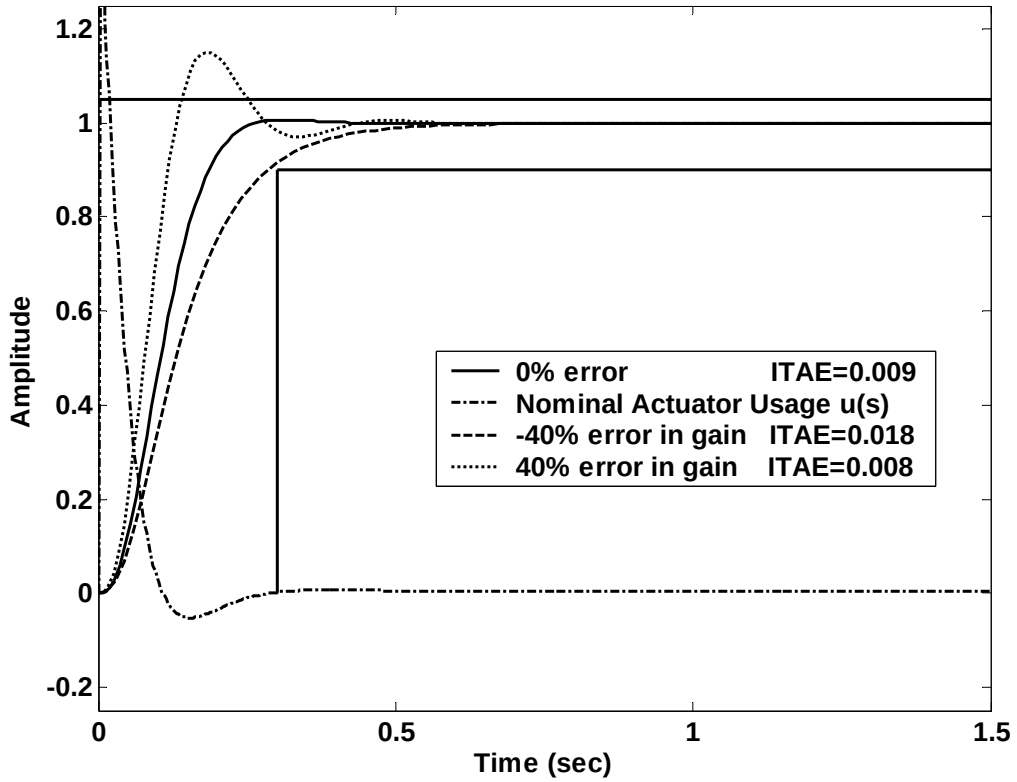

Figure 46: The initial tracking response of the H_∞ Mixed Sensitivity controller for the process defined in Equation (66) for gain estimation error of 0% (with actuator usage), -40%, and 40%. Performance objectives are defined by solid lines.

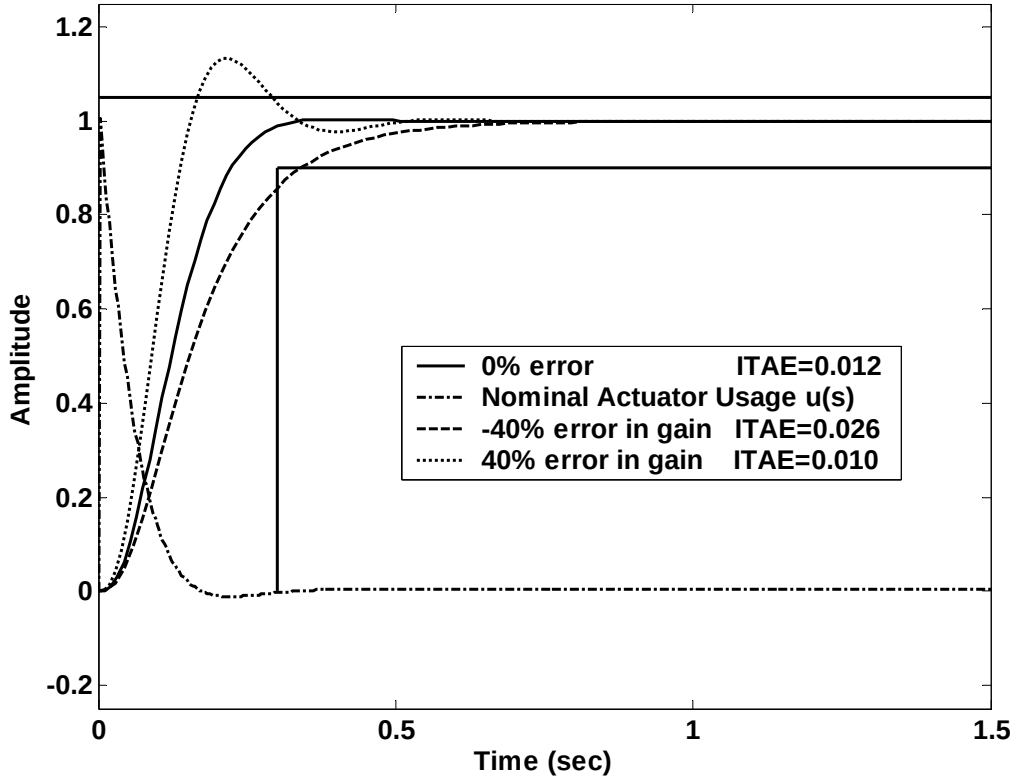

Figure 47: The final tracking response of the H_∞ Mixed Sensitivity controller for the process defined in Equation (66) for gain estimation error of 0% (with actuator usage), -40%, and 40%. Performance objectives are defined by solid lines.

In order to examine the robust performance of PEC, we first need to assemble the two controllers and the model. Since the H_∞ loop-shaping controller uses positive feedback, there is a slight modification needed to the assembly of the final PEC controller. Figure Figure 48 shows the proper way to incorporate a positive feedback controller. The significant point to remember is that the controller in the feedback loop should receive a signal that is the difference between the process and the process model. In the case where positive feedback is used in the feedback loop a sign change is required where the process/model difference is calculated.

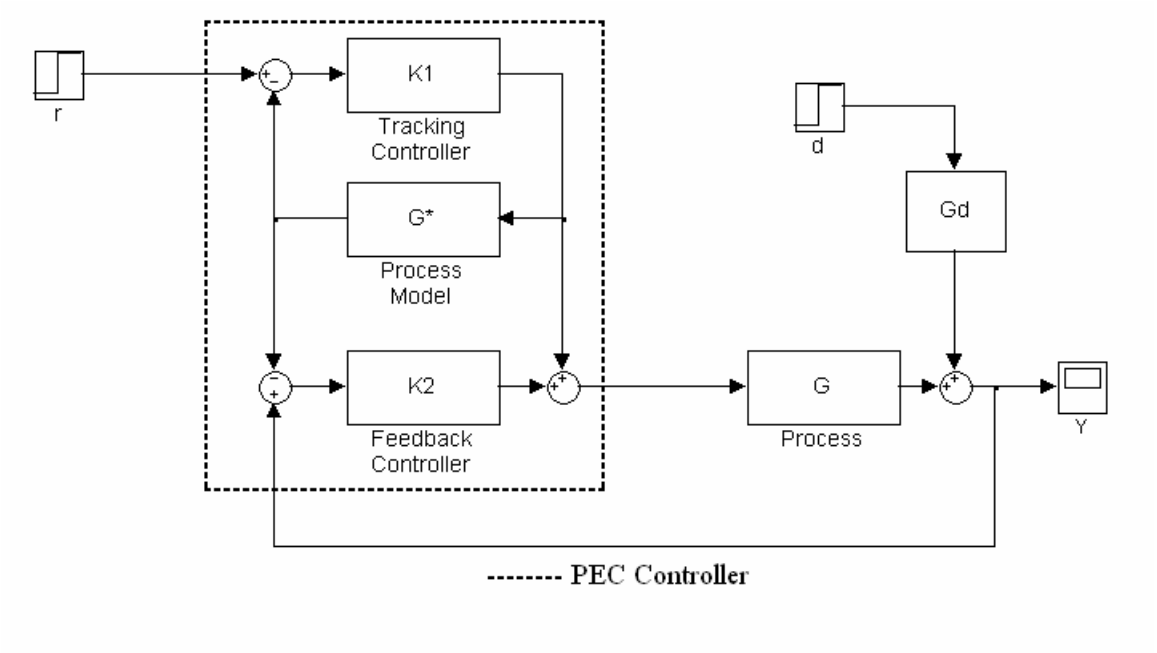

Figure 48: The proper implementation of positive feedback control in the PEC structure

The assembled controller was subjected to modeling error resulting in the tracking and regulatory performance shown in Figure 49 and Figure 50 respectively. As we expected, the nominal performance and nominal actuator usage of the PEC controllers is

identical to the nominal performance and nominal actuator usage of the two controllers which it is comprised of. Upon comparison of Figure 47 and Figure 49 there is a difference in the tracking response in the presence of modeling error between the H_∞ mixed sensitivity controller and the response of the PEC controller. The mixed sensitivity tracking controller has traded performance for robustness, but by placing that controller inside the partitioning loop, we have placed it in a nominal environment, free of robust considerations. All modeling error is compensated for by the feedback controller, resulting in the slower but more robust response of the system in the presence of modeling error.

The resulting PEC controller has 13 states, 2 inputs, and 1 output, including the internal model, which is excessive for a process with only 3 states. The size of the controller is not totally unexpected, since both the H_∞ loop-shaping and H_∞ mixed sensitivity techniques tend to synthesize controllers greater than or equal to the order of the process model. Add the process model to the two fairly large controllers and it can be expected that the overall partitioned error controller with have greater than 3 times the number of states as the process model, and would be cumbersome to implement for large systems. This is a common problem with all H_∞ controllers which is exacerbated by the inclusion of two such controllers it the PEC structure. There are several model reduction techniques available that can be used to alleviate this problem, however.

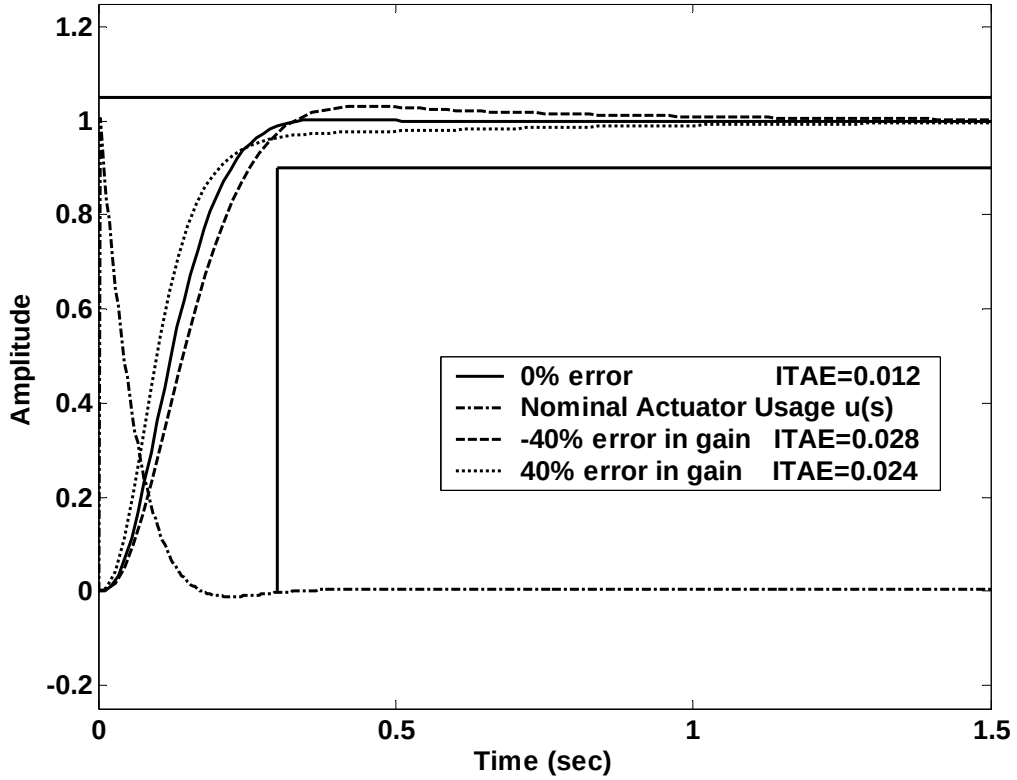

Figure 49: The final tracking response of the PEC controller for the process defined in Equation (66) for gain estimation error of 0% (with actuator usage), -40%, and 40%. Performance objectives are defined by solid lines.

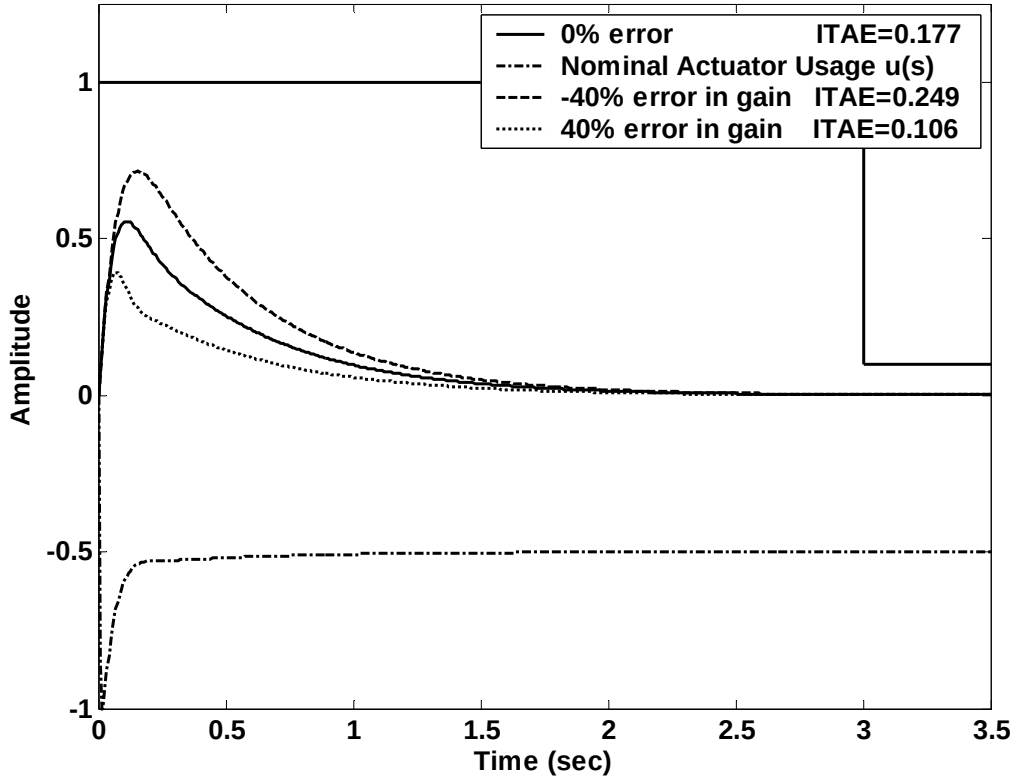

Figure 50: The final regualtory response of the PEC controller for the process defined in Equation (66) for gain estimation error of 0% (with actuator usage), -40%, and 40%. Performance objectives are defined by solid lines.

Model Reduction Techniques and PEC

H_∞ controllers with large numbers of states can generally benefit from the application of model reduction techniques. This also holds true for the H_∞ controllers nested in the PEC structure. Model reduction techniques are applied in three ways. They can be applied to the model before controller design, or after controller design they can be applied to each component separately or to the system as a whole. Each of these techniques provides a slightly different benefit to the system.

First, the system model can be reduced before controller design. For controllers that have a predefined form such as PID controllers, this technique does not have a benefit, but for H_∞ controllers which are generally slightly larger then the process model, any reduction in the order of the process model before the controllers are designed will directly impact the order of the controllers.

Second, all components to the system can be designed and then reduced separately. This would be the recommended procedure if the designer wanted access to the individual outputs of the controllers and model, say for purposes of online model validation. For a SISO system this would result in the reduction of three separate 1 input, 1 output transfer functions, the model output, the partitioning loop controller output, and the feedback controller output. Since, we would be trying to retain the integrity of three output signals we would not expect a significant reduction in the number of states in the controller to occur. This type of reduction is beneficial in the analysis of the system, but a more practical approach would be to preserve only critical information which in the case of PEC is only the total controller output.

The third alternative is to find a less computationally intensive controller by reducing PEC as a whole. For a SISO system we would be reducing the model and both controllers to a single 2 input, 1 output controller, see Figure 48. By only preserving critical information, the controller will be reduced to the lowest order. Since this alternative provides the least computationally intensive controller, it will be the one used in this study.

Now that the type of reduction has been determined, a technique must be chosen. There are a variety of techniques available including truncation, residualization, and Hankel norm approximation. Of these techniques we will be using balanced residualization. The objective of balanced residualization is to first balance the Hankel norm of the process so that it is as controllable as it is observable, Q=P.

$$\|K\|_H = \sqrt{\rho(PQ)} \qquad (70)$$

Where ρ is the spectral radius, P is the controllability Gramian and can be obtained from the solution of the Lyapunov equation $AP + PA^T = -BB^T$, and Q is the observability Gramian and can be obtained from the solution of $A^TQ + QA = -C^TC$. Next the system is ordered by Hankel singular values and the derivatives of the least controllable and observable states are set to zero. Figure 51 displays the Hankel singular values for the unreduced system. The reduction of the partition error controller produced the following 7 state controller:

$$K_{PEC} = \frac{6.7810e\text{-}5s^7 + 1.8585e4s^6 + 1.6459e8s^5 + 4.3218e10s^4 + 2.5068e12s^3 + 5.8533e13s^2 + 5.7864e14s + 9.1671e14}{1.3115e\text{-}5s^7 - 2.0480e5s^6 - 3.6089e9s^5 - 2.6479e11s^4 - 7.7220e12s^3 - 1.0982e14s^2 - 6.9561e14s - 9.1689e14} \qquad (71)$$
$$s^7 + 2.6485e4s^6 + 1.5923e8s^5 + 4.3564e10s^4 + 3.0259e12s^3 + 6.6371e13s^2 + 5.9549e14s + 7845.1$$

A frequency plot of singular values for Kpec was compared to the original 13 state controller and was found to have a negligible residual over all operable frequencies, Figure 52. To further verify the reduction technique the step response of the system was analyzed and found to be indistinguishable from the original controller.

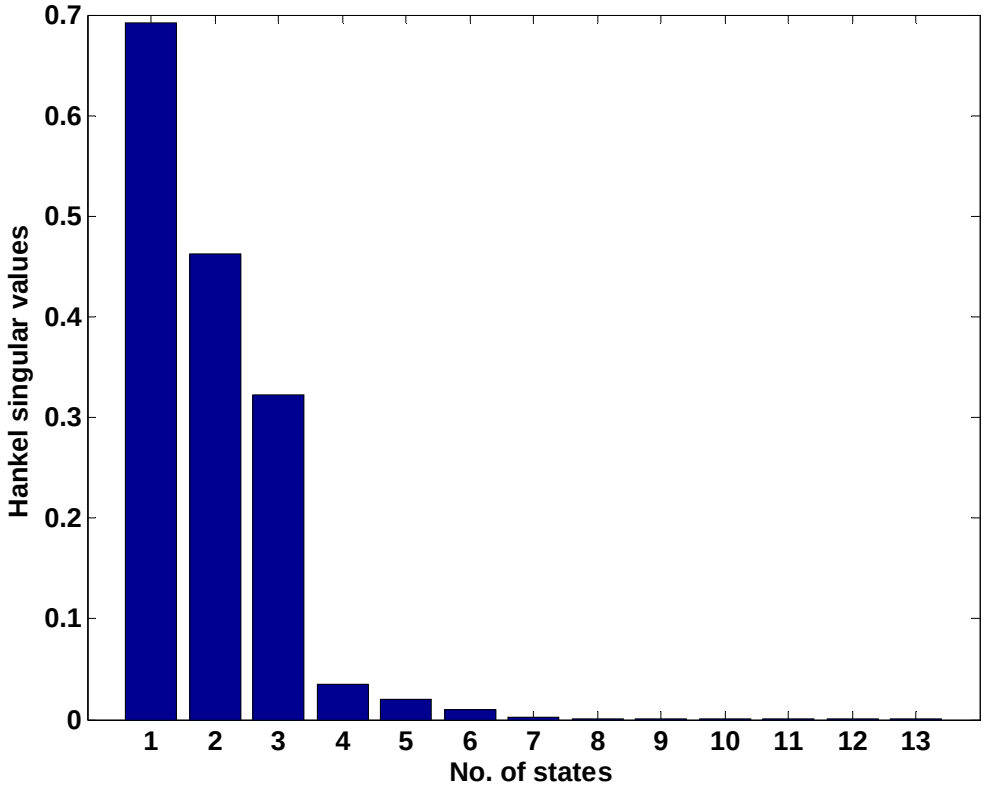

Figure 51: A graphical representation of the Hankel Singular Values of the 13 state PEC controller.

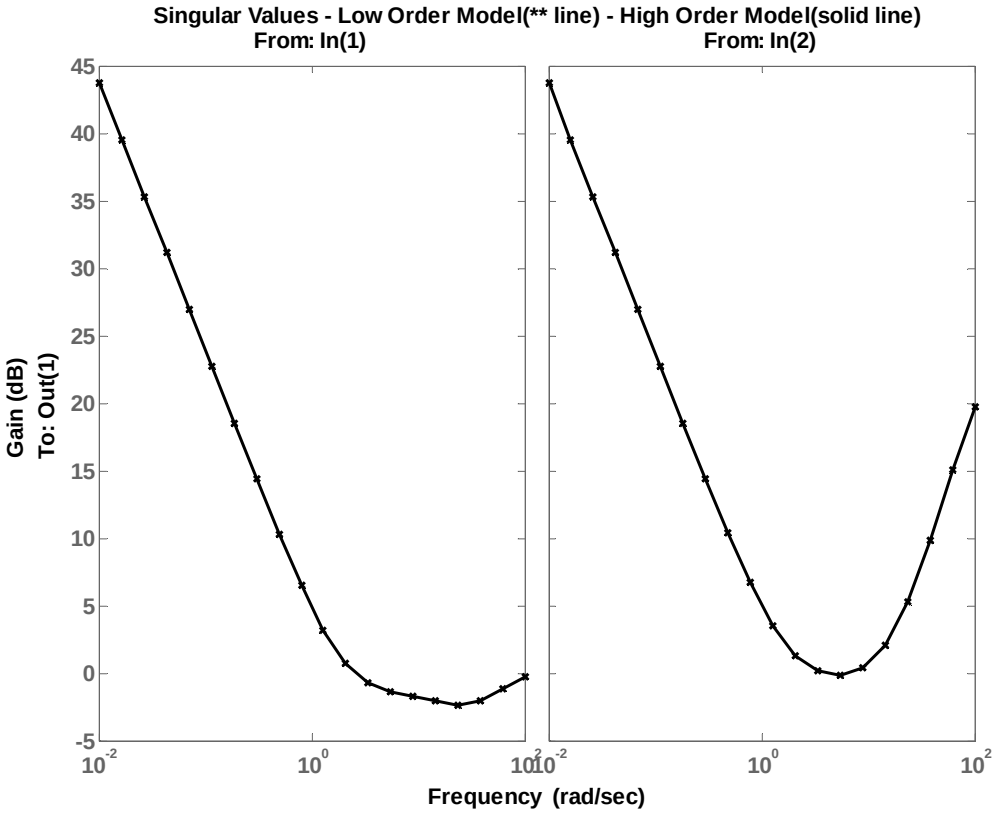

Figure 52: The singular values as a function of frequency for the original 13 state PEC controller and the reduced 7 state PEC controller. Input 1 shows the tracking response, while input 2 shows the disturbance response.

Alternative Two Degree-of-Freedom H_∞ Techniques

Partitioned error control is not the only two-degree of freedom (TDOF) technique, which integrates H_∞ control. H_∞ loop-shaping TDOF control was developed by Hoyle et al.[17] as an adaptation for H_∞ loop-shaping techniques which introduces a tracking element into the controller design through use of a prefilter and a reference trajectory. The general formulation of the H_∞ TDOF controller is shown in Figure 53.

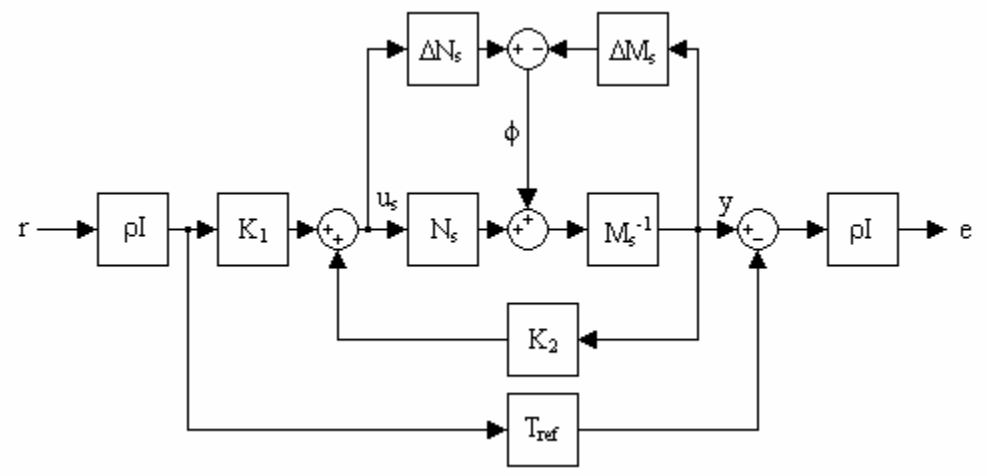

Figure 53: Block diagram describing the H_∞ TDOF problem formulation

This figure directly leads to the following equations:

$$\begin{bmatrix} u_s \\ y \\ e \end{bmatrix} = \begin{bmatrix} \rho(I - K_2G_s)^{-1}K_1 & K_2(I - G_sK_2)^{-1}M_s^{-1} \\ \rho(I - G_sK_2)^{-1}G_sK_1 & (I - G_sK_2)^{-1}M_s^{-1} \\ \rho^2[(I - G_sK_2)^{-1}G_sK_1 - T_{ref}] & \rho(I - G_sK_2)^{-1}M_s^{-1} \end{bmatrix} \begin{bmatrix} r \\ \phi \end{bmatrix} \qquad (72)$$

In the optimization, the H_∞ norm of the block matrix transfer function in Equation (72) is minimized. Hence, the final solution to the problem will be a compromise

between all of these objectives. This is in contrast to mixed sensitivity H_∞ control which only sought to minimize the H_∞ norm two functions, one tracking function and one actuator usage function as seen in Equation (54), and the H_∞ one-degree-of-freedom controller which sought to minimize the H_∞ norm of two functions, one disturbance rejection function and one actuator usage function as seen in Equation (64).

The inclusion of the constant ρ as a gain on the reference signal allows the designer to emphasize the tracking function $\rho^2[(I-G_sK_2)^{-1}G_sK_1 - T_{ref}]$ over the other functions in the matrix providing a method for emphasizing controller tracking during the H_∞ optimization. Better tracking can be achieved by increasing the weighting, ρ, however, using a ρ>1 also deemphasizes controller usage in favor of error tracking. This trade off may be favorable for some categories of problems but in practice large values of ρ tend to cause undesirable effects on multivariable systems. For this reason values of ρ between 1 and 3 are recommended.

At this time it is beneficial to examining the effects of ρ on the block matrix transfer function in Equation (72) in greater detail. By examining the transfer functions from ϕ to u_s and y (Equation (73)), we see that these are the same transfer functions who's H_∞ norm is minimized in the one-degree-of-freedom H_∞ loop-shaping controller (Equation (64)), and that increasing values of ρ have no effect on these transfer functions.

$$\begin{bmatrix} u_s \\ y \end{bmatrix} = \begin{bmatrix} K_2(I-G_sK_2)^{-1}M_s^{-1} \\ (I-G_sK_2)^{-1}M_s^{-1} \end{bmatrix} [\phi] \qquad (73)$$

$$[e] = \left[\rho(I-G_sK_2)^{-1}M_s^{-1}\right][\phi] \qquad (74)$$

The transfer function from ϕ to e does contain the weight ρ, however, as seen in Equation(74). The transfer function from ϕ to y is identical to the transfer function from ϕ to e, so by increasing the value of ρ the minimization problem is being shifted towards disturbance rejection (ϕ to e and thus ϕ to y), and away from actuator usage (ϕ to u_s). The result is that as values of ρ increase more aggressive control will be taken to mitigate the effects of disturbances on the system. Demands on actuator performance can quickly become unrealistic for large values of ρ.

In order to examine the specific effects of the tuning parameter ρ a H_∞ TDOF controller was synthesized for the process defined in Equation (66). The same preweight, $W_1 = \frac{s+2}{s}$, was used to shape the process as was used in the one degree of freedom H_∞ loop-shaping design utilized by the PEC system earlier in this chapter. The reference trajectory, $\left(\frac{y}{r}\right)_{Ref} = \frac{1}{0.1s+1}$, was taken from the work done by Skogestad and Postlethwaite[9] from their lead/lag prefilter design used as an example in chapter 2, and the tracking performance weight, ρ, was set to unity. The resulting controller has 6 states. The nominal ITAE value of 0.265 represents a 10% reduction from the ODOF nominal ITAE of 0.297. These values indicate that the H_∞ Tdof loop-shaping controller is a minor improvement to the ODOF controller stability wise, but roughly equivalent as we would expect. Figure 54 shows the disturbance response of the ρ=1 controller in the presents of modeling gain error.

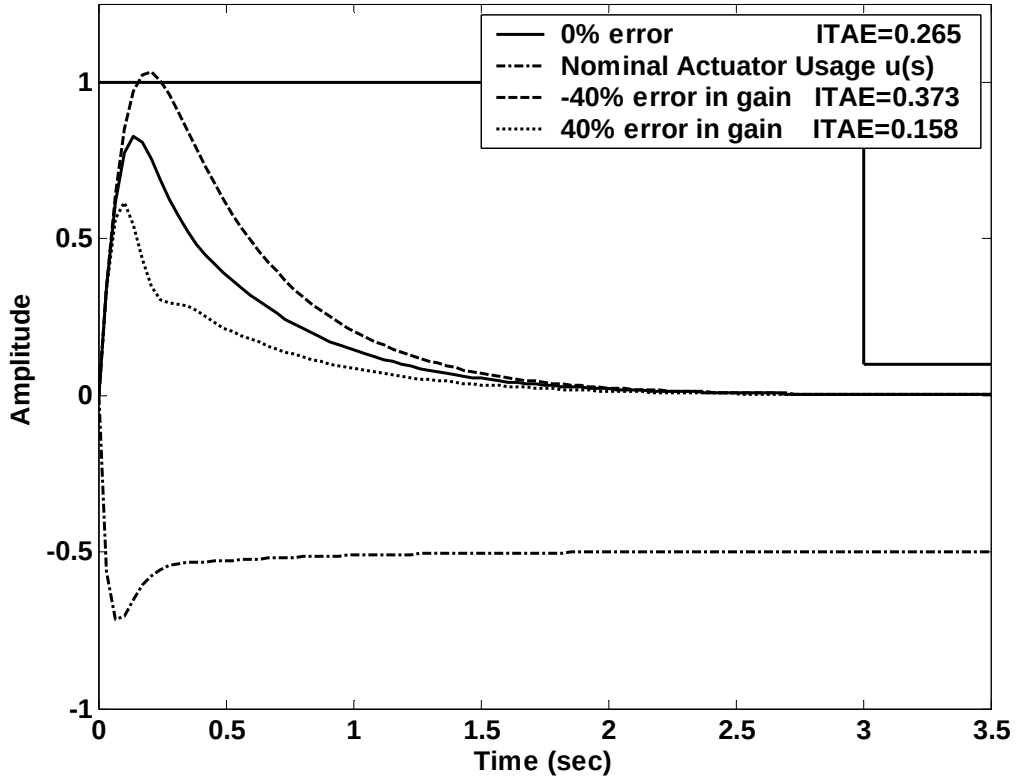

Figure 54: Disturbance rejection of a H_∞ two-degree of freedom controller, ρ=1, for the process defined in Equation (66) for gain estimation error of 0% (with actuator usage), -40%, and 40%. Performance objectives are defined by solid lines.

The system was redesigned by changing the tuning parameter to ρ=4, so the effects of the change could be studied. We have speculated that an increase in ρ will give us better disturbance rejection by loosening restrictions on actuator usage. Figure 55 shows the disturbance response of the ρ=4 controller in the presents of modeling gain error. The nominal ITAE value of 0.212 represents a 29% reduction from the ODoF nominal ITAE of 0.297. Figure 56 shows a plot of the actuator usage of the H_∞ ODOF controller and the H_∞ TDOF controller with ρ=1 and ρ=4 in the nominal setting. This plot clearly confirms the effect of the ρ on disturbance rejection in the design process. This emphasis on disturbance rejection over actuator usage could have been achieved in the ODoF controller by the use of a constant post weight, W_2. The distinction comes from the fact that any change in a tuning parameter of an H_∞ TDoF controller has an impact on multiple characteristics of the process.

Tuning ρ not only has an impact on disturbance rejection, but servo tracking as well. As ρ increases, more emphasis is shifted to the transfer function from r to e, and less is weight is given to actuator usage. Therefore, as ρ increases more aggressive control will be used make the actual system response look like the reference trajectory. It is important to note that as the actual controller tracking approaches the reference trajectory, $\left[\left(I - G_s K_2\right)^{-1} G_s K_1 - T_{ref}\right] \rightarrow 0$, larger and larger values of ρ are required to continue to make this term significant in the norm minimization problem relative to the other transfer functions that are being minimized.

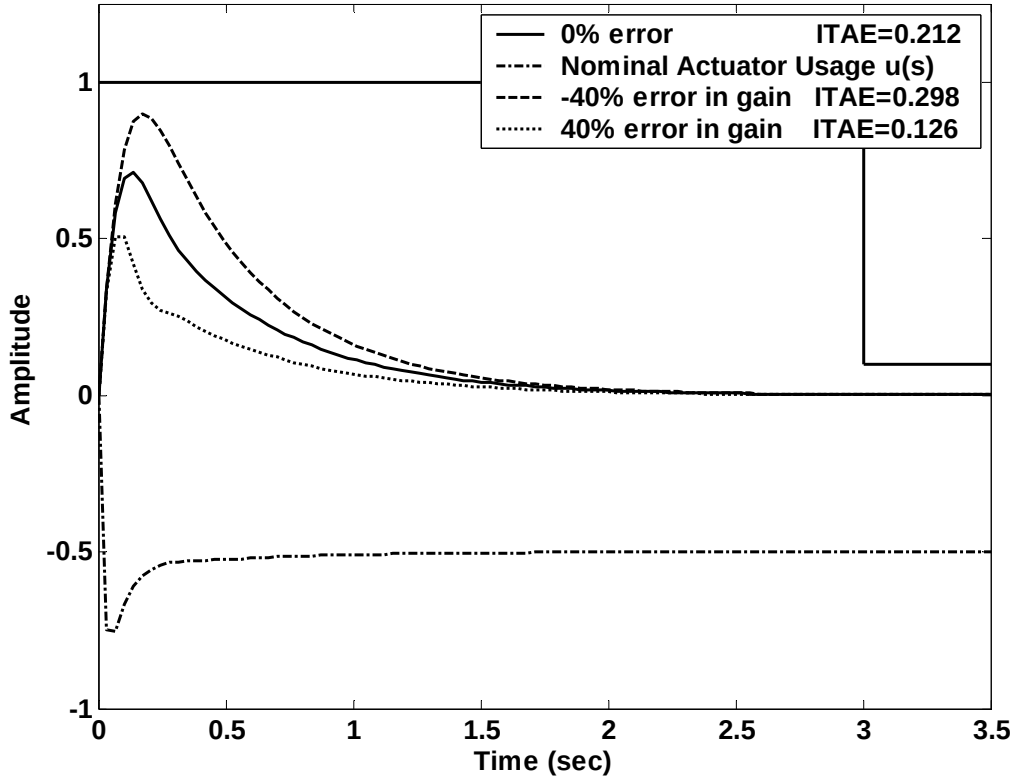

Figure 55: Disturbance rejection of a H_∞ two-degree of freedom controller, ρ=4, for the process defined in Equation (66) for gain estimation error of 0% (with actuator usage), -40%, and 40%. Performance objectives are defined by solid lines.

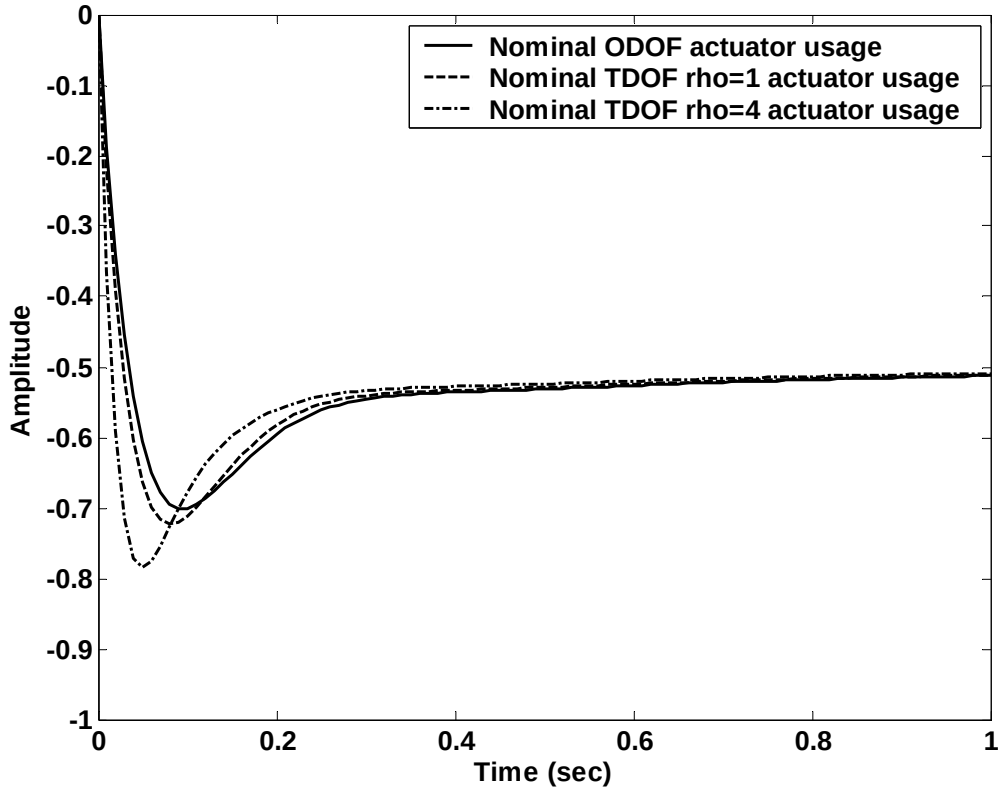

Figure 56: Nominal actuator usage for the ODOF H_∞ controller, TDOF H_∞ controller with $\rho=1$, and the TDOF H_∞ controller with $\rho=4$

Figure 57shows the reference trajectory specified in the design of a controller and the actual response of that controller to a set point change for two values of ρ. The difference between the defined reference trajectory and the actual process response is significant. Even with ρ=4 the process response has an ITAE=0.015. A common technique to cope with this difference is to set ρ=1 and artificially inflate the reference trajectory so the compromised controller has the desired tracking performance. An example of this type of inflation would be when a simple first order reference is used for a system with a dead time. Obviously a system with a dead time will not be able to react like a reference trajectory that does not have a dead time, but by using an unrealistically aggressive reference trajectory the designer is attempting to compensate for the known reference tracking deficiency in H_∞ TDOF design. The use of the reference trajectory as a tunable parameter in TDOF design is less than desirable, but has become a common practice in TDOF H_∞ problems.

A picture of the tuning process is coming into focus for both PEC using H_∞ control and H_∞ TDoF control. In order to further optimize the H_∞ TDoF controller we have four tunable parameters, the pre weight and post weight (W_1 and W_2), ρ, and the reference trajectory. Significant enhancements have been made by using ρ. The regulatory response is noticeably less oscillatory then the intermediate ODoF design for errors in the gain of 40%. At this point it is not necessary to modify the pre weight W_1. What we would like to do is loosen up on restrictions to actuator usage until we reach the maximum allowable usage.

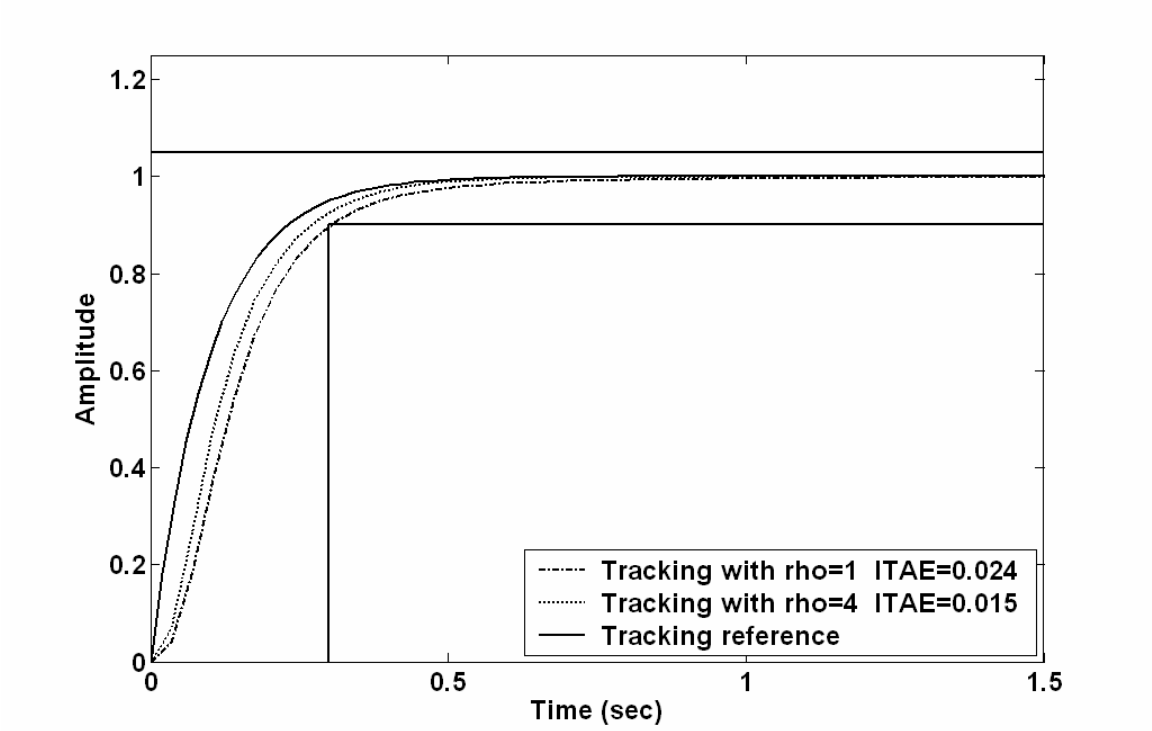

Figure 57: Step response plot of a TDOF H_∞ controller designed with a ρ=1 and ρ=4 plotted against the reference trajectory used in their design.

Up to this point we have increased the value of ρ to shift this balance between performance and actuator usage, but further increases will not continue to enhance the regulatory response because the ρ^2 term used for reference tracking becomes dominant. To manipulate the system further the post weight will be utilized. By iteratively increasing W_2 till it equals 1.43 we arrive at the regulatory response shown in Figure 58 and the tracking response shown in Figure 59. With a nominal ITAE of 0.149 this response is marginally better than the ODoF solution used in the PEC controller (ITAE=0.177). The responses of both systems could be made nearly identical with enough effort, but the small improvement in performance does not warrant the effort.

Instead we will turn our attention to the tracking response. Since increasing ρ beyond its current value of 4 will not achieve our tracking goals we will have to use the reference trajectory as a tunable parameter to continue to shape our tracking response. Currently we are using a first order reference trajectory. As can be seen in Figure 59 this trajectory is sluggish yet still causes our initial actuator usage to exceed unity. Our first option of modifying the reference trajectory would be to lower the time constant of the reference trajectory to make the reference faster, but this action would only aggravate the problem with actuator usage. In fact the designer does not have a good tool for controlling actuator usage. The only way to get the desired result is to use a second order reference trajectory. A critically damped Trajectory was initially chosen, and iteratively modified so that the actuator response was within limits, then the amount of dampening was lowered until the best process response was achieved, $\text{Tref} = \frac{1}{0.005s^2 + 0.1879s+1}$. The controls response is displayed in Figure 60 and produces almost an identical response to the PEC controller.

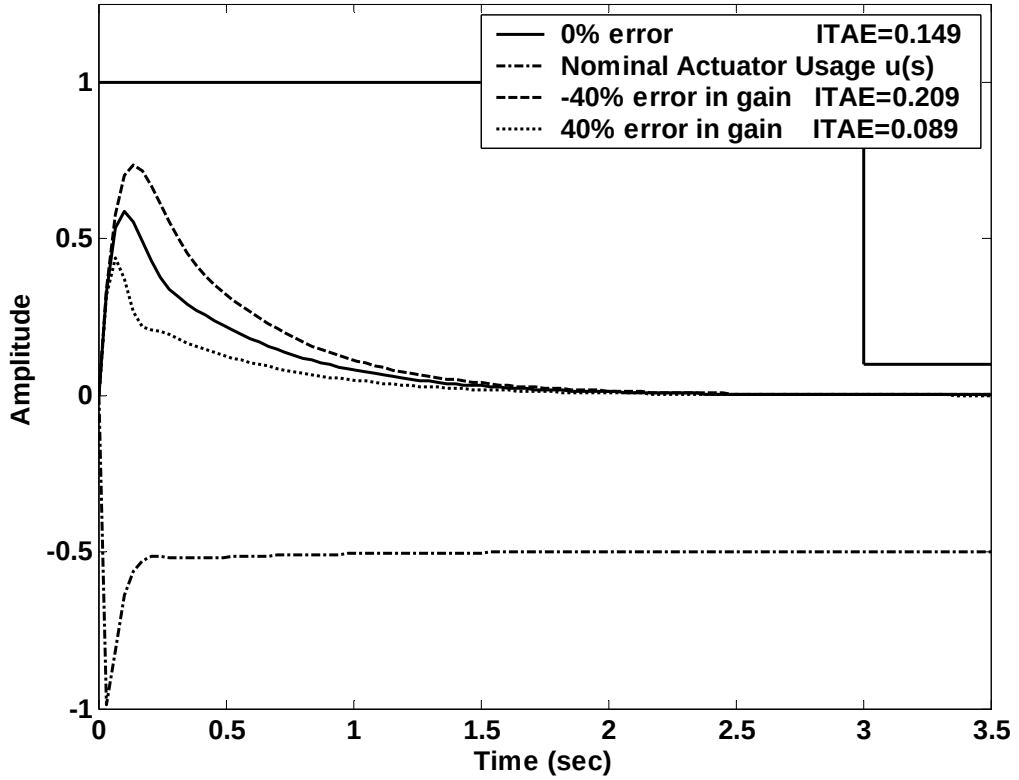

Figure 58: Disturbance rejection of a H_∞ two-degree of freedom controller, $\rho=4$, $W_2=1.43$, for the process defined in Equation (66) for gain estimation error of 0% (with actuator usage), -40%, and 40%. Performance objectives are defined by solid lines.

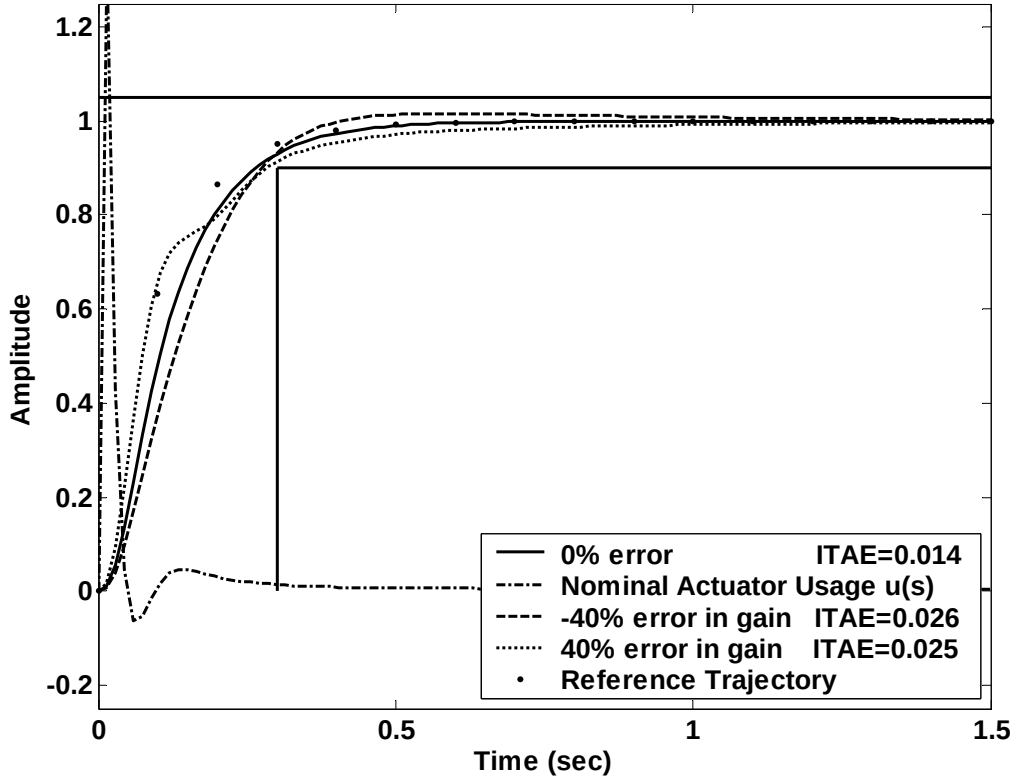

Figure 59: Tracking response of a H_∞ two-degree of freedom controller, first order reference trajectory, for the process defined in Equation (66) for gain estimation error of 0% (with actuator usage), -40%, and 40%. Performance objectives are defined by solid lines.

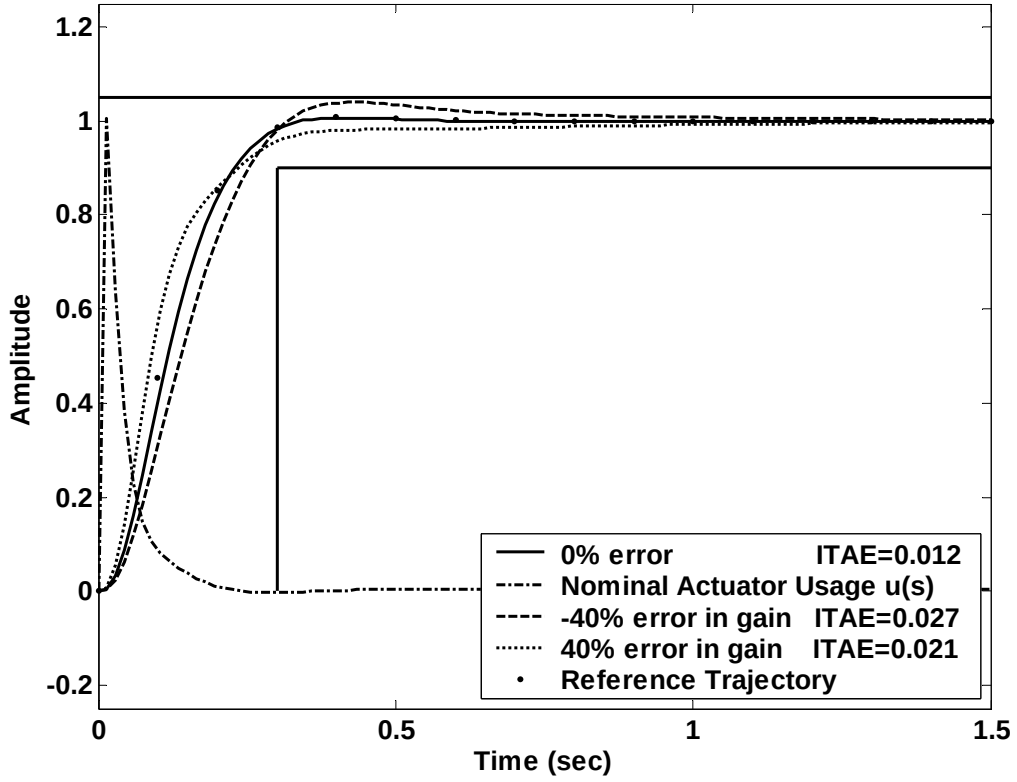

Figure 60: Tracking response of a H_∞ two-degree of freedom controller, second order reference trajectory, for the process defined in Equation (66) for gain estimation error of 0% (with actuator usage), -40%, and 40%. Performance objectives are defined by solid lines.

A summary of the initial and final tunable parameters for the PEC and H_∞ TDoF systems is displayed in Table 2. The corresponding initial and final performances for regulatory and servo responses can be seen in Table 3 and Table 4 respectively.

Table 2. Final tuning values for the control parameters.

Controller	W_1	W_2	W_P	W_u	ρ	T_{ref}
PEC Disturbance (initial)	$\frac{s+2}{s}$	1.0	N/A	N/A	N/A	N/A
PEC Disturbance (final)	$\frac{0.5s+1}{s}\frac{0.05s+1}{0.005s+1}$	2.7	N/A	N/A	N/A	N/A
PEC Servo (initial)	N/A	N/A	M=2 ω_b=15 A=1e-4	1	N/A	N/A
PEC Servo (final)	N/A	N/A	M=2 ω_b=15 A=1e-4	1,8	N/A	N/A
H_∞ TDoF (initial)	$\frac{s+2}{s}$	1	N/A	N/A	1	$\frac{1}{0.1s+1}$
H_∞ TDoF (final)	$\frac{s+2}{s}$	1.43	N/A	N/A	4	$\frac{1}{0.005s^2+0.1188s+1}$

Table 3. Summary of disturbance control performance

Controller	ρ	Load Rejection ITAE for error		
		0%	-40%	40%
PEC (initial)	N/A	0.297	0.419	0.177
PEC (final)	N/A	0.177	0.249	0.106
Tdof H_∞ (initial)	1	0.265	0.373	0.158
Tdof H_∞ (final)	4	0.149	0.209	0.089

Table 4. Summary of tracking control performance

Controller	ρ	Order	Load Rejection ITAE for error		
			0%	-40%	40%
PEC (initial)	N/A	13	0.009	N/A	N/A
PEC (final)	N/A	13	0.012	0.028	0.024
PEC reduced	N/A	7	0.012	0.028	0.024
Tdof H_∞ (initial)	1	7	0.024	N/A	N/A
Tdof H_∞ (final)	4	7	0.012	0.027	0.024

There are several clear observations that can be drawn from this information. The distinction between different two-degree of freedom controllers is best understood by looking at three different aspects of their design.

1. How easily does the design procedure allow designers to take advantage of the second degree of freedom (How easy is it to tune?)
2. What systems can the technique be applied to (When can it be used?)
3. How cumbersome is it to implement the technique (What are the disadvantages of implementation?)

How easy is it to tune?

Given enough time, and the inclination, a designer can achieve nearly identical nominal tracking trajectories with any two-degree of freedom techniques. This is particularly apparent when working with a minimum phase SISO system, as we have been doing in this chapter. How these different systems reach their final design, and the requirements that are placed on the designer are unique to each system, however.

Inverse based prefilters require a reference trajectory to be specified. Under nominal conditions that trajectory will be followed exactly. Alternatively, a lead-lag prefilter can be used to speed up or slow down a response in a simple fashion. Both of these solutions are adequate. As the complexity of a response increases, however, their short comings become more apparent. The value of specifying a reference trajectory diminishes quickly when the optimum response isn't known. The designer must either rely on previous experience with the system to set the proper reference trajectory or gain that experience through trial and error. Likewise, a lead-lag prefilter provides a means of gross correction that is particularly useful in shaping the initial speed of a response, but is not precise enough for fine tuning.

Two-degree of freedom H_∞ controllers specify a trajectory that the design will try to match, but in effect the trajectory specified is approached but not met, and can cause an less intuitive tuning procedure where the designer can try to adjust the speed or amount of overshoot in the reference trajectory so that the final Tdof system exhibits the response that is actually desired. Since the reference trajectory is over specified, it does not have a direct physical correlation to the desired reference trajectory. This makes the tuning process interpretive and less direct. An example of this type of adjustment will be seen in the following chapter. Another alternative is for the designer to increase the tracking weight, ρ. This can have a beneficial effect on disturbance rejection and tracking performance, but when used in conjunction with an overly aggressive reference trajectory can cause undesirable tracking characteristics. It may also have an undesired effect on actuator usage. In a variety of cases, such as the ones explored in chapters 5 and 6 the designer left the weight at unity.

PEC is a flexible two-degree of freedom structure, which is capable of utilizing many different types of controllers. In this chapter we explored the combination of H_∞ loop-shaping and H_∞ mixed sensitivity. This particular combination of controllers does not require a reference trajectory to design the PEC system. Instead it uses the feedback controller, when designed first, to generate a performance weight, W_P. The inverse of this weight approximates the sensitivity function of the feedback loop in the frequency domain. The design of the partitioning controller then reframes the problem in terms of tracking performance to find a partitioning controller, which minimizes $\left\| \begin{matrix} W_P S \\ W_U KS \end{matrix} \right\|_\infty$. This initial step generally provides improved tracking performance. In cases where this improvement is not sufficient, the overall response can be sped up by increasing the bandwidth specification, ω_b, in the performance weight. Furthermore, to increase or decrease the amount of overshoot in a response the value of M in the performance weight can be raised or lowered. The tunable parameters that define the PEC controller have a direct link with the properties of the system they are trying to control, providing a level of intuition to the tuning process that is not available in the H_∞ TDoF controller. Additionally, buy using Mix Sensitivity control in the partitioning loop the designer is able to specify design criteria for actuator usage directly be use of the actuator weight W_U, thus providing a level of control to the tuning process that is not available in the H_∞ TDoF controller.

Applicable systems

Of the Three TDOF systems discussed, inverse based prefilters have the most limited scope. Difficulties are encountered in prefilter design when dealing with non-minimum phase systems, or systems with a significantly larger number of poles then zeros. RHP-zeros, time delays, and high order systems all have different design modifications, which often lead to the use of approximations to the detriment of performance. These complications are often compounded in MIMO systems, limiting inverse based prefilter design significantly.

The application of Tdof H_∞ loop-shaping control or H_∞ loop-shaping and mixed sensitivity under the PEC system are restricted to systems which satisfy the assumptions found in List 1 of this chapter. Glover et al. 1991 has developed a γ-dependent loop shifting transformation, which relaxes these restrictions further, such that for well-posed problems these assumptions are generally not difficult to satisfy.

The PEC structure, however, does not have inherent limitations. It is instead limited only by the controllers, which it utilizes. True independence of design means the limitations imposed by Partitioned Error Control in the feedback loop are the same as those imposed by feedback control. That provides an unprecedented amount of latitude in two-degree-of-freedom design. The partitioning loop is even less restrictive. By eliminating noise and disturbances in the partitioning loop, there is no longer a need for feedback. The need for feedback in the partitioning loop becomes a choice designers can make to suit the type of controller they wish to use. The vast majority of control techniques have designs based on feedback. In order to utilize those designs it is beneficial to use feedback in the partitioning loop, but a designer is capable of using an

open loop controller in the partitioning loop, or even a non-causal controller if the situation calls for it. That is a degree of flexibility that is unmatched by existing two-degree-of-freedom techniques.

Implementation Issues

All two-degree-of-freedom controllers are larger than their one-degree-of-freedom counterparts. It is one of the trade offs for the increased functionality of the control law. PEC is no exception. The implementation of two controllers and process model can seem excessive, however, it has been demonstrated that through model reduction techniques the size of PEC controllers can be brought in line with conventional two-degree-of-freedom systems.

CHAPTER V

CASE STUDY: CONTROL OF AN INVERTED PENDULUM

Introduction

This case study is used to illustrate the design procedures of Tdof H_∞ loop-shaping control and H_∞ loop-shaping/mixed sensitivity PEC, and demonstrate the effects the different procedures can have on controller performance. These controllers will be applied to stabilize and control a classical inverted pendulum, Figure 61. This case study is an extension of work done by Walker[19] who presented a case study, which designed and analyzed the two-degree of freedom H_∞ controller for this particular system. First, a description and explanation of the problem will be given. Second, a one-degree-of-freedom controller will be developed. Third, the benchmark two-degree-of-freedom H_∞ controller designed by Walker[19] will be developed. This will be followed by the development of a PEC controller. Finally, a comparison of techniques will be made.

Problem Description

The objective of this problem is two fold. First, stabilize the inverted pendulum, which may freely pivot at its base and is attached to a small cart. Second, control the lateral position of the cart, which is on a horizontal track, while maintaining the stability of the inverted pendulum.

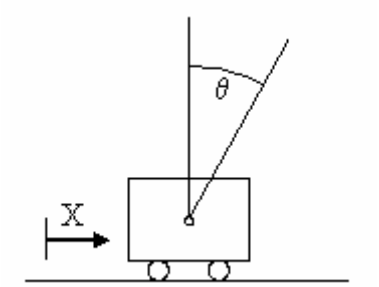

Figure 61: Diagram of an inverted pendulum on a cart

The controller measures the horizontal position of the cart x(t) and the pendulums attitude θ(t), and makes adjustments to the horizontal position of the cart via a DC servo motor acting through 2 pulleys, a timing belt and an N:1 reduction gear (not shown in Figure 61).

The Inverted Pendulum model

The following differential Equations describe the nominal plant.

$$M_{\text{eff}} \frac{\mathrm{d}^2 x}{\mathrm{d}t^2} + ml \frac{\mathrm{d}^2 \theta}{\mathrm{d}t^2} \cos\theta = ml \left(\frac{\mathrm{d}\theta}{\mathrm{d}t} \right)^2 \sin\theta + \left(N/r \right) \left(K_{\text{m}} i - T_{\text{d}} \right) \qquad (75)$$

$$I_0 \frac{\mathrm{d}^2 \theta}{\mathrm{d}t^2} + ml \frac{\mathrm{d}^2 x}{\mathrm{d}t^2} \cos\theta = mgl \sin\theta \qquad (76)$$

$$L \frac{\mathrm{d}i}{\mathrm{d}t} + Ri = -\left(K_{\text{m}} N/r \right) \frac{\mathrm{d}x}{\mathrm{d}t} + V_{\text{in}} \qquad (77)$$

The variables, descriptions, nominal, and (perturbed) values are listed in Table 5.

Table 5. Variable descriptions with nominal and perturbed values

Variable	Description	Nominal value	Perturbed Value
V_{in}	voltage input to the motor (V)	controller output limited to ±15 V	
x(t)	cart position (m)		
θ(t)	pendulum attitude (rad)		
I	motor current (A)		
I_0	the moment of inertia of the pendulum about its pivotal axis	4/3 ml^2 kg m^2 =0.0036 kg m^2	
M	small cart mass	0.283 kg	0.354 kg
N	ratio of the reduction gear on motor	40	
l	half of pendulum length	0.30 m	0.28 m
m	pendulum mass; ()	0.030 kg	0.0375 kg
M_{eff}	$M+m(N/r)^2I_{eff}$		
I_{eff}	effective moment of inertia of rotating parts relative to motor shaft	3.5e^{-7} kg m^2	7.0e^{-7} kg m^2
K_m	motor constant	0.01NmA^{-1}	0.005 NmA^{-1}
L	induction	0.001 H	
R	resistance	4 ohms	
r	effective radius of motor shaft	0.0285 m	0.03 m
g	gravitational constant	9.81 m s^{-2}	

The 5 state model, $X = \left\{ \frac{d\theta}{dt}, \theta, \frac{dx}{dt}, x, i \right\}$, was linearized around the unstable equilibrium point $\{x = 0, \theta = 0\}$, and led to the following 5th order state-space model with outputs {x,θ}

$$\left[\begin{array}{ccccc|c} 0 & 2.6420e^{1} & 0 & 0 & -1.2055e^{2} & 0 \\ 1 & 0 & 0 & 0 & 0 & 0 \\ 0 & -7.5829e^{-1} & 0 & 0 & 4.8221e^{1} & 0 \\ 0 & 0 & 1 & 0 & 0 & 0 \\ 0 & 0 & -1.4035e^{4} & 0 & -6.0000e^{3} & 1000 \\ \hline 0 & 0 & 0 & 1 & 0 & 0 \\ 0 & 1 & 0 & 0 & 0 & 0 \end{array}\right] \quad (78)$$

Open loop poles of the system are located at 0, -115, ±4.95, -5885

The first two poles are associated with the cart position. It can be readily shown that the poles at ±4.95 are associated with the transfer function from cart acceleration to pendulum attitude. The last pole at –5885 is associated with the electrical dynamics of the motor.

Since H_∞ optimization leads to a controller at least the same size as the shaped plant, it is beneficial to work with a model that has been reduced as much as possible before beginning controller design, especially since the electrical dynamics of the motor clearly do not contribute significantly to the overall process. The 5th order linear model was reduced using balanced residualization of coprime factors (McFarlane and Glover[15]). A fourth order approximate was achieved, which retained all the poles of the original system except, as we predicted, the –5885 pole associated with electrical motor dynamics. Figure 62 shows the frequency response of the linear 5th order and 4th order models. No appreciable difference is present over the 5 decades around the crossover frequency.

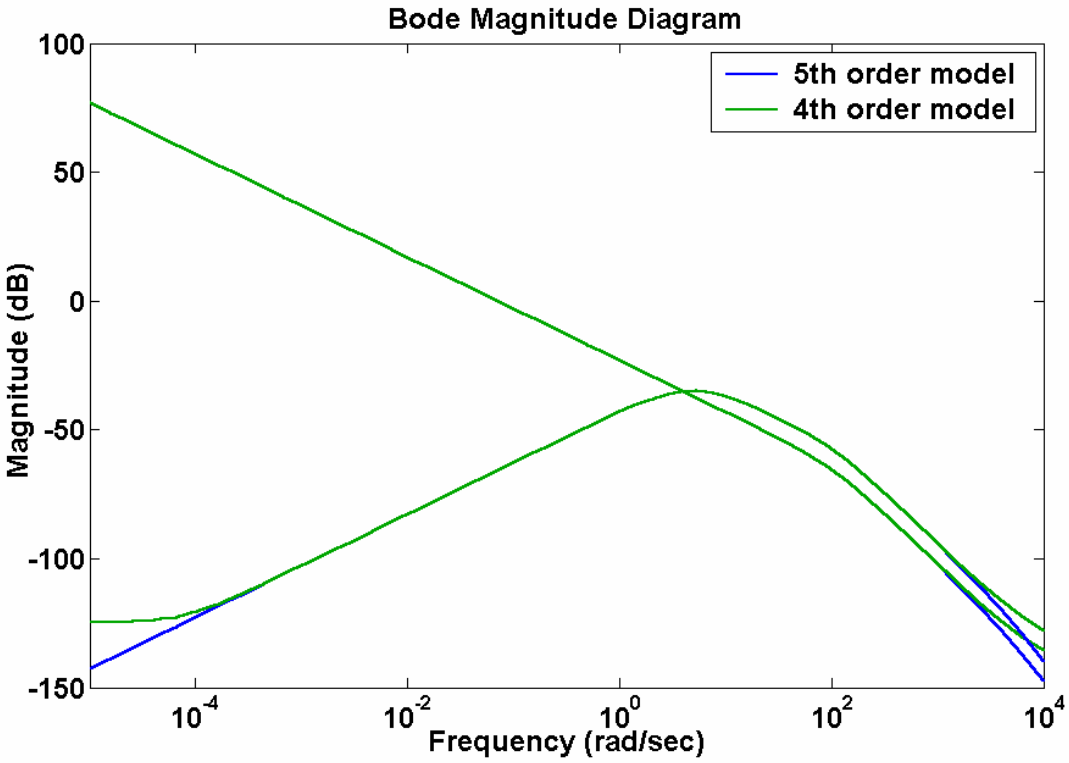

Figure 62: The frequency response of the process model vs. the reduced process model of the inverted pendulum on a cart

Performance specifications

The lateral position of the cart should respond to demands of ±0.3m on a track 1m in length. Furthermore a restriction on the maximum cart velocity of ±0.7m/s should be maintained for the nominal system.

One degree of freedom H_∞ control

It is common in most design problems is to see whether or not a one-degree of freedom controller will successfully meet controller objectives. As such this case study will begin with the design of a one-degree of freedom H_∞ controller. The first step in the design process is to select the weighting functions W_2 and W_1 to form the shaped plant. W_2 is selected to be a constant weighting function, which reflects the importance of pendulum stability over cart position. Hence W_2 is chosen as

$$W_2 = \text{diag}\{1, 2\} \tag{79}$$

For the selection of W_1 we must recognize that the system already contains an integrator, so a good choice of W_1 would be a constant 1x2 matrix, which aligned the singular values of the open plant at the desired bandwidth of the system. To determine the bandwidth of the system we will use the maximum distance of a response, 0.6m, and the maximum velocity of the cart, 0.7m/s and Equation (80)

$$F\left(\frac{\text{rad}}{\text{s}}\right) = \frac{2V}{D} = \frac{2*0.7}{0.6} = 2.3\left(\frac{\text{rad}}{\text{s}}\right) \tag{80}$$

Hence W_1 is chosen to align the singular values of the open plant at 2.3 rad/s. We are in effect converting the system from a one input two output system into a two input two output system and adjusting each input by a constant so that the cross over frequency of each response is roughly 2.3 rads/sec. This alignment is done so that we have effective control over both outputs up to the desired frequency. It would do us no good to have control over the position of the cart at frequencies up to 2.3 rads/sec if we could not also control the pendulum attitude at those frequencies. With this in mind, W_1 was chosen as follows:

$$W_1 = \begin{bmatrix} -18.0685 & 16.0288 \end{bmatrix} \tag{81}$$

H_∞ synthesis produced a 4 state controller with a sub optimal gamma of 4.0963. Under the implementation of Figure 63, where reference signals are scaled and fed directly in to the preweight W_1, K_{Aodof} is given as

$$K_{Aodof} = \begin{bmatrix} \dfrac{17.59s^4 + 6.7801e3s^3 + 6.5863e5s^2 - 4.2108e6s - 6.6837e6}{1s^4 + 385.4523s^3 + 3.7444e4s^2 - 2.3938e5s - 3.7997e5} \\ \dfrac{3.3682e3s^3 + 4.4590e5s^2 + 7.0718e6s + 6.6837e6}{1s^4 + 385.4523s^3 + 3.7444e4s^2 - 2.3938e5s - 3.7997e5} \\ \dfrac{4.7834e4s^3 5.8293e6s^2 3.8156e7s + 5.1019e7}{1s^4 + 385.4523s^3 + 3.7444e4s^2 - 2.3938e5s - 3.7997e5} \end{bmatrix} \tag{82}$$

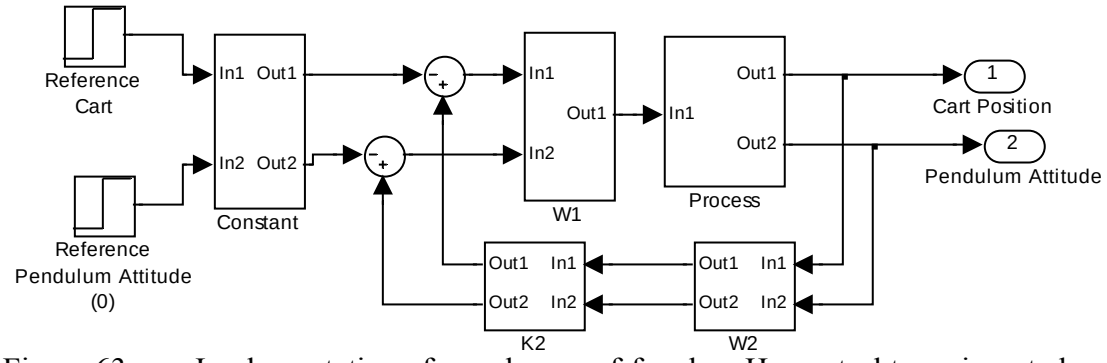

Figure 63: Implementation of one-degree-of-freedom H_∞ control to an inverted pendulum on a cart. This configuration prevents derivative kick for reference changes.

Figure 64shows the cart, pendulum attitude, and cart velocity of this controller for a step response of 0.6m. The controller does not give the desired inverse response because the method chosen to implement the controller sends a scaled reference signal directly into the process. This configuration was chosen to prevent derivative kick not to provide the desired initial inverse response. This suggests that the controller might perform better under the nonstandard implementation shown in Figure 65. The form of this controller is given as K_{Bodof}

$$K_{Bodof} = \left[\frac{3.3682e3s^3 + 4.4590e5s^2 + 7.0718e6s + 6.6837e6}{4.7834e4s^3 5.8293e6s^2 3.8156e7s + 5.1019e7} \right] \qquad (83)$$

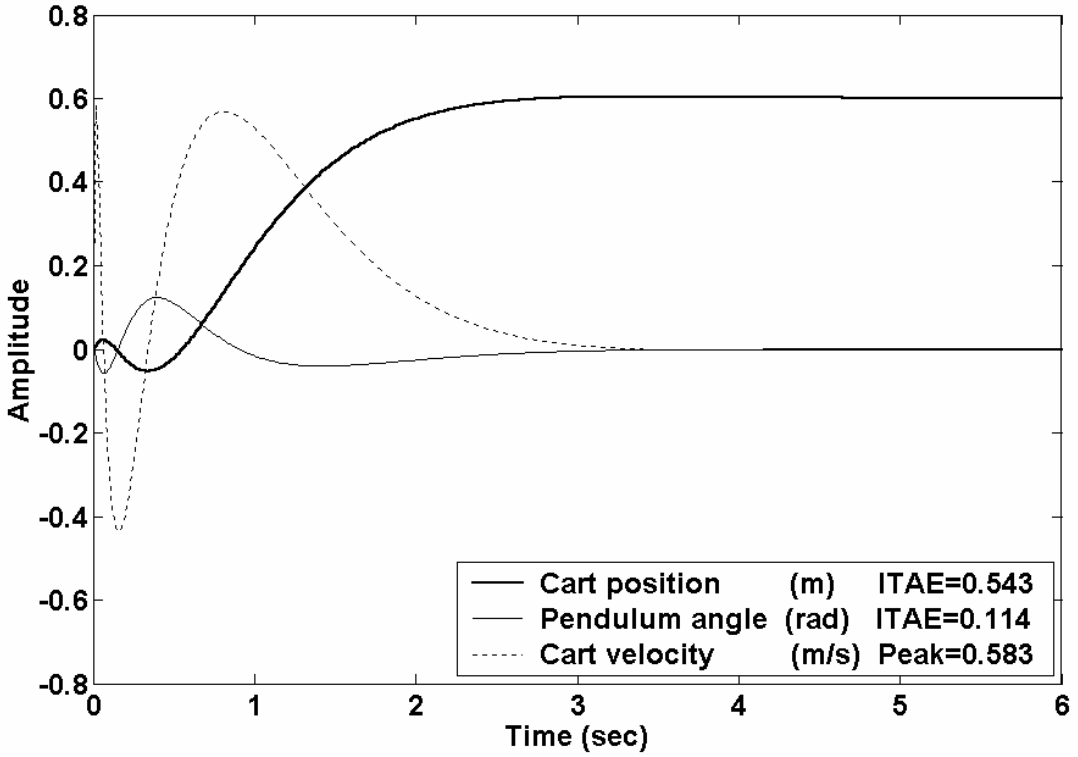

Figure 64: Cart position, velocity, and pendulum attitude for a step response of 0.6 for controller K_{Aodof} on the nominal system

The response of this controller can be seen in Figure 66. This controller has a better initial response then controller K_{Aodof}. A 5% overshoot was observed, which corresponds to a damping factor of 0.69. Comparing our initial requirement for overshoot with the performance of the one-degree of freedom controller, it would seem that the initial requirement was excessive considering H_∞ controllers are of a high order and their objective is to minimize the peak amplitudes of the frequency response, which roughly translates into the time domain as a minimization of overshoot.

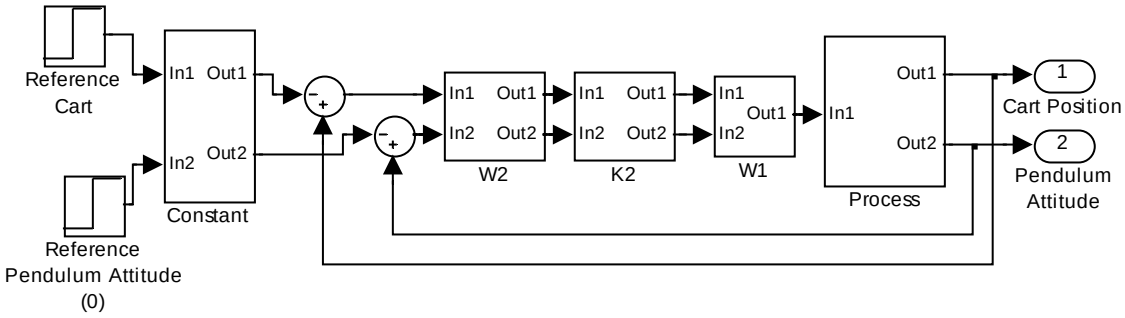

Figure 65: Implementation of H_∞ one-degree of freedom controller where reference is directly compared to the system output

The one-degree-of-freedom design in the non standard implementation provides adequate control over the cart and the pendulum, however, there is no ability to modify the tracking response of the system. We will continue to seek a two-degree-of-freedom controller with better tracking performance.

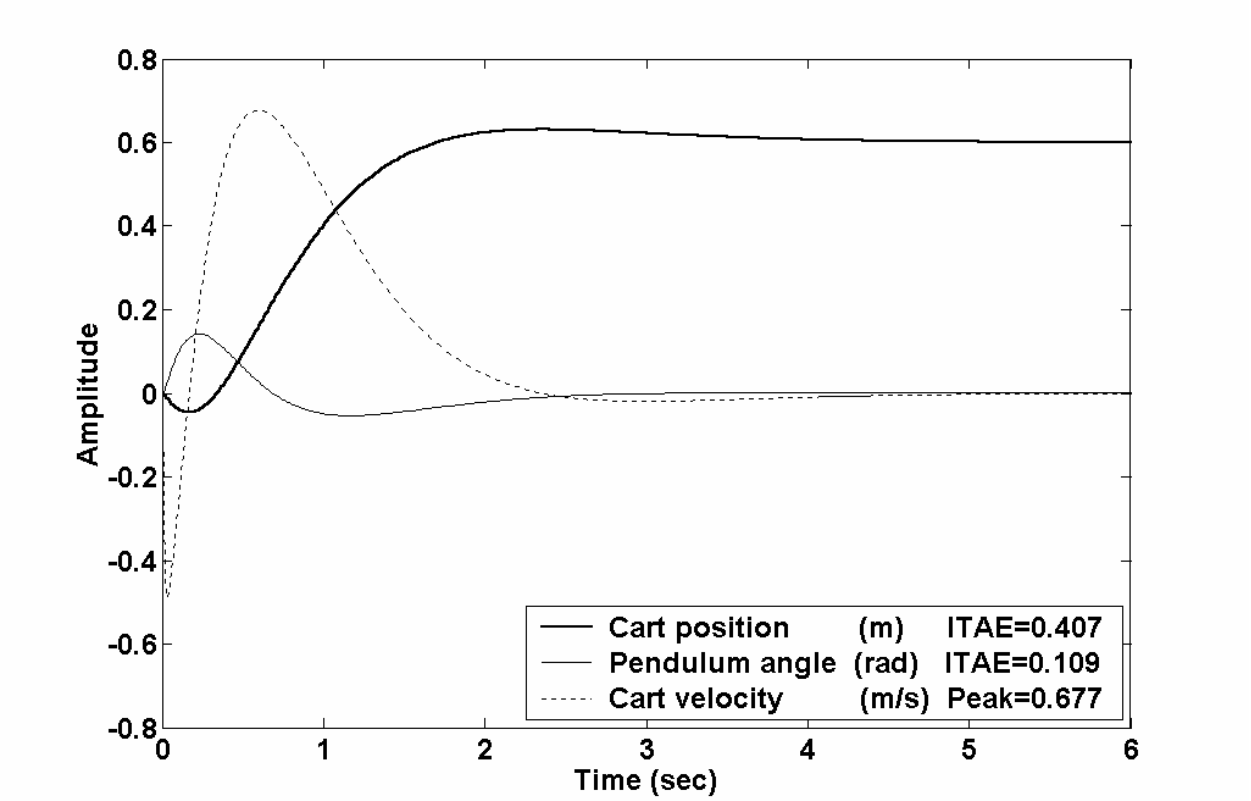

Figure 66: Implementation of H_∞ ODoF controller where reference is directly compared to measured variable

Benchmark control TDoF H_∞ loop-shaping control

The benchmark controller for this study is a two-degree-of-freedom H_∞ controller. The design procedure for this controller was originally developed and published by Walker[19], and is represented here to maintain an unbiased representation of practical two-degree-of-freedom design.

Reference trajectory

Walker's[19] design procedure starts out with the selection of the reference trajectory. The reference trajectory will be designed to incorporate the maximum cart velocity restriction over the maximum step change. From experience with this system it is expected that the controller will have a degree of overshoot, so a second order reference trajectory is chosen of the form

$$M(s) = \frac{\omega_n^2}{s^2 + 2\zeta\omega_n s + \omega_n^2} \qquad (84)$$

where ω_n represents the bandwidth of the system and ζ is the dampening factor which determines the amount of overshoot. The inverse response of the system is not accounted for in this reference trajectory, Walker[19] suggests a better trajectory might have included a RHP-zero, but did not investigate this possibility.

The following calculations show how to determine the bandwidth requirement for a system with an overshoot given by x_1 (<1) assuming a maximum velocity of 0.7 m/s over the maximum possible step change of 0.6 m. The maximum overshoot calculation is solved as:

$$x_1 = \exp\left(-\pi\zeta / \left(1-\zeta\right)^2\right)^{1/2} \quad (85)$$

solving Equation (85) for the damping factor leads to:

$$\zeta = \frac{-\ln\left(x_1\right)}{\left(\pi^2 + \left(\ln x_1\right)^2\right)^{1/2}} \quad (86)$$

The velocity of the system with respect to time is found by noting that the impulse response is identical to the velocity of the step response such that the inverse Laplace transform gives us

$$v(t) = \frac{\omega_n}{\left(1-\zeta^2\right)^{1/2}} \exp\left(-\zeta\omega_n t\right) \sin\left(\left(1-\zeta^2\right)^{1/2} \omega_n t\right) \quad (87)$$

it can be easily shown through differentiation that the maximum velocity of a unit step change is

$$v_{max} = \omega_n \exp\left(\frac{-\zeta}{\left(1-\zeta^2\right)^{1/2}} \arcsin\left(1-\zeta^2\right)^{1/2}\right) \quad (88)$$

Since the maximum step change of the system is 0.6m there needs to be an adjustment to the maximum velocity, 0.7m/s = v_{max}*0.6. Therefore v_{max}=1.167. Rearranging Equation (88) then gives us the bandwidth requirement for the system.

$$\omega_n = 1.167 \exp\left(\frac{\zeta}{\left(1-\zeta^2\right)^{1/2}} \arcsin\left(1-\zeta^2\right)^{1/2}\right) \quad (89)$$

With Equation (89) the designer can determine the approximate bandwidth of the system by specifying a desired overshoot.

Tuning the H_∞ two-degree-of-freedom controller

Walker[19] deemed an overshoot of 0.1 to be appropriate for the process response, though this decision was made without justification. This initial guess works out very favorably for Tdof H_∞ control, which suggests it may have been obtained through an iterative procedure. Regardless, it will be used as a starting point for the controller to further demonstrate the differences in two-degree of freedom H_∞ design and mixed sensitivity/loop shaping H_∞ PEC. For an overshoot of 0.1, the natural frequency of the system is 2.3 rad/s. It is a coincidence that this is the same frequency as was found in the ODoF design. However, this is a coincidence that will help in the analysis of the various systems, since the regulatory response of the controllers should be very similar. Because the desired bandwidth of the systems are identical we will use the pre and post weights (W1 and W2) as they were defined in Equations (79) and (81) for the same reasons.

With the shaped process defined as well as the reference trajectory, T_{ref}, very little additional effort is required by the designer. The only parameter that needs to be specified is the weighting function, ρ. It is common practice to use an initial guess of the weighting function of $\rho=1$, Walker[19] chose to do just this in his controller design. H_∞ synthesis was conducted using commercially available software and a sub optimal two-degree of freedom controller was designed with a gamma of 4.9172.

The 6 state controller K_{Tdof} is given as

$$K_{Tdof} = \begin{bmatrix} -6.6238e4(s+1.1468e2)(s+1.0984e1)(s+3.1334)(s+1.8578 \pm 6.3379e\text{-}1i) \\ 9.0949e4(s+1.1425e2)(s+1.6027e1)(s+1.1435)(s+1.3570 \pm 1.8570i) \\ 1.0476e6(s+1.1501e2)(s+5.0741)(s+1.9032)(s+1.3570 \pm 1.8570i) \\ \hline (s+4.6738e3)(s+1.5276e2)(s\text{-}1.0350e1)(s+1.4167)(s+1.3570 \pm 1.8570i) \end{bmatrix} \quad (90)$$

The corresponding response of this controller for a step change of 0.6 can be seen in Figure 67.

The peak value of the carts position is 6.36 corresponding to an overshoot of 6%. If in fact a 10% overshoot was appropriate this controller would not be able to match the specified trajectory. In this case, however, it is more likely that the designer over inflated the desired overshoot for the process so that the actual response of the plant had the desired tracking. If this is in fact the case, then an iterative procedure was almost certainly used to arrive at the decision to use 10% overshoot in the reference signal. This is a typical example of the over inflation of the reference trajectory to aid in tracking responses in tdof H_∞ control and the iterative adjustments designers make to obtain the desired tracking.

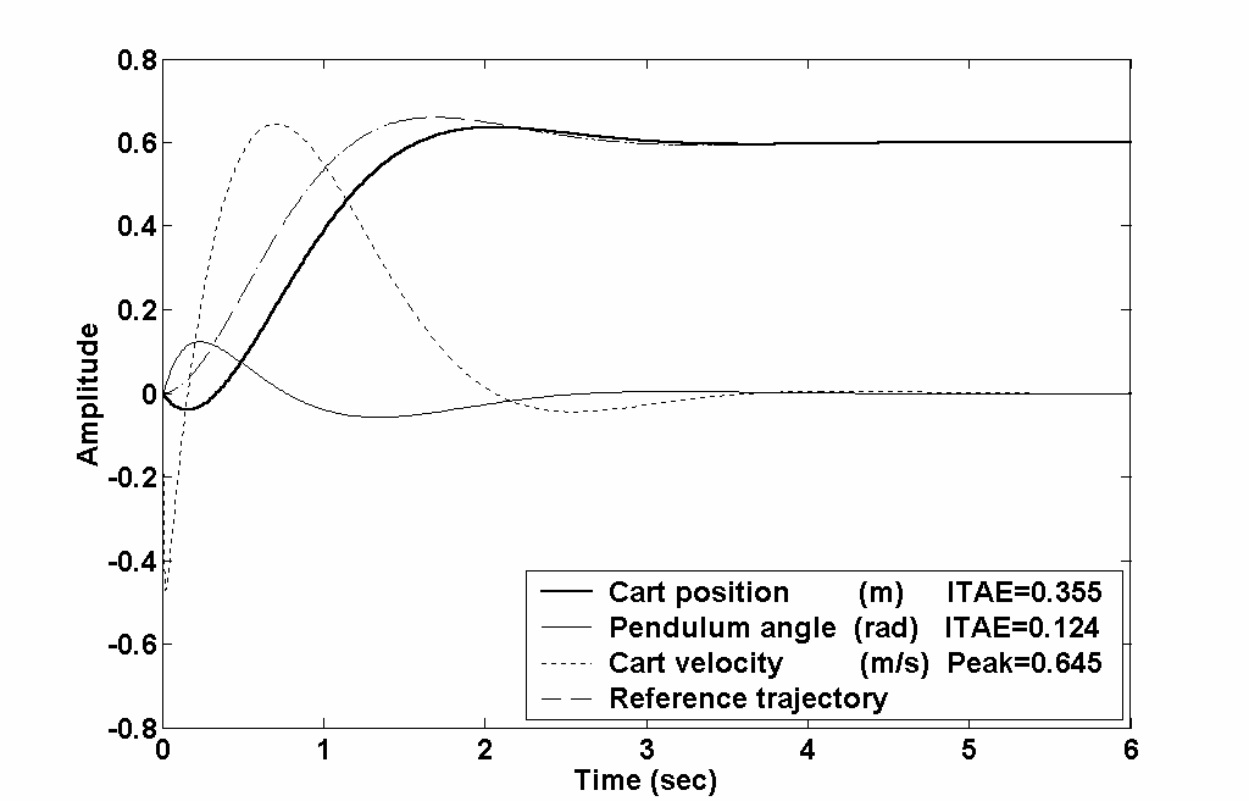

Figure 67: Cart position, velocity, and pendulum attitude for a step response of 0.6 for controller K_{Tdof} on the nominal system

PEC the partitioning controller

The one-degree of freedom controller designed above will be used in the feedback loop of the partitioned error control system. The design of that feedback controller satisfies the first 7 steps in the design procedure to generate a Partitioned error controller outlined in chapter 4. All that remains is to design the mixed sensitivity partitioning controller, validate it for the nominal system, form the partitioned error controller, and possibly use a reduction technique to obtain a lower order final controller. In order to determine the weighting functions required in the mixed sensitivity design of the form shown in Figure 68 that will be used in the partitioning loop it is helpful to plot the frequency response of the sensitivity function of an existing controller and determine the parameters for W_P such that $\left|\frac{1}{W_P}\right| \geq |S|$. The one-degree of freedom H_∞ controller will be used to generate those sensitivity functions. Figure 69 shows the sensitivity function of the cart, while Figure 70 shows the sensitivity function of the pendulum attitude. These figures also include the corresponding plots of $|1/W_P|$.

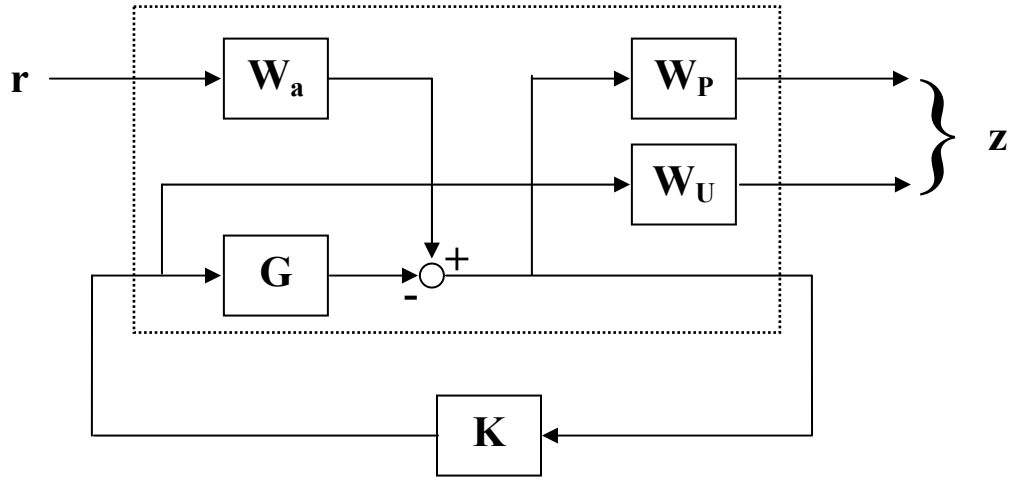

Figure 68: H_∞ mixed sensitivity formulation. The generalized plant is boxed with dashed lines.

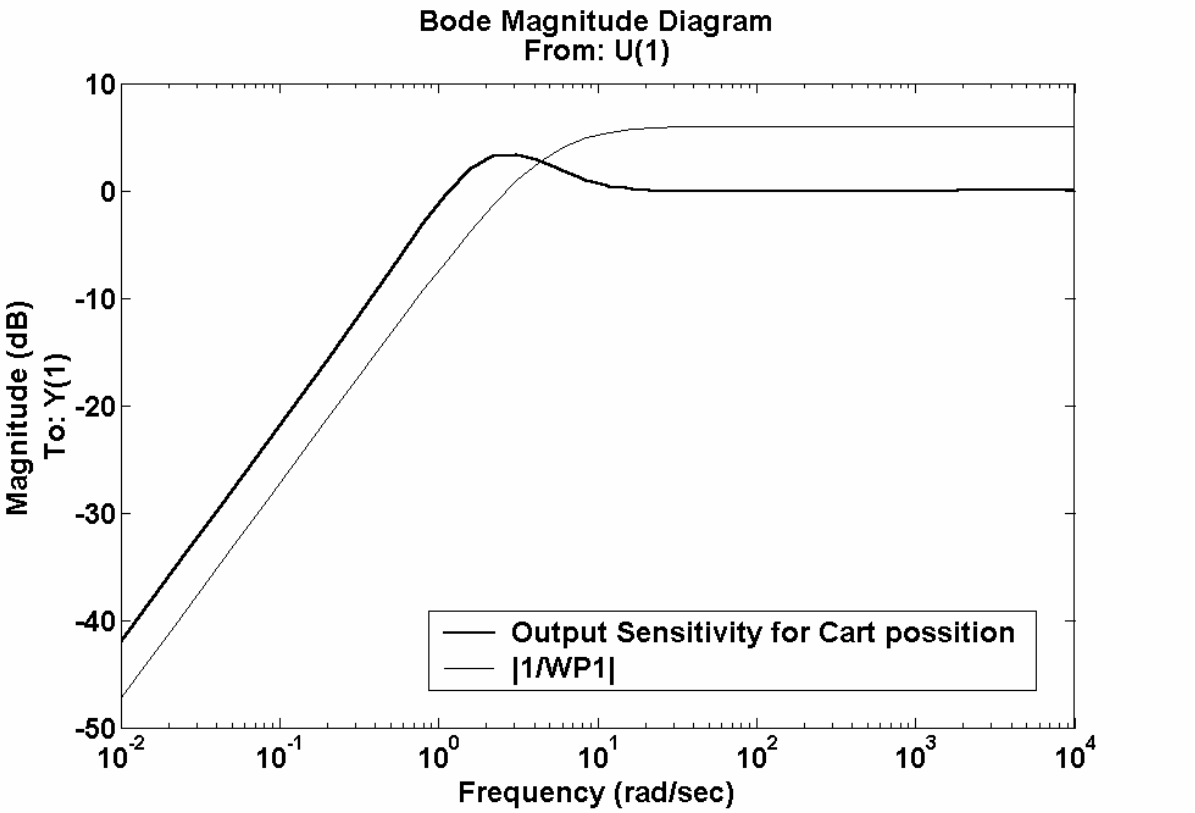

Figure 69: The sensitivity function of the cart position for the ODoF controller plotted against the inverse performance weight.

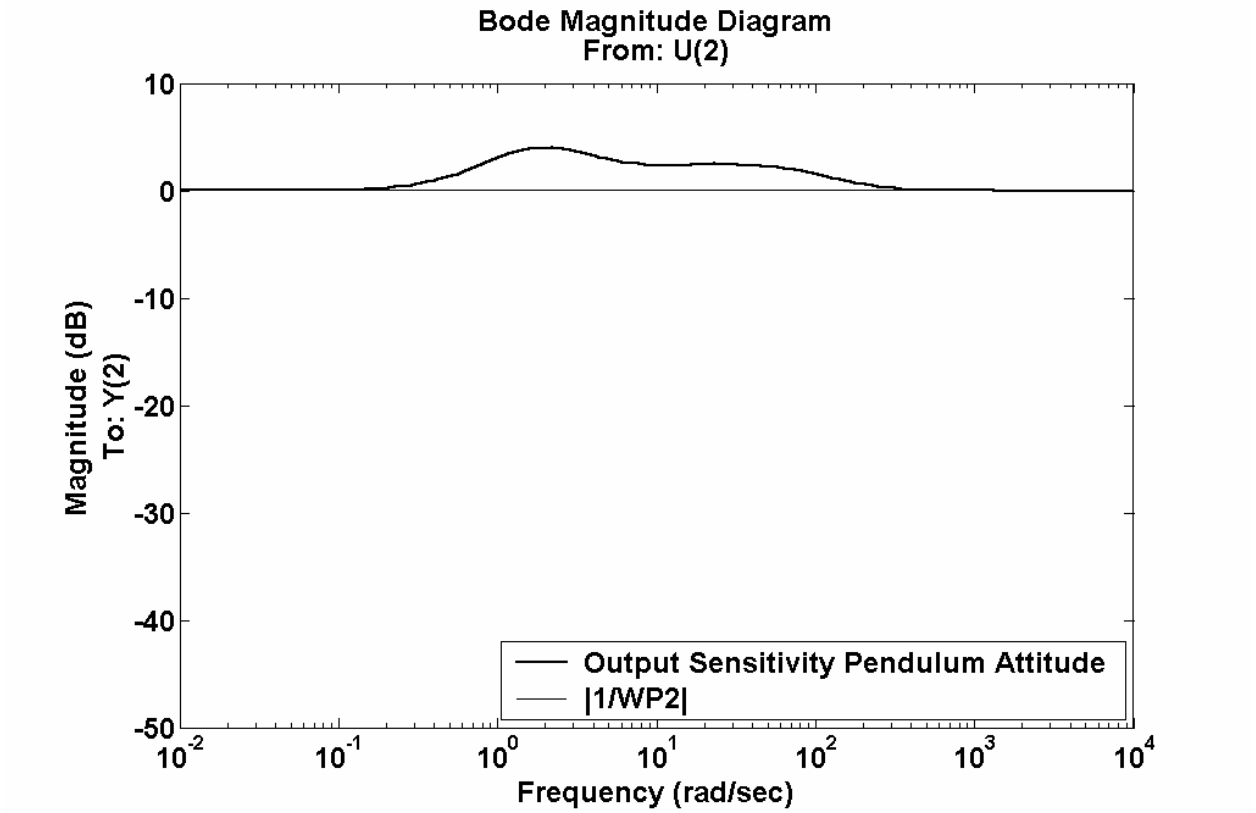

Figure 70: The sensitivity function of the pendulum attitude for the ODoF controller plotted against the inverse performance weight.

The parameterization of the performance weight in Figure 69 is straightforward. We have a system with a bandwidth requirement of ω_{B1}=2.3 rad/s. If the bandwidth requirement was not known or calculated as part of the design of the ODoF H_∞ controller a lower bandwidth that would correspond to output sensitivity of the ODoF controller more closely could have been selected. The upper bound on the bandwidth is set to the default value of M_1=2. To ensure steady state tracking at low frequencies A_1<<1 is chosen. The parameterization of the performance weight in Figure 70 is trivial since the process is self-integrating, as such; W_{P2} is chosen to be a constant equal to unity.

The initial choice of the control sensitivity weight of W_U=I is usually sufficient for most problems. However, since we have an existing controller and a specific maximum velocity we would like to achieve, we could only benefit from examining the frequency response of KS from the one-degree of freedom controller, see Figure 71. The peak of the frequency response of KS for the ODoF system is 27.5(dB) at a frequency of 3.07 rad/s. Neglecting motor dynamics this peak corresponds to the maximum velocity achieved by the ODoF controller, 0.677 m/s. Since this peak is located above 0 dB we know that if Wu=I was chosen the H_∞ optimization would try to reduce this peak. This would result in a very sluggish response with v_{max}<0.677m/s. Similarly, if Wu was chosen to be a sufficiently small constant such that $\left\|W_U KS\right\|_\infty < \gamma$, where γ is assumed to be equal to 1 for a well posed problem, the H_∞ optimization would relax restrictions on actuator usage at all frequencies. For a process with an inverse response this could result in an excessive initial jerk of the cart for a step response. Clearly a frequency dependant weight is needed. Noting that $|W_U KS|<\gamma$ for all frequencies, it follows that $|KS|<\gamma|W_U^{-1}|$. Ideally, assuming γ=1, we would Choose W_U such that $|W_U^{-1}|=|KS|$. Unfortunately the

shape of KS is slightly irregular due to the inverse response and would be hard to approximate with a low order weight.

A better choice for W_U would be a high pass filter, which would flatten the peak of KS and shift it to higher frequencies. Flattening the peak in terms of H_∞ optimization is equivalent to saying we care about suppressing actuator energy over the frequency range of the plateau equally. Choosing a high pass filter, which shifts the peak of the response further to the right, will limit the initial jerk of the cart in the opposite direction. This is because at high frequencies the initial response is the only reaction the system can have.

This high pass filter will be of the form shown in Equation (91).

$$W_U = \frac{1}{\varepsilon}\left[\frac{s + \omega_{bu} M_u}{s + \frac{\omega_{bu}}{\varepsilon}}\right] \qquad (91)$$

where Mu>0,wbu>0, and ε>0.

Lets take a minute to relate the step response characteristics of our system to the frequency response characteristics. The frequency response of a system at any given frequency is simply the amplitude of the response of a system to a sinusoidal input at that frequency. Therefore, the frequency response of systems at high frequencies loosely corresponds to the magnitude of a step response at low times. For a system with an inverse response the peak of the inverse response would occur at some frequency above the bandwidth of the system. With that in mind we will design an actuator weight.

Figure 71 shows the frequency response of the initial weight chosen to produce the effects described above. The actuator weight with initial values is

$W_U = \rho * 0.1\left(\frac{s+0.001}{s+10}\right)$, with ρ=1 is initially chosen. This weight contains a high pass filter, and a scaling factor of 0.1. The parameter ρ serves two purposes. First, the form of the high pass filter was designed assuming γ=1 (this corresponds to the controller meeting all performance and actuator weights) according to $|KS|<\gamma|W_U^{-1}|$. We are satisfied with the controller usage in the ODoF problem, and by choosing Wu such that $\|W_U KS\|_\infty$ is one at frequencies above the bandwidth means we are not attempting to change the initial response of the system from the ODoF design. Should gamma not equal one due to difficulty in lowering $\|W_U KS\|_\infty$ then we can scale the weight by a factor of γ to get the desired result, such that an appropriate second guess would be ρ=γ. By doing this we are saying that the ODoF design was sufficient. In particular we do not wish to change the characteristics of the inverse response. This process of setting ρ=γ could be continued until an acceptable design was reached. If we did wish to change the characteristics of the initial response we could choose Wu to push the $\|W_U KS\|_\infty$ further to the right, however, since Walker[19] did not investigate this possibility in his Tdof H_∞ design (he declined to examine a RHP zero in the reference trajectory), we shall not pursue it either.

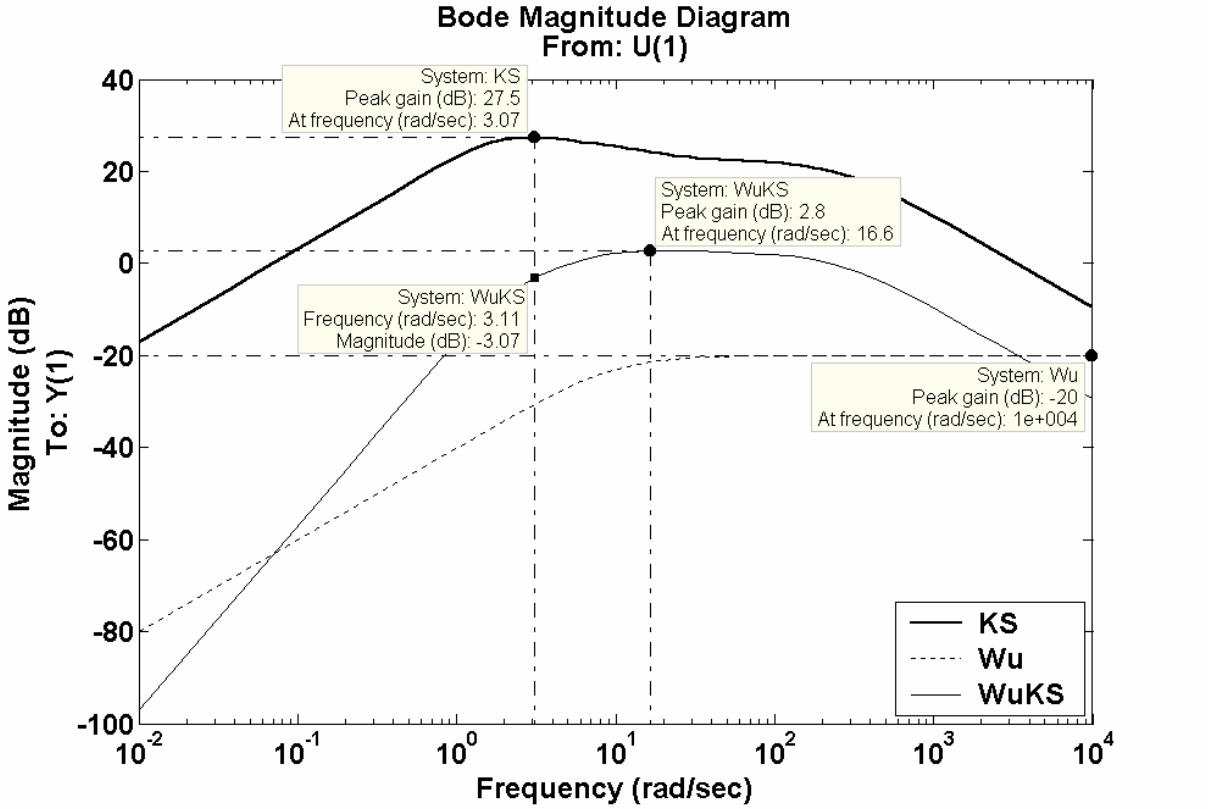

Figure 71: A frequency plot of the KS for the ODoF H_∞ loop shaping controller, the initial choice of the actuator weight Wu, and the function WuKS which is being minimized in the H_∞ mixed sensitivity design. The objective of the performance weight is to push the peak of WuKS above the bandwidth of the system, thus controlling the initial dynamics of the time response of the system, however since the value of the peak is near one, we are specifying that the actuator usage of the ODoF design is acceptable.

A third weight, Wa, is added to the mixed sensitivity problem to emphasize that the pendulums attitude is a regulatory problem, and that tracking of the pendulum to reference commands is significantly less important than cart tracking. Hence,

$\mathrm{Wa} = \begin{bmatrix} 1 & 0 \\ 0 & 0.01 \end{bmatrix}$ is chosen to signify the pendulum attitude is to be regulated, not tracked.

The final forms and values of the weights used in the mixed sensitivity design are listed in Table 4.2.

Table 6. Mixed sensitivity weight parameter values for inverted pendulum on a cart tracking

Weight	Form	Parameter values
W_P	$w_P = \begin{bmatrix} \frac{s/M_1 + \omega_{B1}}{s + \omega_{B1} A_1} & 0 \\ 0 & 1 \end{bmatrix}$	M_1=2 ω_{B1}=2.3 A=1e-6
W_U	$W_U = \rho * 0.1\left(\frac{s+0.001}{s+10}\right)$	$\rho_{initial}$=1 ρ_{final}=1.8
Wa	$\mathrm{Wa} = \begin{bmatrix} w_{a_1} & 0 \\ 0 & w_{a_2} \end{bmatrix}$	$\mathrm{Wa} = \begin{bmatrix} 1 & 0 \\ 0 & 0.01 \end{bmatrix}$

The step response of the initial design of the mixed sensitivity controller can be seen in Figure 72. This design had a γ value of 1.8 signifying that all performance specifications were not met. From this information we would expect that actuator usage would exceed our maximum tolerance, which figure Figure 72 clearly shows. The parameter, ρ, was then set to 1.8 and the controller was designed again. The controller synthesis returned $\gamma = 2.0$. Again we would expect that our controller was more aggressive then the one-degree of freedom H_∞ controller, yet as the step response of this new system in Figure 73 indicates this yielded an acceptable design probably because the one-degree of freedom controller had a max velocity slightly under v_{max} to begin with.

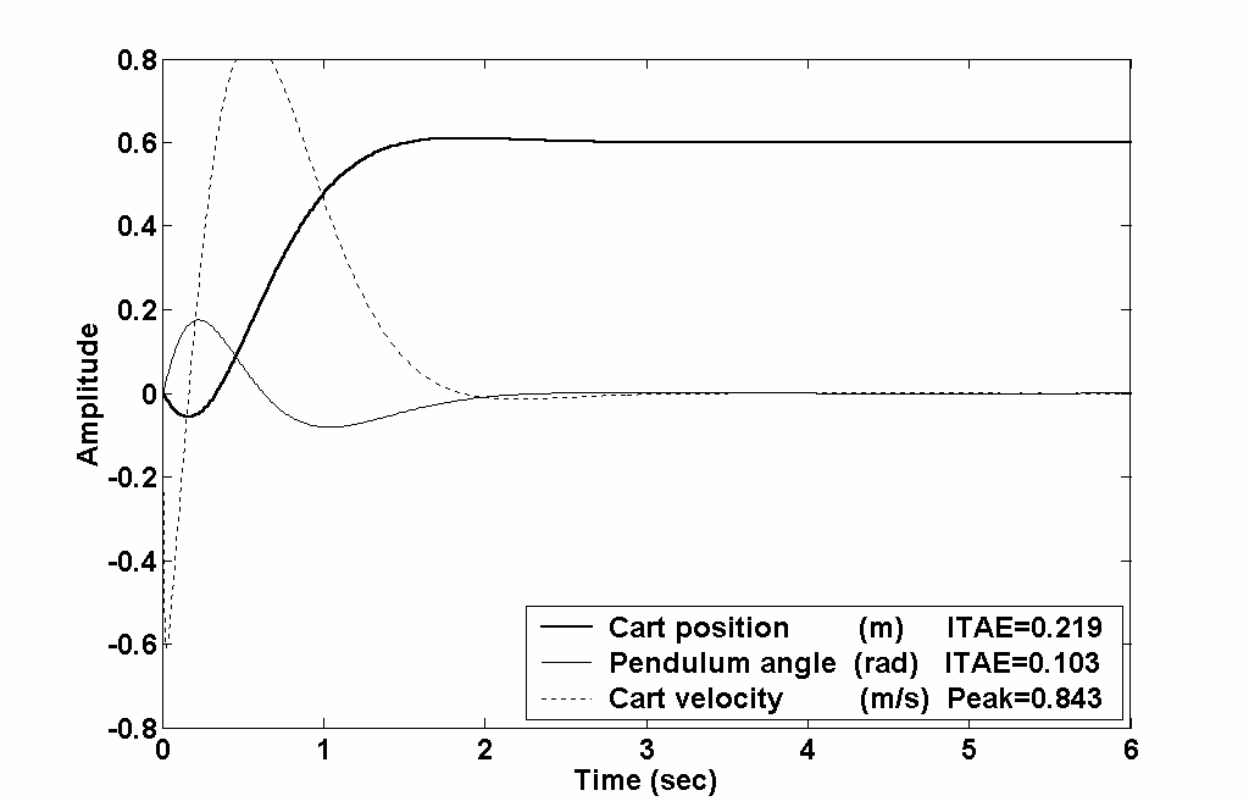

Figure 72: Initial H_∞ mixed sensitivity design.

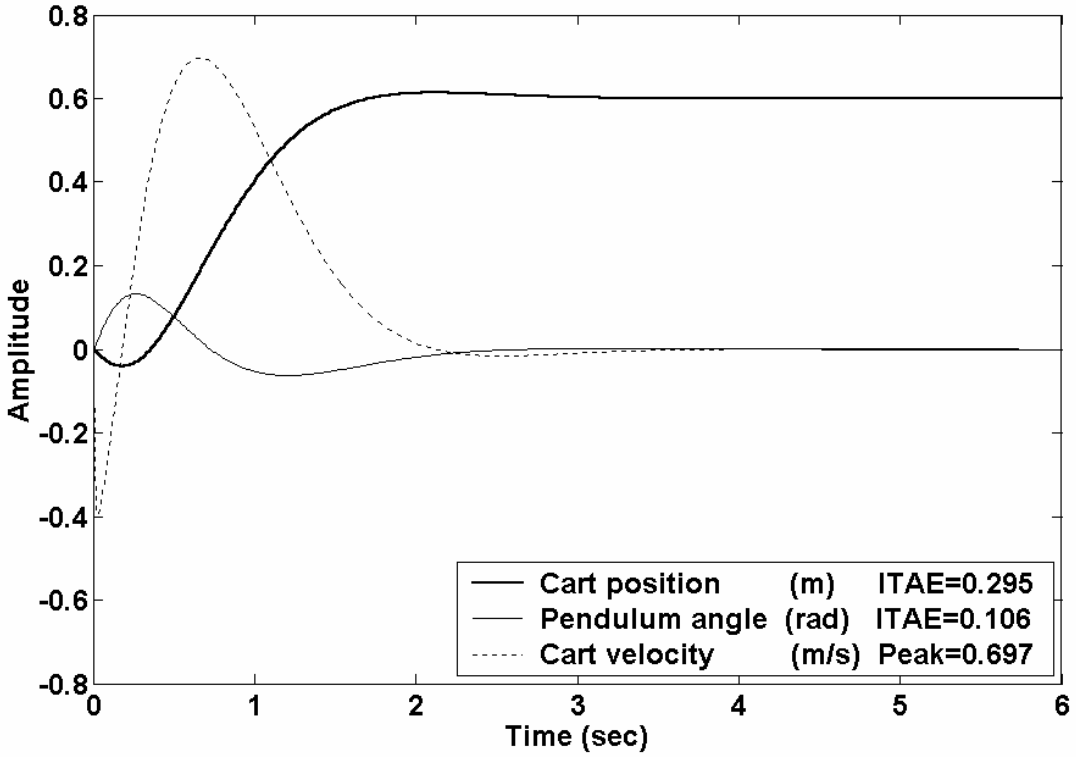

Figure 73: Final H_∞ mixed sensitivity design.

Ensuring there are no RHP poles in the closed partitioning loop establishes nominal stability, satisfying step 10 in the PEC design procedure. The location of the poles are listed:

(s+6.7578e+2)(s+1.1495e+2)(s+1.1501e+2)(s+2.0564 ±1.7288i)

(s+5.0061 ±8.3508e-1i)(s+2.0000e-5)(s+4.9603)(s+4.9434)

The mixed sensitivity controller has 6 states is shown in Equation (92).

$$K_{PL} = \left[\frac{(s+1.1501e+2)(s+1.0e+1)(s+4.9603)(s+4.9434)(s+2.0003e-5)}{(s+1.1501e+2)(s+1.0e+1)(s+4.9434)(s+2.3e-4)(s+2.0002e-5)} \right] \quad (92)$$

$$\frac{}{(s+6.6888e+2)(s+1.4672e+2)(s-1.1713e+1)(s+9.7705)(s+1.1171)(s+2.3e-4)}$$

PEC Assembly and Controller order

The three elements that are used to form the partitioned error controller are the feedback controller (4 states), the process model (4 states), and the partitioning controller (6 states). Simply assembling these parts would result in a controller with 14 states. This is not unexpected. The work done in chapter 3 showed that partitioned error controller would have at least 3 times as many states as the process model used in the design procedure. Hence the final stage in the PEC design is to explore controller minimization. Balanced residualization of coprime factors was employed for the unstable system since the feedback controller contains a RHP pole. The principle behind balanced residualization of coprime factors is to split the process up into stable and unstable parts using coprime factors, then to apply the now familiar technique of balanced residualization to the stable portion of the process. This technique resulted in a 6^{th} order approximate controller with three inputs and one output. Verification that the 6^{th} order

approximate controller was satisfactory was obtained by plotting the bode magnitudes of the 14 state controller and its 6 state approximate. These results are shown in Figure 74. As we can see the reduced controller has a slight residual around frequencies of 100 rad/s. This is well above the bandwidth of the system. A step response of the reduced controller was generated and found to be indistinguishable from the original controller.

System stability

The robustness of the controller designs to unstructured perturbations was analyzed by breaking the feedback loop at point A and B shown in Figure 75. The Guaranteed stability margins were then calculated using the following equation

$$1 - 1/\|T\|_\infty \leq \text{guaranteed G.M.} \leq 1 + 1/\|T\|_\infty \quad (93)$$

$$\text{Guaranteed P.M.} = \pm \sin^{-1}\left(1/2\|T\|_\infty\right) \quad (94)$$

The results are summarized in Table 7 through Table 9.

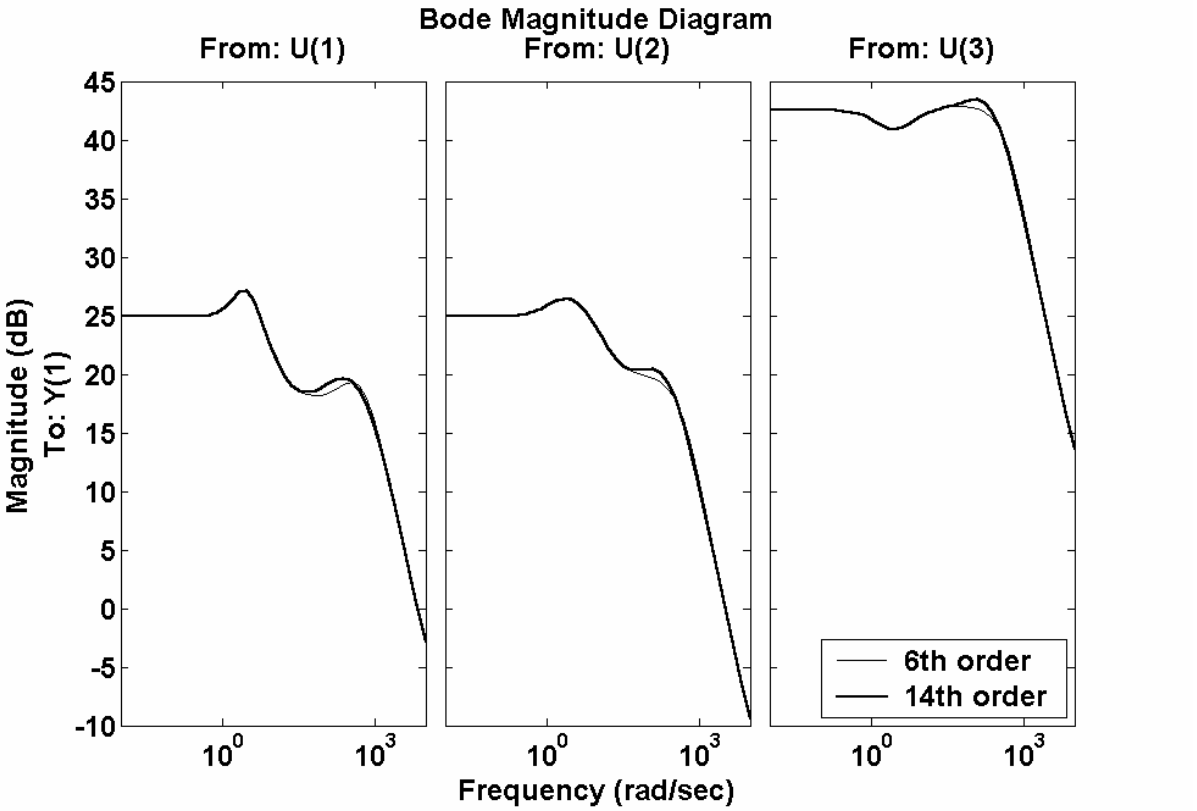

Figure 74: Bode magnitude diagram of the original 14 state PEC controller vs. the 7 state reduced PEC controller.

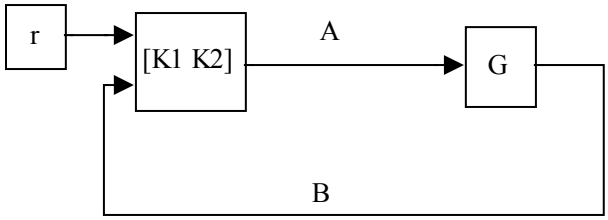

Figure 75: Points at which the loop is broken for stability analysis.

Table 7. Stability margins of 14 state Partitioned Error Controller/ H_∞ ODoF controller (identical)

Loop broken at	$\|T\|_\infty$	Guaranteed G.M.	Guaranteed P.M. (deg)
B	$\left\|\left(I-GK_2\right)^{-1}\right\|_\infty$	1.1299 to 0.8701	±7.4476
B	$\left\|GK_2\left(I-GK_2\right)^{-1}\right\|_\infty$	1.1299 to 0.8701	±7.4476
A	$\left\|\left(I-K_2G\right)^{-1}\right\|_\infty$	1.7649 to 0.2351	±44.9718
A	$\left\|K_2G\left(I-K_2G\right)^{-1}\right\|_\infty$	1.4673 to 0.5327	±27.0244

Table 8. Stability margins of H_∞ Tdof controller

Loop broken at	$\|T\|_\infty$	Guaranteed G.M.	Guaranteed P.M. (deg)
B	$\left\|\left(I-GK_2\right)^{-1}\right\|_\infty$	1.1615 to 0.8385	±9.2633
B	$\left\|GK_2\left(I-GK_2\right)^{-1}\right\|_\infty$	1.1615 to 0.8385	±9.2633
A	$\left\|\left(I-K_2G\right)^{-1}\right\|_\infty$	1.7931 to 0.2069	±46.7239
A	$\left\|K_2G\left(I-K_2G\right)^{-1}\right\|_\infty$	1.4542 to 0.5458	±26.2503

Table 9. Stability margins of 6th order reduced partitioned error controller.

Loop broken at	$\|T\|_\infty$	Guaranteed G.M.	Guaranteed P.M. (deg)
B	$\left\|\left(I-GK_2\right)^{-1}\right\|_\infty$	1.1299 to 0.8701	± 7.4476
B	$\left\|GK_2\left(I-GK_2\right)^{-1}\right\|_\infty$	1.1299 to 0.8701	± 7.4476
A	$\left\|\left(I-K_2G\right)^{-1}\right\|_\infty$	1.7427 to 0.2573	± 43.5952
A	$\left\|K_2G\left(I-K_2G\right)^{-1}\right\|_\infty$	1.4707 to 0.5293	± 27.2229

Comparison of designs

The nominal linear step response of the two-degree of freedom controllers designed in this study are compared in Figure 76. Table 10 lists the percent overshoot of these responses as well as the maximum velocity obtained, maximum pendulum attitude, and ITAE for cart tracking.

The advantage of H_∞ two-degree of freedom control is in its simplicity. It requires little additional effort to specify a simple reference trajectory, especially when that trajectory can be unrealistically aggressive. The cost of this simplicity is flexibility, however. In the end Walker shied away from introducing RHP zero into his reference trajectory simply because it increases the complexity of the problem to a point where it becomes a deterrent to designers. This makes precision tuning of tracking performance very difficult. By specifying a reference trajectory the designer is asked to make arbitrary choices without any tools for analysis. It is no surprise that a technique like this would result in designers simplifying their selection and accepting the resulting suboptimal results.This is the reason H_∞ tdof control provided inferior tracking performance in this case study.

On the other hand, PEC was able to use a very powerful controller design, mixed sensitivity, for a very specific problem, nominal tracking. The design procedure of the partitioning controller also greatly benefited from the use of the feedback controller to generate initial values for the weight parameters, making the mixed sensitivity design significantly easier then it may have been. The result of which was superior use of the second degree of freedom to meet tracking specifications, and overall better tracking performance. Granted this tracking performance gain required a higher degree of analysis and interpretation, but with the proper tools and an initial starting point in the design procedure, the designer is able to interpret and affect the process with surgical precision. One example of this is the use of the actuator weight. If the actuator usage is unacceptable for some reason then the mixed sensitivity controller gives the designer a specific tool for modifying this aspect of the design, the actuator weight Wu. In the inverted pendulum problem it would be a simple matter to address the initial jerk of the cart with the weight currently used. In fact, all it would require is the multiplication of the weight by a scalar. The introduction of a RHP zero to the reference trajectory of the TDoF H_∞ controller would have several undesired affects. First it would lower the bandwidth of the reference trajectory, bringing it more in line with the actual process response. This has a direct impact on the driving force behind reference tracking. This impact could be countered by increasing the value of the tracking weight ρ, but that would have unforeseen effects on the disturbance response, particularly in a multivariable problem.

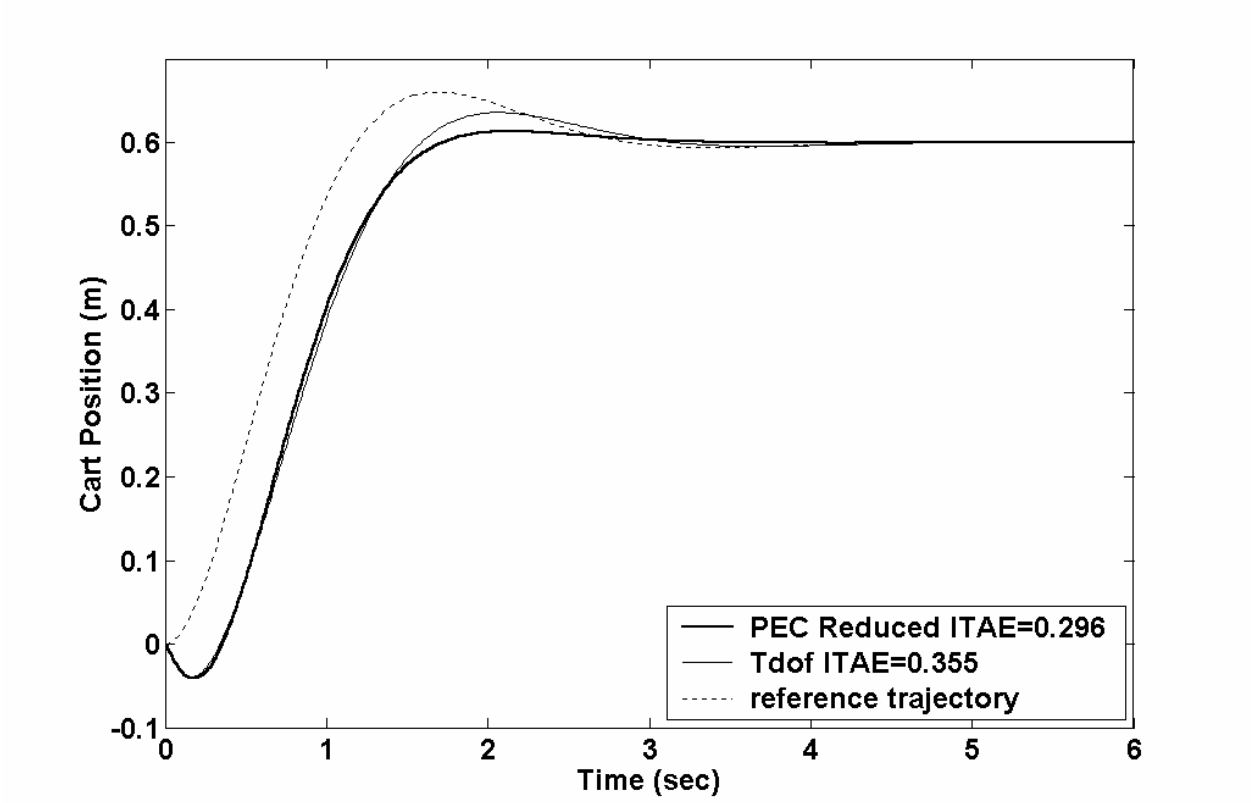

Figure 76: Tracking Performance of the Cart for both the PEC controller and the benchmark H_∞ TDoF controller.

The PEC design procedure returned a controller with superior tracking abilities over the H_∞ TDoF design and the H_∞ ODoF design. By minimizing the overshoot of the process and by operating at the boundaries of the design criteria with a max velocity of 0.696 m/s PEC returned an ITAE that was 16% lower then the benchmark system. The ITAE of the deflection of the pendulum was also significantly less then that of the benchmark system.

Table 10. Response characteristics of the Cart and Pendulum for various controllers.

Controller	% overshoot	Max Velocity m/s	ITAE	ITAE θ
Odof H_∞	5.13	0.677	0.407	0.109
Tdof H_∞	6.00	0.645	0.355	0.124
PEC	1.32	0.696	0.296	0.106

Simulation results

A step change of 0.6 meters was simulated for the perturbed nonlinear pendulum under control of both PEC and the H_∞ tdof controller. The results of this simulation can be seen in Figure 77 plotted next to the same step change for the nominal nonlinear pendulum. Both controllers exhibited degraded performance under the perturbed conditions, yet remained stable. The PEC controller displays better robust performance mainly because its nominal response does not exhibit as much overshoot as the TDoF H_∞ controllers.

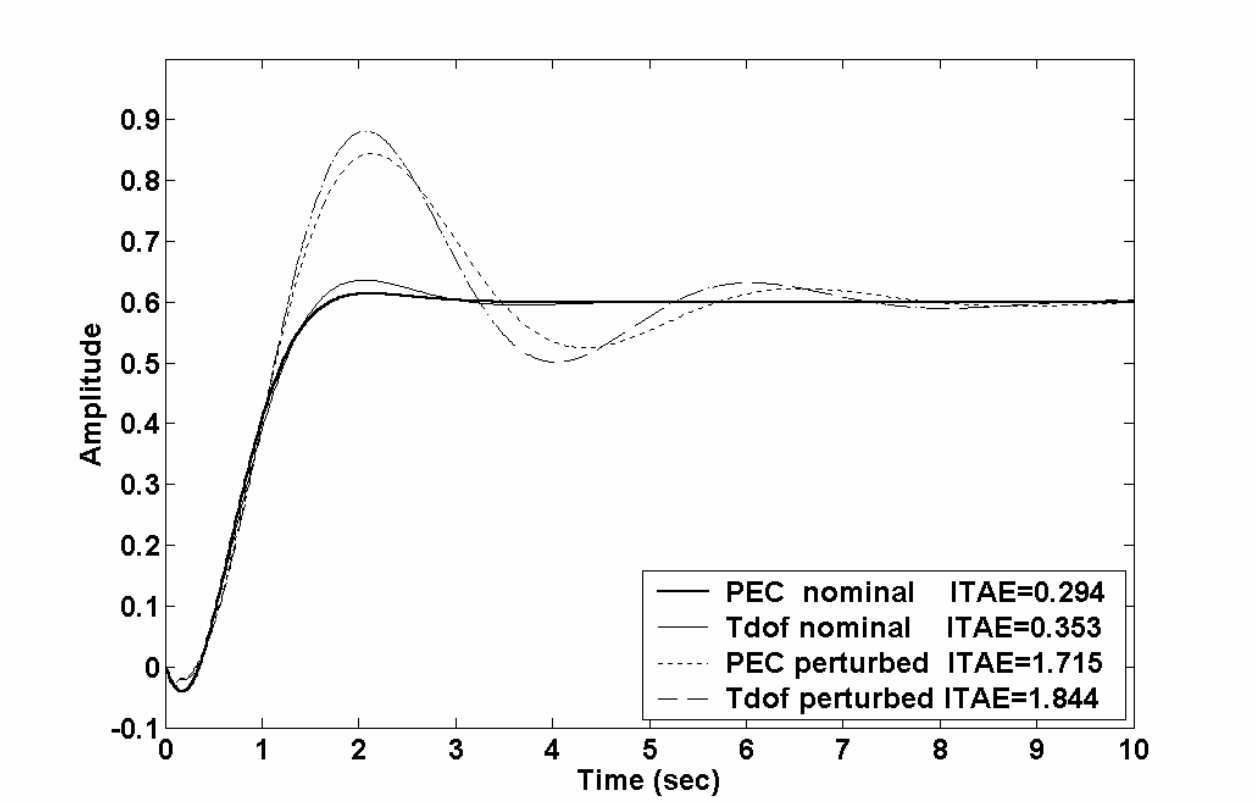

Figure 77: Nominal and perturbed responses of the reduced PEC controller and the H_∞ TDoF controller.

Conclusions

This case study demonstrated the PEC design procedure and led to favorable performance over Tdof H_∞ controller design, even though both of these controllers are two-degree-of-freedom systems. The PEC design did require more effort but also provided help in the design procedure by using the feedback controller to generate initial conditions for the tracking controller.

One of the concerns with the implementation of PEC is the overall controller size. This concern was successfully mitigated by the use of model reduction techniques. The final PEC controller had an equivalent number of states as the benchmark system.

Through this case study, it has been demonstrated that PEC is a flexible, powerful, and viable two-degree-of-freedom design technique.

CHAPTER VI

CASE STUDY: TWO-DEGREE OF FREEDOM CONTROL OF A BINARY DISTILLATION COLUMN

Introduction

This case study is used to illustrate the design procedures for a discrete implementation of an H_∞ loop-shaping/mixed sensitivity PEC controller. The controllers will be applied to stabilize and control the classic Wood and Berry binary distillation column, Figure 78. A review of the performance of the PEC controller will be given relative to a two-degree of freedom H_∞ internal model controller (IMC) developed by Murad et al.[20]

Problem Description

Wood and Berry noted in their original publication that most industrial columns are operated under SISO control where only one composition is automatically regulated, and that this form of control is wasteful of both product and energy. Attempts to control both overhead and bottoms compositions with reflux and steam flow are complicated by the inherent coupling in high purity processes. These strong interactions make the system very sensitive to inaccuracies in the manipulated variables. This requires a rigorous method for dealing with process uncertainties. This high demand of robust considerations leaves little room for tracking issues to be addressed with a one-degree of

freedom controller. As such we seek to design a two-degree of freedom controller, which provides both the required disturbance rejection and a degree of tracking performance.

Notable attempts to improve upon the original work of Wood and Berry were made by Garcia and Morari[21], who designed a one-degree of freedom IMC controller, Zhou el al.[22], who designed a modified one-degree of freedom LQG/LTR (linear quadratic Gaussian/loop transfer recovery) controller, Rouhani and Mehra[23], who designed a model predictive controller, and Murad et al. [20], who designed a two degree of freedom H_∞ IMC controller. Of these attempts Murad's two-degree of freedom design performed similarly to if not better than the other designs, and will be used as the benchmark in this study.

The Distillation Column Model

An evaluation of the effectiveness of mixed sensitivity/loop-shaping PEC will be achieved through the simulation of the Wood and Berry Distillation column. The system is a typical MIMO plant with strong loop interactions and significant time delays. The process is described in Equation (95).

$$\begin{bmatrix} y_1(s) \\ y_2(s) \end{bmatrix} = \begin{bmatrix} \dfrac{12.8e^{-s}}{16.7s+1} & \dfrac{-18.9e^{-3s}}{21.0s+1} \\ \dfrac{6.60e^{-7s}}{10.9s+1} & \dfrac{-19.4e^{-3s}}{14.4s+1} \end{bmatrix} \begin{bmatrix} u_1(s) \\ u_2(s) \end{bmatrix} + \begin{bmatrix} \dfrac{3.5e^{-8s}}{14.9s+1} \\ \dfrac{4.9e^{-3s}}{13.2s+1} \end{bmatrix} d(s) \qquad (95)$$

The time constants of the system are in minutes. The significance of the variables is given in Table 11 along with the nominal operating conditions of the process.

Table 11. Input and Output descriptions and associated steady-state values.

Variable	Description	Steady-state value
y_1	Overhead MeOH composition	96.00 mol%
y_2	Bottoms MeOH composition	0.50 mol%
u_1	Reflux Rate	1.95 lb/min
u_2	Reboiler steam rate	1.71 lb/min
d	Column feed rate	2.45 lb/min

Uncertainty in the process will be modeled as perturbations in the time delays (θ_Ps) as suggested by Zhou et al.[22], such that:

$$\left[G_P\right]_{ij} = \frac{\left[K_P\right]_{ij} e^{-\left[\theta_P\right]_{ij} s}}{\left[\tau_P\right]_{ij} s + 1} \qquad (96)$$

Uncertainty limits associated with the plant time delays are listed in table 5.2

Table 12. Perturbation values of the time delays of the distillation column.

Parametric Uncertainty	i,j	Max	Normal	Min
$\left[\theta_P\right]_{ij}$	1,1	2	1	1
	1,2	4	3	2
	2,1	10	7	4
	2,2	4	3	2

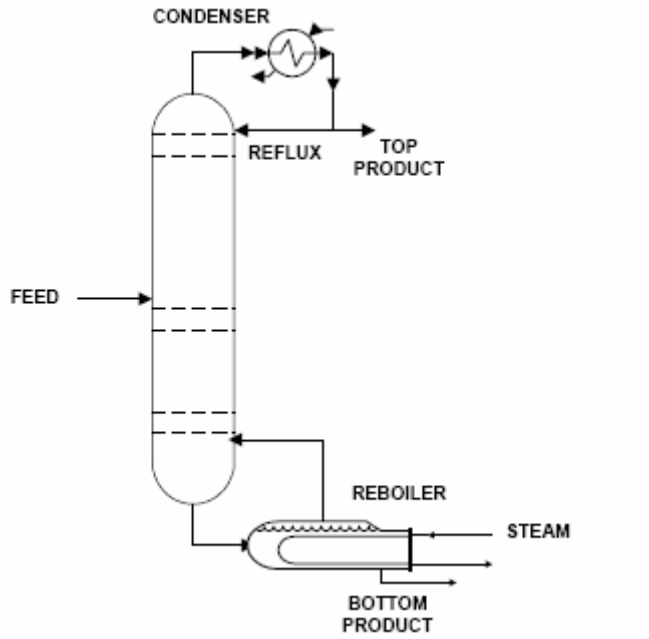

Figure 78: Diagram of the Wood and Berry binary distillation column.

Performance specifications

The design specifications suggested by Murad[20] will be used for this process

1. The final steady-state values of all variables should be at their desired value
2. Robust stability within the model uncertainty limits defined in Table 12
3. For overhead composition, where a change is demanded, the composition should be within 10% of the desired final value in less than 30 minutes.
4. Disturbances of 14% in the feed rate should be rejected to the desired steady-state value within 30 minutes.
5. All control signals should be sensible and smooth

Benchmark Controller

The benchmark controller for this study will be a two-degree-of-freedom H_∞ loop-shaping internal model controller based on the work originally presented by Murad et al. [20]. The original motivation for the work of Murad et al. [20] was to demonstrate the direct synthesis of an H_∞ two-degree-of-freedom internal model controller. The advantage of such a controller would come from the fact that IMC designs such as the one shown in Figure 79 are based on an inverse process. This type of design is not well suited for ill conditioned processes. H_∞ two-degree-of-freedom internal model controllers (TDoF H_∞ IMC) are based on minimization of the H_∞ norm and do not utilize an inverse model in their design procedures. It then follows that TDoF H_∞ IMC design could be applied to a class of problems that other IMC schemes would not be suited for.

There are a couple of benefits to IMC. The first benefit was summed up nicely by Garcia and Morari[21] who concluded that, "the IMC structure allows a rational controller design procedure where controller quality and robustness can be influenced in a direct manner", sighting a high level of transparency and intuitive appeal, making IMC an attractive alternative to classic feedback approaches. Under the perfect model assumption IMC controllers are open loop controllers. The intuitiveness and directness springs directly from the relation of the controller to the inverse process. TDoF H_∞ IMC severs this relationship. The form of an H_∞ controller is a state space model where the parameters have no interpretable meaning. This is the direct opposite of classic IMC controllers. Take for instance the gain of an open loop controller. It is known that the overall gain of the response should equal unity, therefore it follows that the gain of the controller must be the inverse of the gain of the process. The second benefit of IMC control is that it can be used to determine the present dynamic state of the process, states that may be otherwise unobservable. Control based on the present dynamic state of a process (not just observable states) falls into a category called full information control. This ability is not limited to IMC control, however; it is simply that this additional information can be accessed fairly readily through use of the internal model. The access of this additional information requires that the current disturbance input is known. A similar technique could be applied to the PEC structure in the partitioning loop. The benefit would be that the disturbance would not need to be measured, because there is no disturbance in the partitioning loop. This would open up the application of full information control to a much wider category of systems. The down side to this implementation is that the full information controller would only be responsible for

nominal servo performance. Disturbances would be handled without the benefit of full information. This application may be more beneficial for ill-conditioned processes, but that has not been investigated yet.

These nuances of TDoF H_∞ IMC are interesting, but the performance of this controller as it was applied to the Wood and Berry distillation column by Murad et al. [20] is almost identical to the performance of a standard TDoF H_∞ controller; so much so that the differences are not worth quantifying.

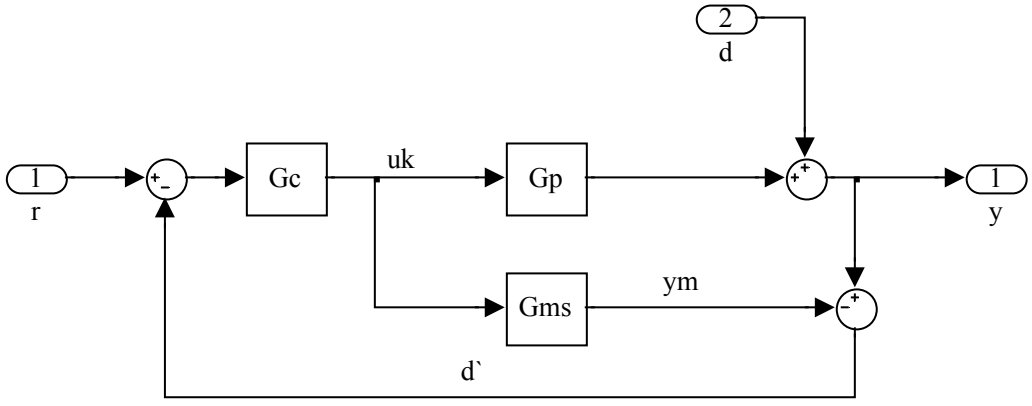

Figure 79: The general implementation of Internal Model Control.

The design configuration for TDOF H_∞ IMC is presented in Figure 80. This configuration is similar to that of the TDOF H_∞ controller discussed in previous chapters. Equation (97) is the algebraic representation of this configuration. When compared to the configuration of a TDoF H_∞ controller shown in Equation (98) we see that the IMC controllers Q1 and Q2 are expressed as open loop controllers instead of feedback controllers like K1 and K2, but other than this distinction, the block matrices of these two

systems possess the same functionality. It is interesting to note that Murad et al. [20] left out the tuning parameter ρ in their formulation of the design configuration. This tuning parameter could be used if desired, but its absence suggests that the parameter is not commonly used in controller design.

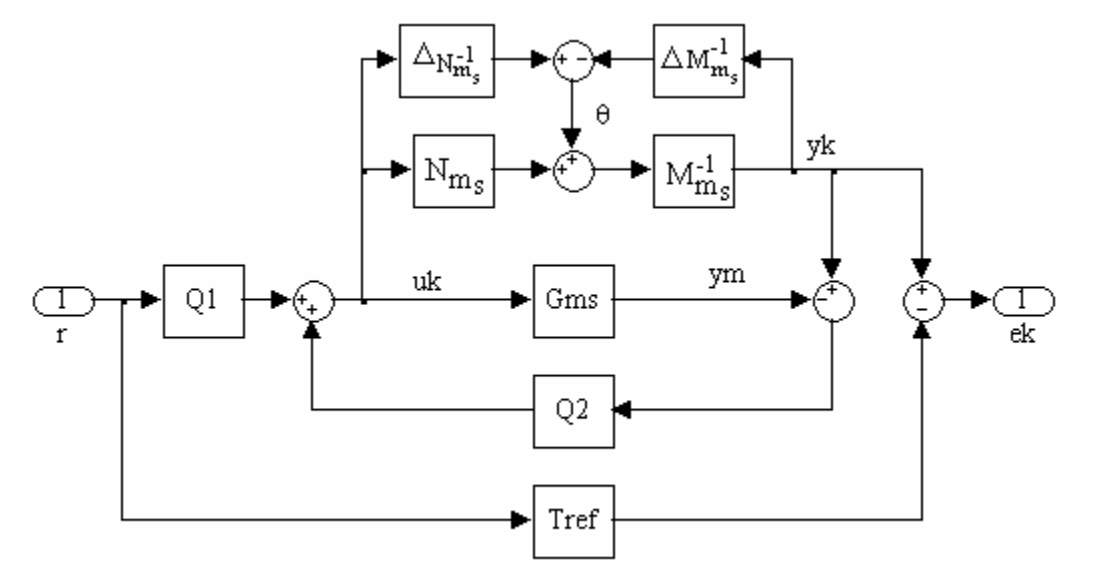

Figure 80: TDOF H_∞ IMC design configuration

$$\begin{bmatrix} uk \\ yk \\ ek \end{bmatrix} = \begin{bmatrix} Q_1 & Q_2 M_{ms}^{-1} \\ G_{ms} Q_1 & \left(I + G_{ms} Q_2\right) M_{ms}^{-1} \\ G_{ms} Q_1 - Tref & \left(I + G_{ms} Q_2\right) M_{ms}^{-1} \end{bmatrix} \begin{bmatrix} r \\ \theta \end{bmatrix} \tag{97}$$

$$\begin{bmatrix} u_s \\ y \\ e \end{bmatrix} = \begin{bmatrix} \rho(I - K_2 G_s)^{-1} K_1 & K_2 (I - G_s K_2)^{-1} M_s^{-1} \\ \rho(I - G_s K_2)^{-1} G_s K_1 & (I - G_s K_2)^{-1} M_s^{-1} \\ \rho^2 [(I - G_s K_2)^{-1} G_s K_1 - T_{ref}] & \rho(I - G_s K_2)^{-1} M_s^{-1} \end{bmatrix} \begin{bmatrix} r \\ \phi \end{bmatrix} \tag{98}$$

Modification to the design procedure and simulation of the benchmark system

Upon examining the work done by Murad et al.[20] it was noted that the performance of the TDoF H_∞ IMC controller was exceptional. In fact the system response was so good it was given extra scrutiny. Upon further examination it was noted that the systems bottoms composition was instantly responding (if ever so slightly) to set point changes in the overhead. According to our process model there should be a minimum delay of three minutes (due to process delays) before any change in the bottoms composition is observed. Eventually the design was reproduced and the root cause of this discrepancy was determined to be modeling error brought about by using approximations of approximations to represent time delays in the system. First order pade approximations were made of the time delays in the model, and then discrete approximations were made of the pade approximations. The discrete model was then used to synthesize the controller AND to run simulations to test that controller. The impact of discretizing the first order pade approximation can be seen in Figure 81. This figure displays the discretization of a first order response with a dead time. The final approximation has an all pass element; at time zero the gain of the response is slightly negative. This dynamic is negligible for a P+I controller because the control law is too simple to take advantage of this dynamic, an H_∞ controller with 28 states like the one developed by Murad et al.[20] is a different story, however. These seemingly negligible dynamics coupled with the complexity of the controller and the questionable use of the approximation of the model in simulations form the reason the TDoF H_∞ IMC controller functions almost as if the system was under a full frequency decoupler.

Two corrective actions were made to method used in this study.

First, controllers will be designed in the Laplace domain, then after the controller designs are complete they will be discretized. Murad et al.[20] defined the frequency decoupler, the shaped plant, and the reference trajectory in the Laplace domain, then discretized them, and then designed the controller. This splits the design procedure up between two domains (s and z), and adds error into the design that is inherent when approximating systems from one domain to the other. By designing the controllers entirely in the Laplace domain this source of error will be mitigated.

Second, the nominal model defined in Equation (95) will be used without approximation during simulations. Any approximations that need to be made to design controllers should not affect the process model. When Wood and Berry first modeled the binary distillation column simulation techniques often required the use of pade approximations of time delays, however, modern software packages can easily simulate time delays without using approximations. As a result, first order pade approximations will be used for controller design, but during simulation runs process time delays will not be approximated. This will introduce process/model mismatch into the design. Higher order approximations can be used, but it is more beneficial to this study to examine worst case scenarios.

As a side note the original data published by Wood and Berry suggests that approximated time delays may describe the process better than true time delays. Based on this information, running simulations against approximated models was considered, but in the end it was determined to be of greater interest to see how controller designs performed in systems with unapproximated time delays.

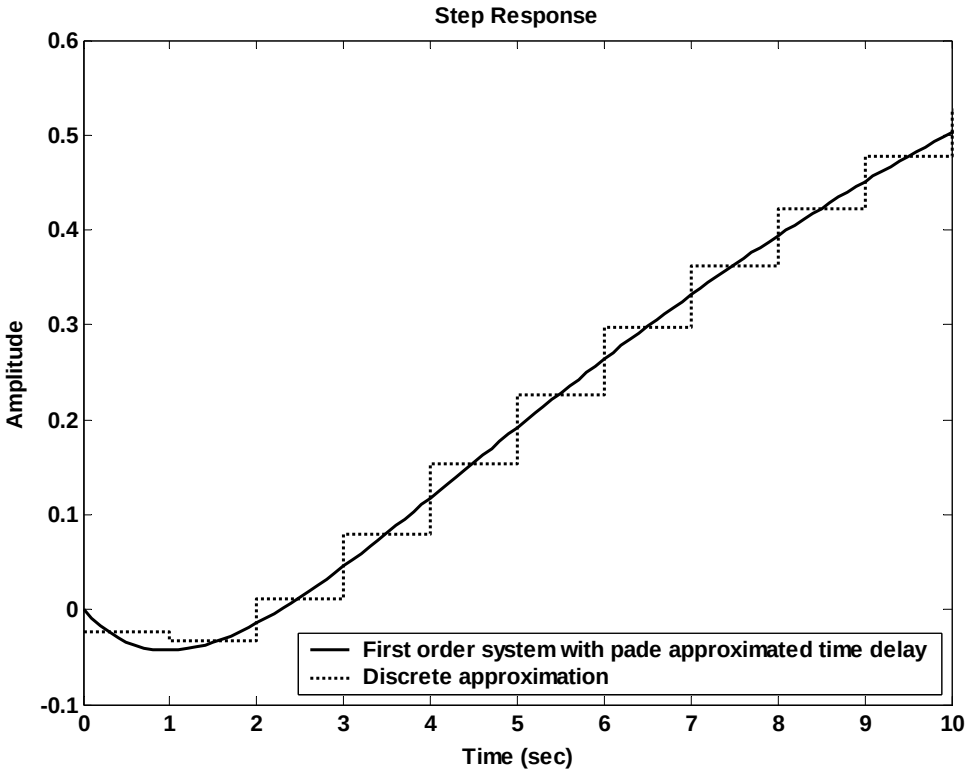

Figure 81: The step response of a first order system with the pade approximation of a 3 minute delay, and the discretization of that response.

Design Procedures: Shaping the Process

As we learned in the previous chapters, we would like the shaped plant, Gs, to exhibit high gains at low frequencies, a roll off rate of approximately 20dB/decade at the desired bandwidth, and integral action to enhance low frequency performance. Generally this requires a preweight in the shape of a P+I controller. This makes it very tempting to use the P+I controller designed by Wood and Berry as our preweight, but due to stability conditions of an IMC scheme integral action must be approximated. In deference to this restriction the initial weighting function, $\hat{W}$, that was chosen can be seen in Equation (99). To keep the various controllers used in this study similar, approximate integral action will be used for both the TDoF H_∞ IMC controller and the ODoF H_∞ controller that will be used in the PEC controller. This approximation adds an additional state to the overall PEC controller which is not needed, but will be removed with the application of model reduction techniques after the controller is designed.

$$\hat{W} = \frac{1}{\left(s+10^{-6}\right)\left(s+30\right)} I_2 \qquad (99)$$

The final step in determining the preweight is to align $G_m\hat{W}$ at the desired closed loop bandwidth of the system, where G_m is the process model. This will be done by approximating the real inverse of the system at a specified frequency, the closed loop bandwidth of the system. The alignment term Ka is in effect a constant decoupler. The concept is similar to that of a steady state decoupler. The decoupling frequency was chosen to be 0.3 rad/sec after examining the singular values of the original process. The final preweight is then chosen to be $W_1=\hat{W}Ka$. The singular values of the original and

shaped plant are displayed in Figure **82**. By examination we note that all the desired characteristics of the shaped process were achieved.

Decoupling and TDoF Processes

The use of a constant decoupler to define the shaped process brings up the as of yet unexplored question of how decoupling could work in the PEC structure. There currently is not way to implement decoupling in a two-degree-of-freedom fashion using standard two-degree-of freedom techniques. Any decoupler that is used for feedback must also be used for tracking and vice versa. The independence of design that is allowed by partition error control also allows a designer the option of using different decoupling techniques for feedback and tracking control. The question then becomes under what circumstances would a designer desire to implement different decouplers for tracking and regulatory control? The obvious answer to that question is when the implementation of full decoupling is restricted by the uncertainty found in all real systems. Take for instance the following three common restrictions. The theoretical application of full decouplers relies on the exact cancellation of system dynamics. This cancellation translates RHP zeros into RHP poles resulting in unstable decouplers. Similarly systems with erroneous models can lead to similar stability issues. The last restriction may come from the realizability of system dynamics, for instance the designs for some systems result in a decoupler with a predictive element.

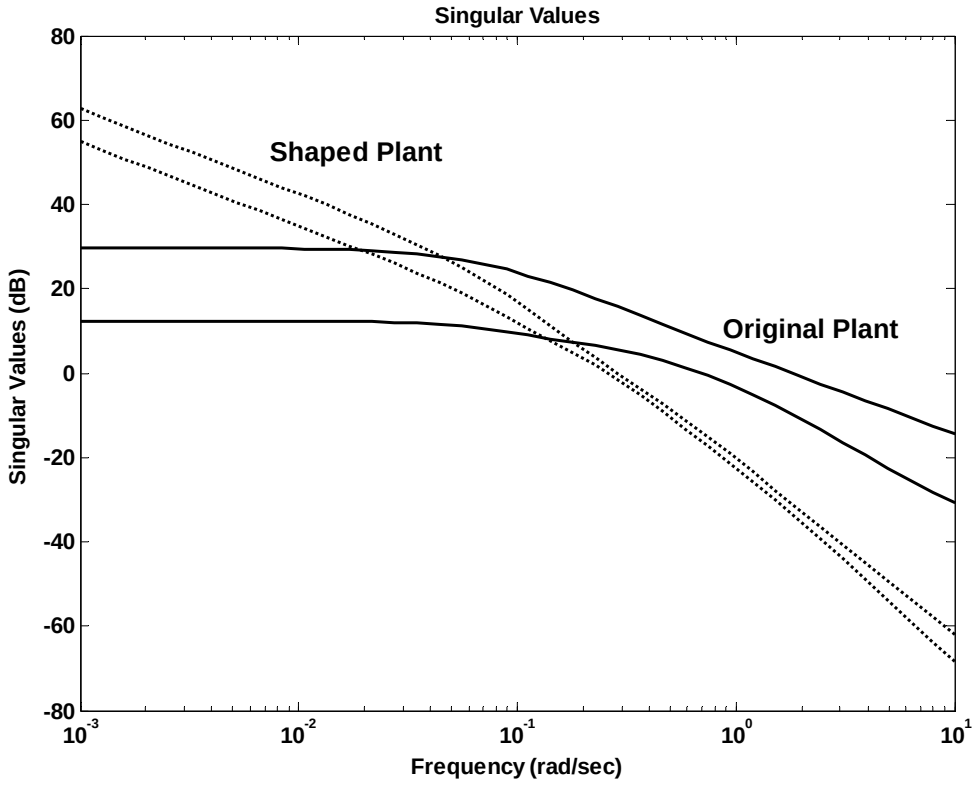

Figure 82: Singular values of the original and shaped process.

All of these restrictions are mathematical in nature, and all of the restrictions come from the implementation of these theories on real systems. The partitioning loop is not a real system, it is a mathematical abstraction of the process. The partitioning loop may allow a relaxing of the restrictions placed on decouplers, so that tracking responses can benefit from reduced loop interactions. A detailed study of this topic will be left for future research. However, before we continue the design of the controllers for the binary distillation column, I would like to suggest a specific application to prod the imagination of the reader.

The system defined in Equation (100) only contains time delays. It is impossible to fully decouple this system because the theoretical decoupling design relies on the ratios of G_{12}/G_{11} and G_{21}/G_{22}. In this case the G_{21}/G_{22} would be predictive and unrealizable. Inside the partitioning loop a time delay could be used to add a 2 minute delay to the U_1 control signal. In effect this would shape the process, slowing down the tracking response of the y_1 process variable by 2 minutes. For the shaped process, G_{21}/G_{22} would no longer be predictive and a full decoupler could be implemented for tracking. This would result in a slower yet smoother tracking response. Such a response may be desirable in continuous chemical processing where set point changes are not frequent and are often planned well in advance. The regulatory response of this system would not be decoupled because it would be undesirable to add a delay to a disturbance rejection response.

$$\begin{bmatrix} y_1 \\ y_2 \end{bmatrix} = \begin{bmatrix} G_{11} & G_{12} \\ G_{21} & G_{22} \end{bmatrix} \begin{bmatrix} U_1 \\ U_2 \end{bmatrix} = \begin{bmatrix} e^{-1s} & e^{-3s} \\ e^{-3s} & e^{-5s} \end{bmatrix} \begin{bmatrix} U_1 \\ U_2 \end{bmatrix} \qquad (100)$$

Benchmark control: TDoF H∞ loop-shaping Internal Model Control (IMC)

With the shaped process determined, the final design element for the TDoF H_∞ IMC controller is the choice of a reference trajectory, T_{ref}. Murad et al. [20] selected the trajectory shown in Equation (101). No justification for this selection was given.

$$T_{ref} = \frac{1}{1.43s+1} I_2 \qquad (101)$$

There are some note-worthy characteristics. First, T_{ref} is specifying that there should be no interactions between process outputs. Second, there is no accounting for the time delays in the system. We know there will be at least a 1 minute delay on the overhead tracking response, and a 3 minute delay on the bottoms tracking response. The ability to set unrealistic and arbitrary reference trajectories in TDoF H_∞ control is something that we have seen in the other applications that have been explored. With simpler systems this was a minor inconvenience; however, with the addition of non-minimum phase dynamics the design choices for shaping the tracking responses are becoming limited. It would be possible to specify time delays in these trajectories, but in order to synthesis the controller those trajectories would have to be approximated. Low order approximations could introduce an inverse response in the reference trajectory, while higher order responses can have a significant impact on the size of the controller. Couple these drawbacks with an inability to directly specify actuator usage and it becomes apparent that the ability to utilize the second degree of freedom is limited.

Ignoring a one minute delay on a response that will take 10 to 15 minutes is not a bad assumption. Leaving it out of the reference trajectory for the overheads increases the driving force on overhead tracking during the H_∞ minimization, in that same vain, leaving the time delay out of the reference trajectory for the bottoms increases the driving force

on the bottoms during the H_∞ minimization process. With this understanding, it can be predicted that the response to setpoint changes in the bottoms composition will be more aggressive than corresponding overhead changes, because the reference trajectory of the bottoms is much more unrealistic than the overheads.

The sub-optimal controller was designed through gamma iteration. The controller along with the internal model was discritized, then a balanced residualization was then performed on the discrete controller reducing the overall number of states in the controller from 25 to 15. Negligible residuals were found when the frequency responses of the original and reduced controllers were compared over four decades around the cross over frequency of the system.

PEC Control Design

With the shaped process determined, the ODoF H_∞ loop shaping controller was designed through gamma iteration. The sensitivity response was plotted for the ODoF controller to help with weight selection for the design of the mixed sensitivity controller in the partitioning loop as shown in Figure 83. The form of the performance weight and the tuning parameters chosen are displayed in Equation (102). The default values of 2 and $1e^{-4}$ were applied to the weighting parameters M_i and A_i respectively. The crossover frequency of the process, 0.3 rad/sec, was used as the bandwidth requirement ω_{b1}. ω_{b2} was chosen as 0.1 rad/sec to match the ODoF sensitivity response.

$$\begin{aligned} W_P &= \mathrm{diag}\{w_{Pi}\} \\ w_{Pi} &= \frac{s/M_i + \omega_{bi}}{s + \omega_{bi}A_i} \\ M_1 &= 2;\ \omega_{b1} = 0.3;\ A_1 = 1e^{-4} \\ M_2 &= 2;\ \omega_{b2} = 0.1;\ A_2 = 1e^{-4} \end{aligned} \qquad (102)$$

The form of the actuator weight and the tuning parameters chosen are displayed in Equation (103). The default values of 2 and $1e^{-4}$ were applied to the weighting parameters M_{ui} and A_{ui} respectively. The crossover frequency of the process, 0.3 rad/sec, was used as the bandwidth requirement ω_{ui}. The use of an actuator weight of this form will limit high frequency actuator use in the system.

$$\begin{aligned} W_u &= \mathrm{diag}\{W_{ui}\} \\ W_{ui} &= \frac{1}{A_{ui}}\left(\frac{s + \omega_{ui}M_i}{s + \frac{\omega_{ui}}{A_{ui}}}\right) \\ M_i &= 2;\omega_{ui} = 0.3;A_{ui} = 1e^{-4} \end{aligned} \qquad (103)$$

The H_∞ mixed sensitivity controller was designed by gamma iteration. Performance evaluations were then conducted on the loop shaping and mixed sensitivity controller to assure adequate performance before assembling the final PEC controller. During these evaluations it was determined that the loop shaping controller used for feedback was taking aggressive control action, a desirable trait for nominal disturbance rejection, but not for robust disturbance rejection. To correct this characteristic a post weight W2 was introduced to the shaped plant. Recalling from our previous experience that post weight values greater than one emphasize disturbance rejection by loosening restrictions on actuator usage, we select a post weight less than one to tighten up restrictions on actuator usage. A post weight of 0.5*I2 was added to the shaped plant and the loop shaping controller was resynthesized. Performance evaluations of the new controller were adequate.

The final PEC controller, which contained the H_∞ loop shaping controller for feedback control and the H_∞ mixed sensitivity controller with an internal model for tracking control, was assembled and discritized resulting in a 24 state controller. A balanced residualization was then performed on the discrete controller reducing the overall number of states in the controller from 24 to 12. Negligible residuals were found when the frequency responses of the original and reduced controllers were compared over four decades around the cross over frequency of the system.

Figure 83: Frequency response of the sensitivity function of the ODoF H_∞ controller plotted with the inverse performance weight W_P.

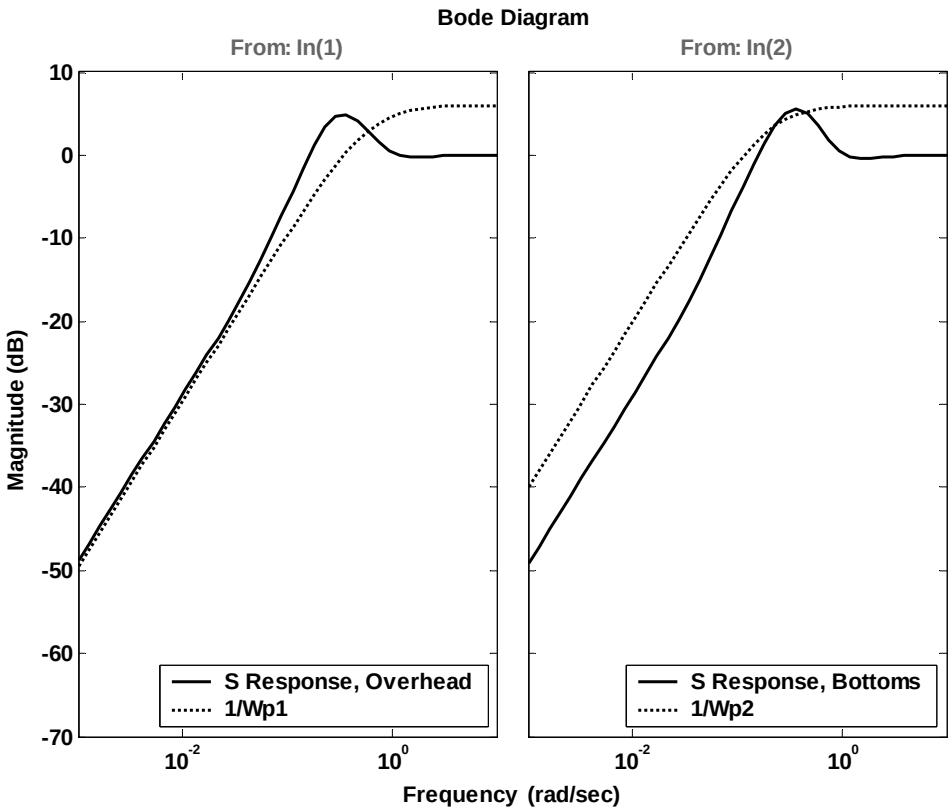

Simulation Results and Controller Comparison

The nominal performance of the TDoF IMC and PEC controllers in response to a 0.75% increase in the setpoint of the overhead can be seen in Figure 84. Actuator usage for the responses can be seen in Figure 85. Several observations can be drawn from these figures. First, the TDoF IMC controller has a more aggressive tracking response. The overhead response of the TDoF IMC controller has a rise time of 8 minutes, while the PEC controller has a rise time of 11 minutes. This is not surprising seeing as the reference trajectory used in the TDoF IMC design has a rise time of 4 minutes. Second, the bottoms response is also aggressive. The oscillatory shape of the bottoms response and the roughness seen in the overhead response are the results of having aggressive control with modeling error. Recall the controllers were designed with a first order Pade approximation, while the simulated process used true time delays. The approximated dynamics brought about during controller synthesis are now reemerging as modeling error in the performance analysis, and as with all systems, performance and robustness are conflicting objectives. Very aggressive control will make very aggressive mistakes when modeling error is present. The PEC response set performance objectives based on the bandwidth of the system. This approach has resulted in a slower more stable response with a settling time to a nominal setpoint change in the overheads of 30 minutes.

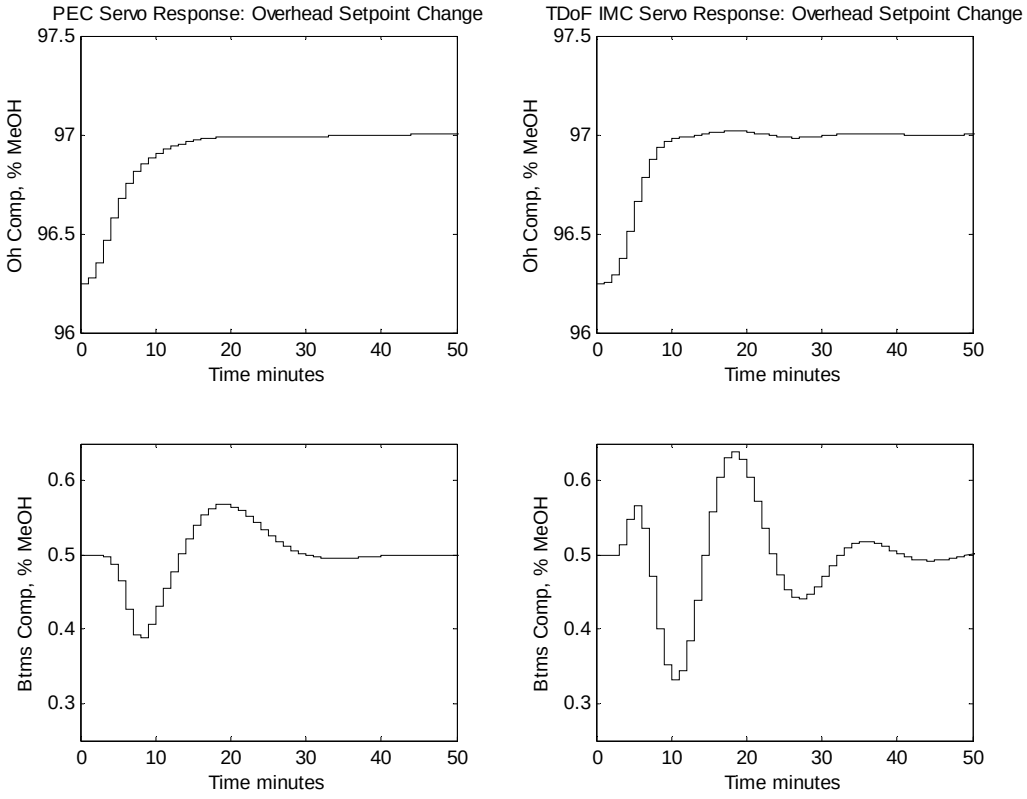

Figure 84: The step response to a 0.75% change in overhead composition for PEC and TDoF IMC control

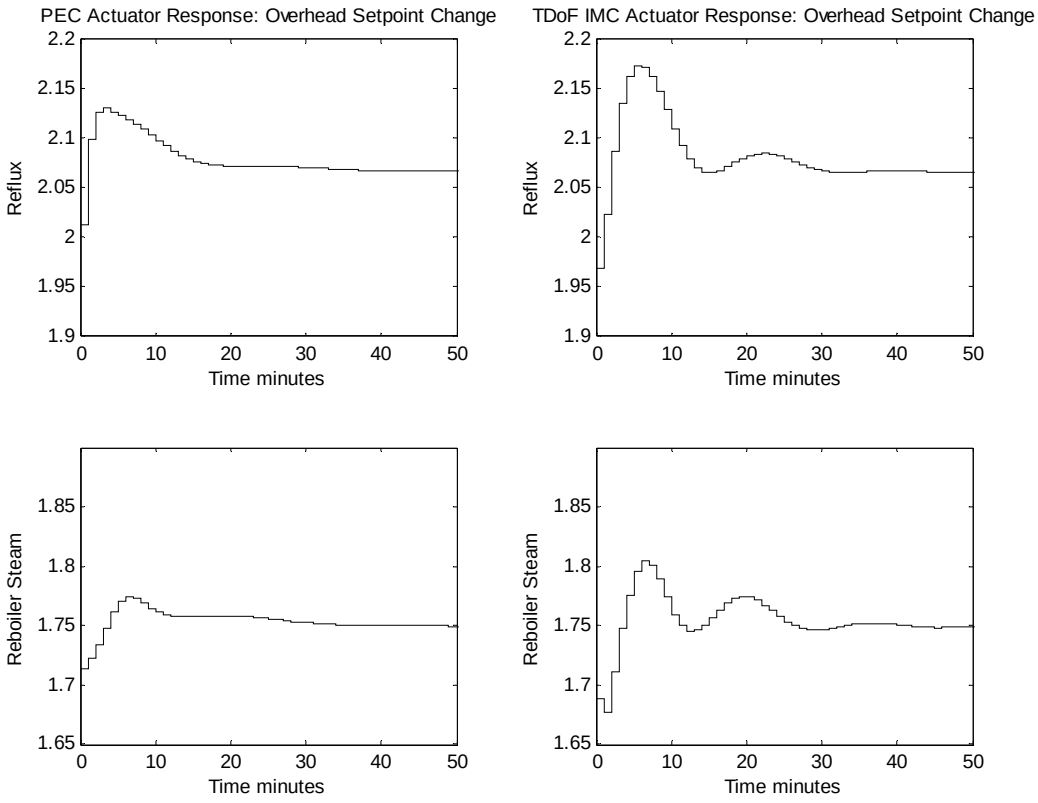

Figure 85: The actuator response to a 0.75% change in overhead composition for PEC and TDoF IMC control.

The nominal performance of the TDoF IMC and PEC controllers in response to a 0.75% increase in the setpoint of the bottoms can be seen in Figure 86. The TDoF IMC controller response contains some overshoot, but on the whole both, the IMC and PEC controllers were able to track the bottoms set point with minimal impact on the overheads composition. Both controllers were found to have an acceptable response to bottoms changes.

Figure 87 displays the system response to a 0.34 lb/min increase in the feed flow rate to the column. The TDoF IMC controller exhibits a faster recovery time than the PEC controller for both the overhead and bottoms composition. The PEC response is, however, smoother. Since the regulatory response of these controllers were both based on the same loop shaping techniques, it is safe to conclude that the enhanced performance of the TDoF IMC controller is a direct result of the interaction between tracking and regulatory considerations during the H_∞ optimization. In this case the interaction between the degrees-of-freedom during the optimization process has enhanced this particular portion of the response.

All three nominal responses have similar results. Both controllers were able to meet the nominal design criteria with responses that approach steady state within 30 minutes. The TDoF controller exhibits a faster response with more controller action, while the PEC response is smoother. Figure 88, Figure 89, and Figure 90 detail the robust performance of the controllers for the perturbed process. Two robust responses were generated. Using the parametric uncertainty outlined in Table 12 the first response utilized the maximum time delays for each transfer function, while the second response utilized the minimum time delays for each transfer function. Both controllers have a

stable response, satisfying the robust stability requirement. The aggressive nature of the TDoF IMC controller is producing a highly oscillatory response under the maximum time delay conditions.

With additional tuning the responses of both of these two-degree-of-freedom controllers could be modified to obtain nearly identical results for both the nominal and perturbed system. The fine tuning procedures for these controllers would vary significantly, however. The PEC system provides the designer with independently tunable parameters for the performance of the system, (W_p, W_1) as well as the actuator usage of the system, (W_u, W_2). TDoF H_∞ IMC control provides a conceptually simpler, but less intuitive tuning process. The use of the reference trajectory as a tunable parameter has the potential to provide the desired response, the designer is forced to use one tunable parameter to meet tracking and actuator goals.

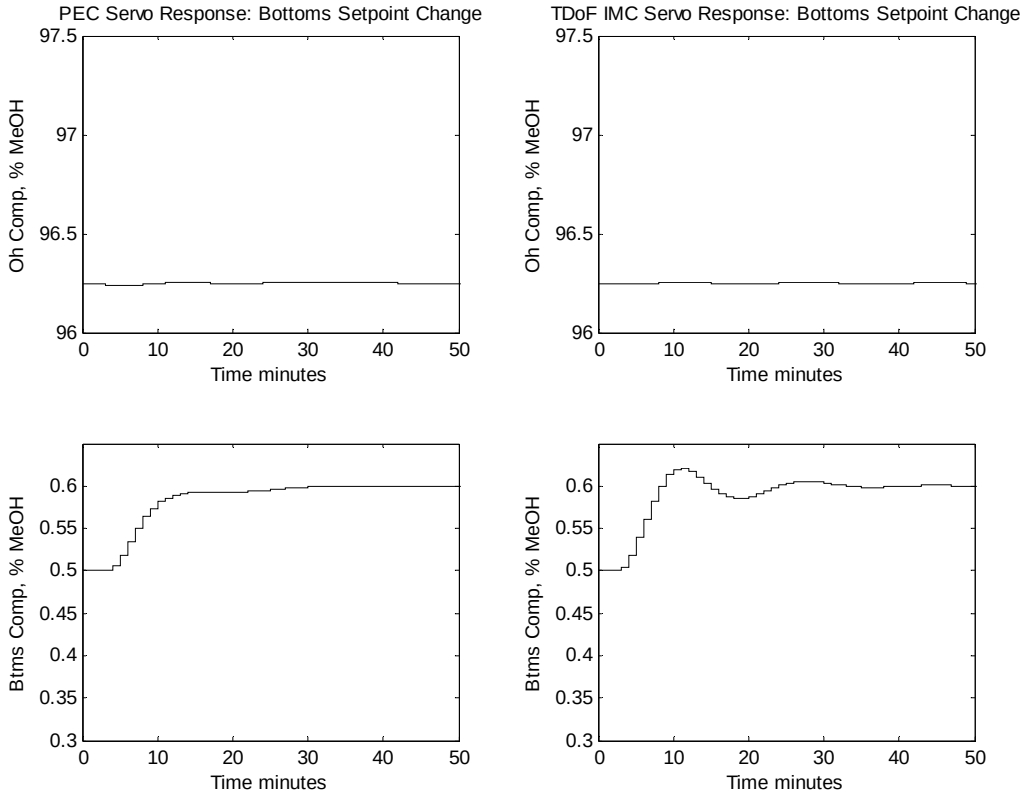

Figure 86: The step response to a 0.75% change in bottoms composition for PEC and TDoF IMC control

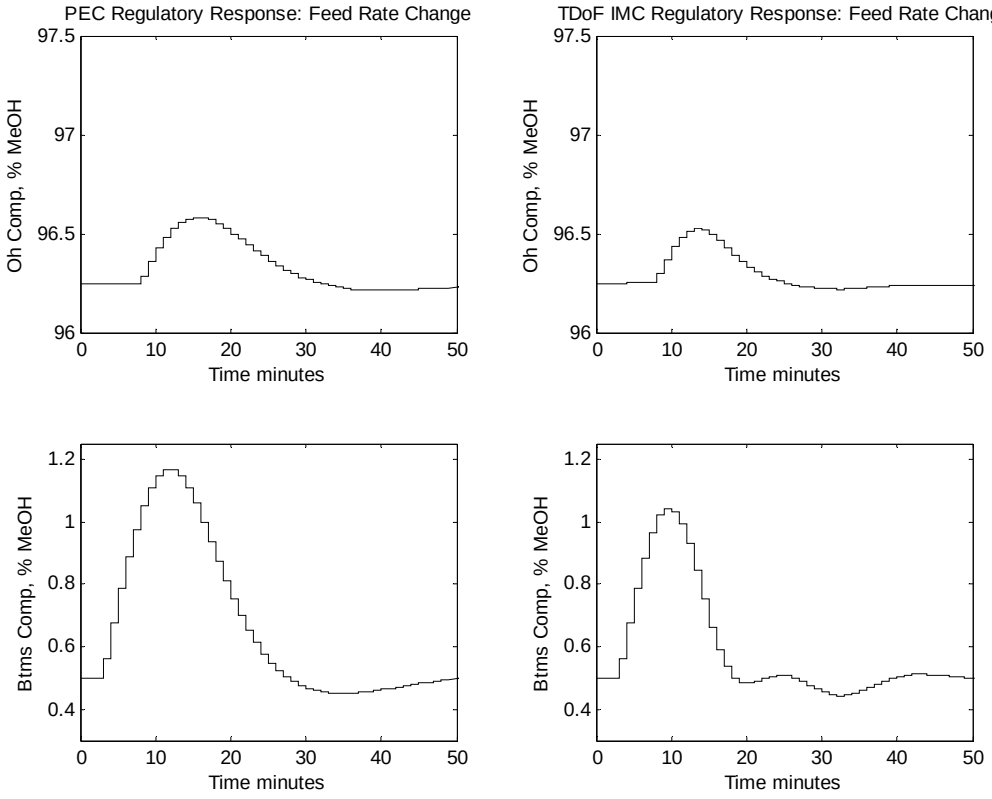

Figure 87: The regulatory response to a 0.34 lb/min change in the column feed rate for PEC and TDoF IMC control.

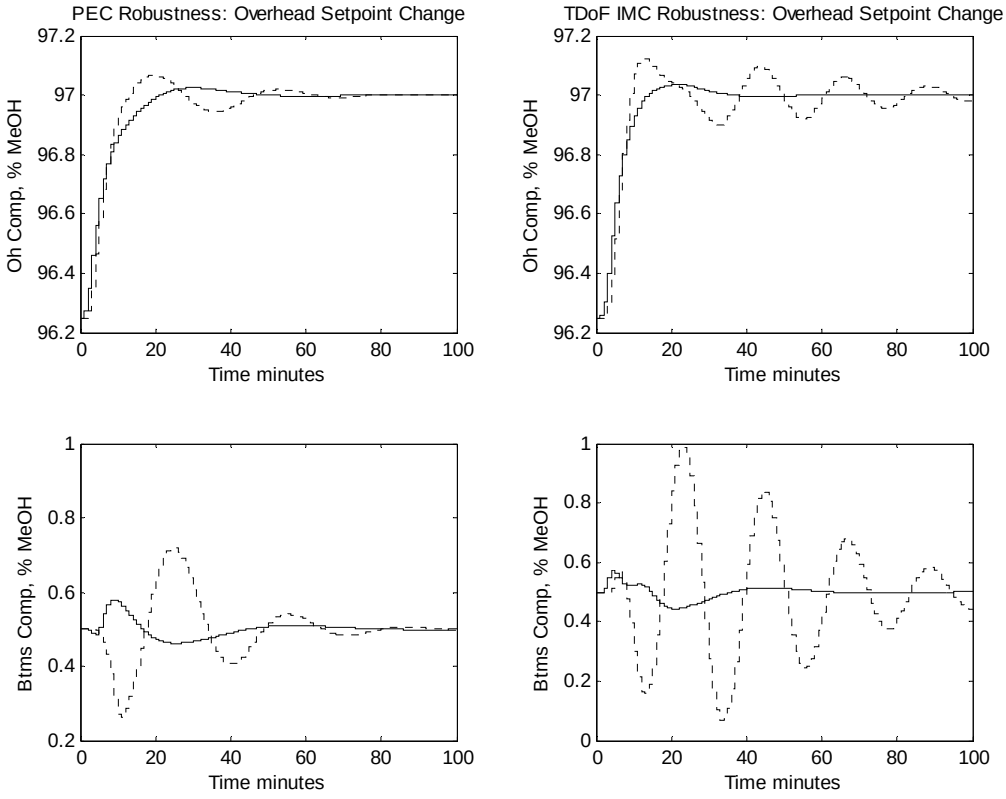

Figure 88: The step response of the perturbed process to a 0.75% change in overhead composition for PEC and TDoF IMC control. The solid line represents the process with the minimum time delays. The dotted line represents the process with the maximum time delays.

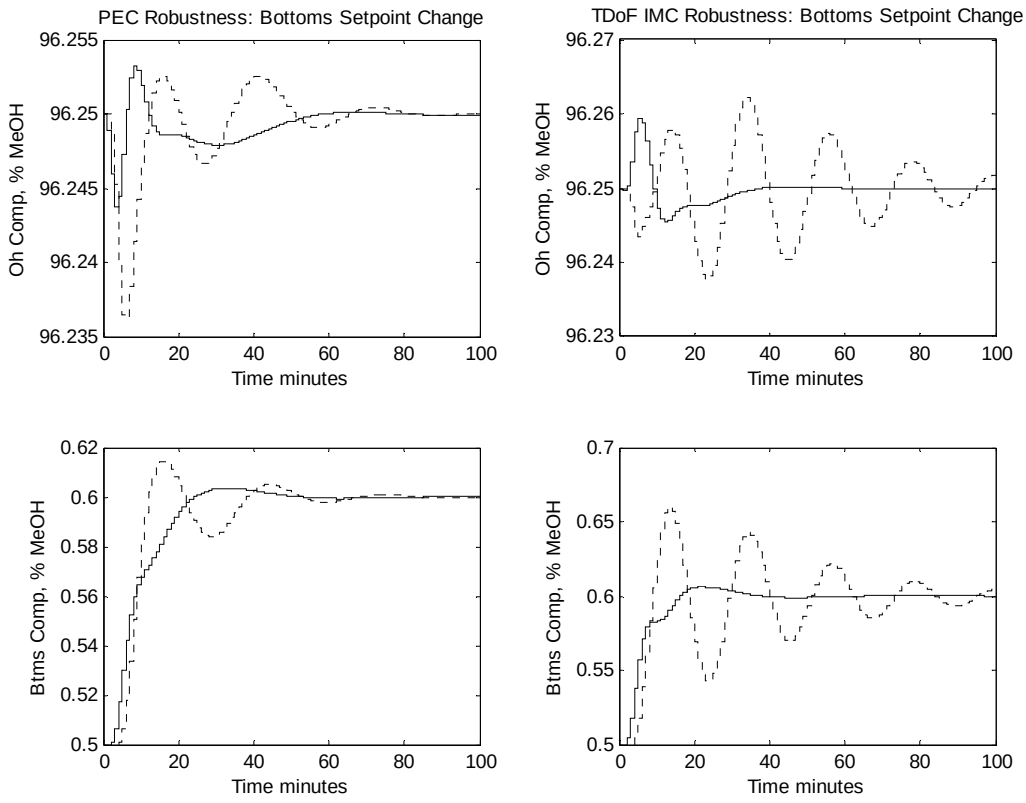

Figure 89: The step response of the perturbed process to a 0.75% change in bottoms composition for PEC and TDoF IMC control. The solid line represents the process with the minimum time delays. The dotted line represents the process with the maximum time delays.

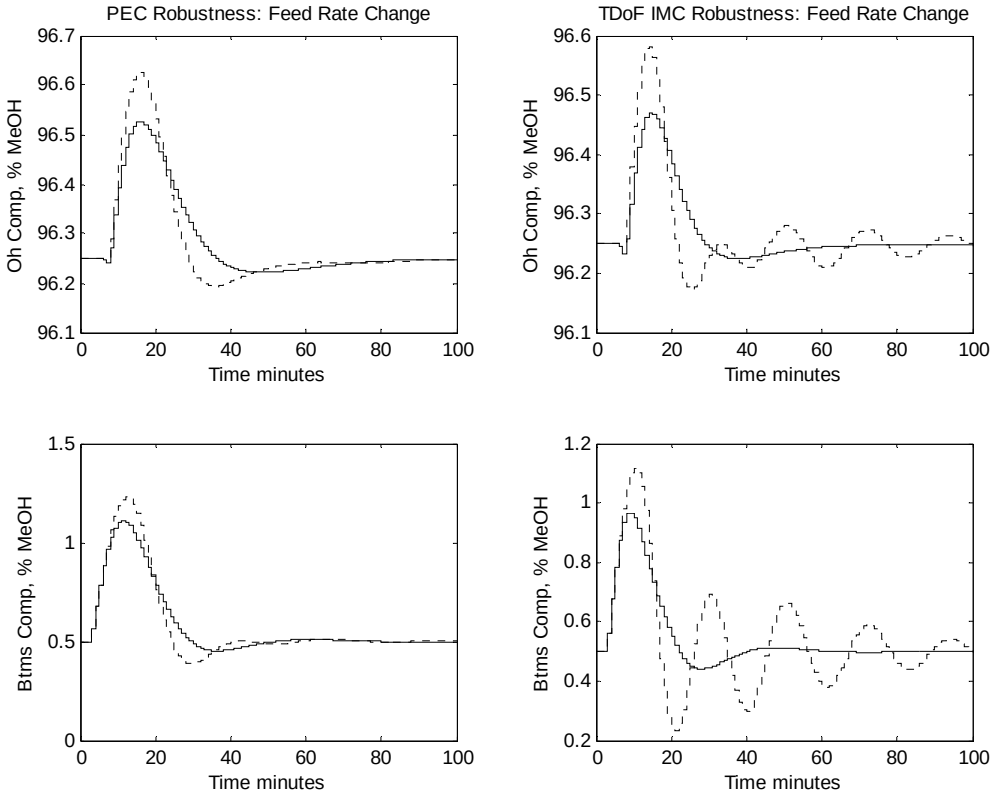

Figure 90: The regulatory response of the perturbed process to a 0.34 lb/min change in the column feed rate for PEC and TDoF IMC control. The solid line represents the process with the minimum time delays. The dotted line represents the process with the maximum time delays.

Conclusions

Both PEC and H_∞ IMC control were able to utilize a second degree-of-freedom to meet the design criteria for the process. The PEC design procedure, though more complex then its TDof H_∞ IMC counterpart, was able to leverage the feedback design and default values for tunable parameters to achieve a good initial performance with little design effort. TDof H_∞ IMC controller, on the other hand, demonstrated a favorable interaction during the H_∞ optimization which enhanced the disturbance rejection response of the system, and a more arbitrary yet simpler tracking design procedure. In the end both controllers were able to use model reduction techniques to obtain reasonably sized controllers for the problem.

CHAPTER VII

CONCLUSIONS: A SUMMARY OF RESULTS

This research developed the theory of Partition Error Control. An extensive literature and patent search was conducted to verify the novelty of the PEC system and to find comparable control structures. During this search the novelty of PEC was confirmed and two competitive two-degree-of-freedom designs were identified: Inverse model prefilters, and H_∞ two-degree-of-freedom control. The designs of both of these systems use a prefilter and are based on shaping the reference signal so the feedback controller exhibits the desired tracking response. Inverse model prefilters utilize an inverse model to achieve this result, while H_∞ two-degree-of-freedom control parameterized the prefilter based on the solution to an H_∞ norm minimization problem. Partitioned Error Control was compared to these techniques in a SISO setting to help provide insight into the workings of these various controllers in simplified control problems. Once the benefits and limitations of the various systems were understood, the research was expanded into a MIMO setting; first by examining controller design for an inverted pendulum on a cart, then by examining controller design for a binary distillation problem in the discrete domain. These classic systems were chosen because they provided a cross section of process dynamics and because competitive two-degree-of-freedom designs were already explored by other researchers for these systems. The inverted pendulum represents a single input, multiple output system. The challenges presented by controlling two outputs with one manipulated variable make the inverted pendulum a standard system for

the study of two-degree-of-freedom control. The binary distillation column was chosen because it included time delays (non minimum phase dynamics), and required a discrete domain controller.

Partitioned Error Control uses a process model to partition the error signal from the process into that which is caused by reference changes and that which is from other sources. Once the error signal is partitioned, two independent controllers can be designed to address regulatory and servo problems separately. Several advantages were found to this technique when compared to other two-degree-of-freedom controllers. First, it was demonstrated that PEC systems share the same respond to modeling error as other two-degree-of-freedom controllers when they are designed on the same basis. Second, the Approach was found to be more intuitive and flexible. Third, information about the response of the feedback controller can be used to reduce the design effort of the partitioning controller. Fourth, PEC can be applied to a wider variety of systems then inverted model prefilters. The main disadvantage of PEC was found to be the inherent size of the controller. By using an internal model and two independent controllers, PEC controllers have a larger number of states then competitive systems. This disadvantage was countered through the successful use of model reduction techniques.

The effect of modeling error on the PEC system was studied in detail. It was shown that the response of the system to error was governed by the feedback control law. However, performance and robustness objectives are always at odds. Therefore as the aggressiveness of the nominal tracking response increased, the robust stability of the tracking response decreased. This relationship is the same for all two-degree-of-freedom

controllers. As such PEC has neither superior nor inferior robustness when compared to other systems.

PEC allows for the independent design of servo and regulatory controllers. All other two degree of freedom techniques shape the reference trajectory so that the feedback controller exhibits the desired tracking response. This inextricably links their servo response to their regulatory response. Since PEC controllers are independent they can be chosen for their performance or robustness as well as for desirable tuning parameters. As a result, PEC designs are more intuitive and more flexible then both inverted model prefilters and H_∞ two-degree-of-freedom control. This is particularly evident when it is realized that standard feedback techniques can be applied directly to the controller within the partitioning loop. In comparison the use of a reference trajectory as a tunable parameter by H_∞ two-degree-of-freedom controllers was found to be a simple but limiting means of obtaining two degree of freedom control. Designers must over-specify the reference trajectory, and often neglect significant dynamics because fine tuning procedures can be bogged down with additional complexity.

During the design of H_∞ Mixed Sensitiviy/H_∞ loop shaping PEC systems, it was demonstrated that information about the response of the feedback controller could be used to assist in the design of the partitioning controller, significantly reducing the overall design effort. This design synergy generated superior initial nominal tracking responses for both the inverted pendulum and the binary distillation column when compared to the initial H_∞ two-degree-of-freedom design.

PEC control is applicable to a wider variety of systems than other two-degree-of-freedom techniques. Prefilter design relies on inverse models; however, not all systems

are invertible. This limitation discourages the use of inverse model prefilters on non minimum phase or even multivariable problems. Likewise, two-degree-of-freedom H_∞ controllers are limiting in that they dictate the use of H_∞ control. It has been demonstrated that PEC uses simple feedback structures and can accommodate any controller type.

Along with the flexibility to use many different types of controller, PEC also inherits the shortcomings of controllers it uses. One particular shortcoming of H_∞ control is that the controllers often contain more states then the process model. This problem was exacerbated by using two H_∞ controllers simultaneously in the PEC structure, one for servo and the other for regulatory control. Model reduction techniques were successfully applied to the overall PEC controller in both multivariable systems examined. The size of the reduced controller was roughly equivalent to the size of the H_∞ two-degree-of-freedom controllers examined.

PEC provides a viable alternative to current two-degree-of-freedom techniques, which has greater breadth of application and flexibility.

CHAPTER VIII

FUTURE RESEARCH

The tremendous adaptability of Partitioned Error Control opens the system up to a wide variety of research possibilities. Of particular interest is that designers can now implement control strategies for tracking in a nominal, environment with full access to model outputs. Three ideas that scratch the surface of this new environment will now be presented.

Decoupling

There currently is not way to implement decoupling in a two-degree-of-freedom fashion using standard two-degree-of freedom techniques. Any decoupler that is used for feedback must also be used for tracking and vice versa. The independence of design that is allowed by partition error control also allows a designer the option of using different decoupling techniques for feedback and tracking control. The question then becomes under what circumstances would a designer desire to implement different decouplers for tracking and regulatory control? The obvious answer to that question is when the implementation of full decoupling is restricted by the uncertainty found in all real systems. Take for instance the following three common restrictions. The theoretical application of full decouplers relies on the exact cancellation of system dynamics. This cancellation translates RHP zeros into RHP poles resulting in unstable decouplers. Similarly systems with erroneous models can lead to similar stability issues. The last

restriction may come from the realizability of system dynamics, for instance the designs for some systems result in a decoupler with a predictive element.

All of these restrictions are mathematical in nature, and all of the restrictions come from the implementation of these theories on real systems. The partitioning loop is not a real system, it is a mathematical abstraction of the process. The partitioning loop may allow a relaxing of the restrictions placed on decouplers, so that tracking responses can benefit from reduced loop interactions.

Full Information Control

The second benefit of IMC control is that it can be used to determine the present dynamic state of the process, states that may be otherwise unobservable.

Control based on the present dynamic state of a process (not just observable states) falls into a category called full information control. This additional information can be accessed readily in the internal model used inside the partitioning loop. The benefit would be that in the nominal environment of the partitioning loop any disturbances would not need to be measured in order to estimate the states of the process. This would open up the application of full information control to a much wider category of systems. The down side to this implementation is that the full information controller would only be responsible for nominal servo performance. Disturbances would be handled without the benefit of full information. This application may be more beneficial for ill-conditioned processes, but that is a matter for future investigation.

Smith Predictor Adaptation for Batch Processing

Batch processes present a difficult set of dynamics for control problems. In addition to all the dynamics present in continuous systems, batch systems are continuously moving away from the setpoint. Inversion techniques are often unavailable due to these dynamics. Large batch systems often have significant time delays as well, complicating the issue further. One solution to this problem would be to use a smith predictor to separate out the dynamics of the system model from the time delays. This would allow the controller to take swifter action. However, any error in the estimate of the time delay would cause a slight phase shift in the process models response that would also be handled swiftly. In this case it may be advantageous use a slower response to feedback error so as not to over react to small phase differences in the process and model outputs. We have just identified a performance benefit from a swift servo response and a slower regulatory response for a class of systems that current two-degree-of-freedom controllers can not be readily applied to. The internal model in the partitioning loop can be split into a dynamic portion and a time delay portion with ease. The dynamic portion would provide a feedback signal for the partition loop controller while the output of the time delay portion of the model would be used to compare against the actual process output to generate an error signal for the feedback controller.

BIBLIOGRAPHY

(1) Horowitz, I.M. *Synthesis of Feedback Systems*; Academic Press: London, 1963.

(2) Morari, M.; Zafiriou, E. *Robust Process Control*; Prentice Hall: Englewood Cliffs, NJ, 1989.

(3) Lundstrom, P.; Skogestad, S; Doyle, J.C. Two-Degrees-of-Freedom Controller Design for an Ill-Conditioned Distillation Process Using μ-Synthesis. *IEEE Trans. Control Sys. Technol.* **1999**, *29*, 157.

(4) Limbeer, D. J. N.; Kasenally, E. M.; Perkins, J. D. On the Design of Robust Two-Degrees-of-Freedom Controllers. *Automatica* **1993**, *29*, 157.

(5) Van Digglen, F.; Glover, K.A. Hadamard Weighted Loop Shaping Design Procedure. *Proc. IEEE Conf. Decision Control* (Tucson, AZ) **1992**, 2193.

(6) Skogestad, S.; Morari, M.; Doyle, J.C. Robust Control of Ill-Conditioned Plants: High Purity Distillation. *IEEE Trans. Automat. Control* **1988**, 1092.

(7) Lopez, A. M.; Murrill, P.W.; Smith, C.L. Controller Tuning Relationships Based on Integral Performance Criteria. *Instrum. Technol*. **1967**, *14*, 57.

(8) Rovira, A. A.; Murrill, P. W.; Smith, C. J. Tuning Controllers for Set-point Changes. *Instrum. Control Syst.* **1969**, *42*, 67.

(9) Skogestad, S. and Postlethwaite, I., *Multivariable Feedback Control: Analysis and Design.* John Wiley, West Sussex, England, 1996.

(10) Debelak, K. A.; Rutherford M. L., Partitioned Error Control. *Ind. Eng. Chem. Res.* **1999**, *38*, 4113-4119.

(11) Tyreus, B. D.; Luyben, W. L. Tuning PI Controllers for Integrator/Dead Time Processes. *Ind. Eng. Chem. Res.* **1992**, *32*, 2625.

(12) Astrom, K. J. and Wittenmark, B., Adaptive Control. Addison-Wesley, second edition, 1995.

(13) Glover, K. and Doyle, J. C., State-space formulae for all stabilizing controller that satisfy an H_∞ norm bound and relations to risk sensitivity, *Systems and Control Letters*. **1988**, *11*, 167-172.

(14) Doyle, J. C., Glover, K., Khargonekar, P. P. and Francis, B.A., State-space solutions to standard H_2 and H_∞ control problems, *IEEE Transactions on Automatic Control* **1989**, *AC-34*(8), 831-847.

(15) McFarlane, D., and Glover, K., Robust Controller Design Using Normalized Coprime Factor Plant Descriptions, Lecture Notes in Control and Information Science Series 1990, (Berlin: Springer-Verlag).

(16) Hyde, R., and Glover, K., Application of scheduled H_∞ controllers to a VSTOL aircraft. *IEEE Transactions on Automatic Control*, **1993**, *38*, 1021-1039.

(17) Hoyle, D., Hyde, R., and Limebeer, D., An H_∞ approach to two degree of freedom design. *Proceedings of the 30th IEEE Conference on Decision and Control*, Brighton, U.K. **1991**, pp.1581-1585.

(18) Walker, D., Postlethwaite, I., High performance full authority active control system design for the Lynx helicopter. *June Quarterly Progress Report on Research Agreement 2026/32 RAE(b)-DRA*, Bedford, U.K. **1992**.

(19) Walker, D. J.; *On the structure of two-degree-of-freedom H_∞ loop shaping controller*. International Journal of Control, 1996, vol. 63, no. 6, 1105-1127.

(20) Murad, G., Postlethwaite, I., and Gu, D., *A discrete-time internal model-based H_∞ controller and its application to a binary distillation column*. Journal of Process Control, 1997, vol. 7, no. 6, 451-465.

(21) Garcia, C. E. and Morari, M., *Internal Model Control. 6. Multiloop Design*. Industrial Engineering Chemical Process Design and Development, 1985, no. 24, pp. 472-484

(22) Zhou, C., Whiteley, J. R., Misawa, E. A. and Gasem, K. A. M., *Application of enhanced LQG/LTR for distillation control*. IEEE Control Systems Magazine, 1995, 15(4), 56-63.

(23) Rouhani, R. and Mehra, R. K., *Model algorithmic control (MAC); basic theoretical properties*. Automatica, 1982, 18, 401-414.